

University of Windsor

## Scholarship at UWindor

---

Electronic Theses and Dissertations

Theses, Dissertations, and Major Papers

---

2014

# The Development of Polymer-coated Electrodes for Chemical Detection

Xuefeng Hu  
*University of Windsor*

Follow this and additional works at: <https://scholar.uwindsor.ca/etd>

---

### Recommended Citation

Hu, Xuefeng, "The Development of Polymer-coated Electrodes for Chemical Detection" (2014). *Electronic Theses and Dissertations*. 5129.

<https://scholar.uwindsor.ca/etd/5129>

This online database contains the full-text of PhD dissertations and Masters' theses of University of Windsor students from 1954 forward. These documents are made available for personal study and research purposes only, in accordance with the Canadian Copyright Act and the Creative Commons license—CC BY-NC-ND (Attribution, Non-Commercial, No Derivative Works). Under this license, works must always be attributed to the copyright holder (original author), cannot be used for any commercial purposes, and may not be altered. Any other use would require the permission of the copyright holder. Students may inquire about withdrawing their dissertation and/or thesis from this database. For additional inquiries, please contact the repository administrator via email ([scholarship@uwindsor.ca](mailto:scholarship@uwindsor.ca)) or by telephone at 519-253-3000ext. 3208.

# **The Development of Polymer-coated Electrodes for Chemical Detection**

By

**Xuefeng Hu**

A Thesis  
Submitted to the Faculty of Graduate Studies  
through the Department of Chemistry and Biochemistry  
in Partial Fulfillment of the Requirements for  
the Degree of Master of Science  
at the University of Windsor

Windsor, Ontario, Canada

2014

© 2014 Xuefeng

The Development of Polymer-coated Electrodes for Chemical Detection

by

Xuefeng Hu

APPROVED BY:

---

X. Nie

Mechanical, Automotive & Materials Engineering

---

R. Aroca

Department of Chemistry & Biochemistry

---

J. Wang, Advisor

Department of Chemistry & Biochemistry

June 13, 2014

## Declaration of Co-Authorship / Previous Publication

### I. Co-Authorship Declaration

I hereby declare that chapters 2 and 4 of this thesis incorporate materials that are the result of joint research with Jun Li, who was also under the supervision of Dr. J. Wang. A publication presented in Chapter 5 is a review article on electrochemical sensor, accomplished while taking a graduate course with Dr. Mutus.

I am aware of the University of Windsor Senate Policy on Authorship and I certify that I have properly acknowledged the contribution of other researchers to my thesis, and have obtained written permission from each of the co-author(s) to include the above material(s) in my thesis.

I certify that, with the above qualification, this thesis, and the research to which it refers, is the product of my own work.

### II. Declaration of Previous Publication

This thesis includes [*insert number*] original papers that have been previously published/submitted for publication in peer reviewed journals, as follows:

Thesis Chapter	Publication title/full citation	Publication status*
Chapter 2	Electrochemical Recognition of Chiral Molecules with Poly-(4-bromoaniline) Modified Gold Electrode, Electroanalysis, J. Li, X. Hu, J. W, Electroanalysis <b>2013</b> , 25, 1975.	Published
Chapter 4	Designed Deposition of Copper Nanoparticles on/inside a Conductive Polymer Matrix, X. Hu, J. Li, J. Wang, ECS Electrochemistry Letters, <b>2014</b> , 3, D13.	Published
Chapter 5	Electrochemical Detection of Sulfide, X. Hu, B. Mutus, Reviews in Analytical Chemistry, <b>2013</b> , 32, 247.	Published

I certify that I have obtained a written permission from the copyright owner(s) to include the above published material(s) in my thesis. I certify that the above material describes work completed during my registration as graduate student at the University of Windsor.

I declare that, to the best of my knowledge, my thesis does not infringe upon anyone's copyright nor violate any proprietary rights and that any ideas, techniques, quotations, or any other material from the work of other people included in my thesis, published or otherwise, are fully acknowledged in accordance with the standard referencing practices. Furthermore, to the extent that I have included copyrighted material that surpasses the bounds of fair dealing within the meaning of the Canada Copyright Act, I certify that I have obtained a written permission from the copyright owner(s) to include such material(s) in my thesis.

I declare that this is a true copy of my thesis, including any final revisions, as approved by my thesis committee and the Graduate Studies office, and that this thesis has not been submitted for a higher degree to any other University or Institution.

## ABSTRACT

This research focuses on the development of simple and cost effective approaches for making electrochemical sensors with a great sensitivity and selectivity. As an economic and abundant starting material, organic substrates were investigated to making conductive polymers that showed promising electrocatalytic activities. Firstly, a poly(4-bromoaniline) film was successfully synthesized on a gold electrode and the porous film which was made up of nano-ribbons on the Au electrode was used for the recognition of amino acids enantiomers. Secondly, different halogen ions were introduced to manifest the properties of the synthesized polymers. The results show that bromide ions have significantly inhibited the transition of leucoemeraldine to emeraldine, letting the PANI polymer to be in Pernigraniline form, which exhibited much improved performance in pH sensing. In addition, a simple way to controllably deposit copper nanoparticles inside poly-2,5-dimethoxyaniline matrix, which can be employed as a glucose sensor, was developed.

## DEDICATION

This work is dedicated to my husband, Jun Li, who is also my fellow in the same lab, as well as my precious daughter, Grace Li. I definitely could not have completed my Master's program without their love.

This work is also dedicated to my parents for their love, support and encouragement. It is because of them I am here on the first place.

God bless!

## ACKNOWLEDGEMENTS

This thesis becomes a reality with the kind support and help of many individuals. I would like to extend my sincere thanks to all of them.

First and foremost, I would like to thank God for his blessing and kindness. I thank him for the gift of life, health, wisdom and all life opportunities.

I would like to express the deepest appreciation to my supervisor, Professor Jichang Wang. Without his guidance, encouragement and persistent help this thesis would not have been possible.

I would like to thank all my committee members, Professor Ricardo Aroca and Professor Xueyuan Nie. Thanks to the Professor Ricardo Aroca for his wonderful teaching, I have learned so much knowledge about photochemistry. With the nice help and suggestion of Professor Xueyuan Nie, I was encouraged during my graduate study.

I would like to thank Professor Bulent Mutus, who has taught me the electrochemistry course. With your guidance, support and kindness, I could complete all the experiments I wanted to try. Also I would like to thank Professor James Green, who is really an excellent instructor.

Many thanks to all the members in Professor Wang's group, especially to Jeffrey Bell, who always gives me very nice help not only in academic and language but also daily life.

Also, I wish to express my sincere thanks to the University of Windsor, Department of Chemistry and Biochemistry, and all the faculty members who have helped and



supported me in the past 2 years. Especially thanks to Mrs. Marlene Bezaire, for her constant help during my stay at the University of Windsor.

Lastly, my thanks and appreciations go to all my family members, who love me and support me all the time.

## TABLE OF CONTENTS

DECLARATION OF ORIGINALITY	III
ABSTRACT	V
DEDICATION	VI
ACKNOWLEDGEMENTS	VII
LIST OF TABLES	XII
LIST OF FIGURES	XIII
LIST OF APPENDICES	XVII
LIST OF ABBREVIATIONS/SYMBOLS	XVIII
<b>CHAPTER 1 Introduction</b>	<b>1</b>
1.1 Overview of Electrochemical Sensors	1
1.2 Electrochemical Sensing with Carbon Nanotubes	2
1.3 Metal Nanoparticles in Electrochemical Sensing	6
1.4 Polymer-based Electrochemical Sensors	11
1.4.1 Historic Development	11
1.4.2 Conducting Polymer	13
1.4.3 Polyaniline	14
References	17
<b>CHAPTER 2 Electrochemical Synthesis of Poly-(4-bromoaniline) for the Recognition of Chiral Molecules</b>	<b>34</b>
2.1 Introduction	34
2.2 Experimental	35

2.3 Results and Discussion	36
2.4 Conclusions	42
References	43
<b>CHAPTER 3 Controlled Synthesis of Polyaniline on Glassy Carbon Electrodes for Improved pH Sensing</b>	<b>48</b>
3.1 Introduction	48
3.2 Experimental	49
3.3 Results and Discussion	50
3.4 Conclusions	57
References	58
<b>Chapter 4 Designed Electrodeposition of Copper Nanoparticles inside/on Poly-2, 5-dimethoxyaniline and Applications as Non-enzymatic Glucose Sensor</b>	<b>62</b>
4.1 Introduction	62
4.2 Experimental	64
4.3 Results and Discussion	65
4.4 Conclusions	74
References	75
<b>Chapter 5 Electrochemical Detection of Sulfide: A Review</b>	<b>80</b>
5.1 Introduction	80
5.2 Classical Detection Methods	81
5.3 Electrochemical Methods	83
5.3.1 Anodic Stripping Voltammetry	83
5.3.2 Amperometric Method	84

	XI
5.3.3 Cyclic Voltammetry	87
5.3.4 Photoelectrochemical Method	89
5.3.5 Electrochemical Detection Methods Coupled with Other Devices	90
5.4 Summary	94
References	96
<b>Chapter 6 Summary and Perspectives</b>	106
6.1 Summary	106
6.2 Future Works	108
References	109
<b>APPENDICES</b>	111
Appendix A: Copyright Releases Electroanalysis	111
Appendix B: Copyright Releases ECS Electrochemistry Letter	119
Appendix C: Copyright Releases Reviews in Analytical Chemistry	120
<b>VITA AUCTORIS</b>	121

## **LIST OF TABLES**

Table 1. Different methods used in different periods

Table 2. Different analytical characteristics by different electrochemical method

## LIST OF FIGURES

**1.1** Schematics of an individual (A) SWCNT and (B) MWCNT.

**1.2** SEM images of different morphologies of PANI: (A) Needle-like shapes (B) Nanowires (C) Nanotubes (D) Hollow Microsphere.

**2.1** CVs of 4-bromoaniline (a), EIS of the PBA films (b), Electrolyte used in (b) consists of 5.0 mM  $K_3Fe(CN)_6$  and 0.1M NaCl, (5 and 10 means CV cycles for PBA film; sim means simulated EIS and exp means experimental EIS, in which 12 data points were recorded per frequency decade at 0.262 V).

**2.2** SEMs of the PBA films fabricated with 5 cycles (a) and 10 cycles (b).

**2.3** DPVs of DGA (a) and LGA (b) at the Au-PBA Au electrode, (c) DPVs of DGA and LGA at a bare Au electrode. The concentration of LGA and DGA in (c) is 15.0 mM.

**2.4** The relationship between the peak current and the scan rate in the cyclic voltammetry experiments. The concentration of LGA and DGA used in these experiments is 15.0 mM, The scan rate was adjusted between 5 and 200 mV/s.

**2.5** DPVs of (a) LAA and (b) DLAA at the Au-PBA electrode. The aspartic concentration was increased from 0 (curve 0) to 30.0 mM (curve 6) with an increment of 5.0 mM.

**3.1** Cyclic voltammogram ( $50 \text{ mV s}^{-1}$ ) of electrochemically synthesized PANI in 0.05 M aniline and 1 M  $HNO_3$  at glassy carbon electrode in the absence (a) and presence (b) of 0.05 M NaBr ; (c) EIS measurements of polymer film (a) in 5 mM  $K_3Fe(CN)_6$  with the electrolyte 0.1M NaCl solution within the range from 100 mHz to 100 kHz, with an amplitude of 5 mV rms, the fixed potential of the film corresponded to the anodic

potential; (d) Experimental and simulated EIS curves of polymer film (b) under the same condition in (c).

**3.2** SEM images for 10 cycles of bromide-absence PANI (a) and bromide-presence PANI (b) on glassy carbon electrode, the conditions of electropolymerization of PANI were the same as Figure 1a and 1b, respectively.

**3.3** pH vs. OCP (open circuit potential) curve tested by bromide-free PANI (square) and bromide-added PANI (circle) modified GC electrode. pH buffered solution was prepared by pH = 7 phosphate buffer, hydrochloric acid (0.1 M) and sodium hydroxide (0.1 M) were used to adjust the pH to the desired value.

**3.4** Open circuit potential responses to a successive addition of 0.01 M NaOH in pH = 1 phosphate buffer, curve 1 and 2 represent bromide-added PANI and bromide-free PANI modified GC electrode, respectively.

**4.1** (A) CVs of 20.0 mM 2,5-dimethoxyaniline in 0.5 M H<sub>2</sub>SO<sub>4</sub> solution at a scan rate of 100 mV/s. (B) pulsed deposition of Cu in 0.1 M CuSO<sub>4</sub> solution with or without KCl additives. The number of cycles is 20 in both (A) and (B).

**4.2** SEM images of the PDMA file after the Cu deposition. No additive such as KCl was added to the electrolyte solution.

**4.3** SEM images of the PDMA file after the Cu deposition. The pulsed electrodeposition of copper took place in the presence of 20.0 mM KCl in the electrolyte.

**4.4** (A) CVs of glucose at (1) GC/PDMA/Cu(cube), (2) GC/PDMA/Cu(pyramid), (3) GC/PDMA and (4) bare GC electrodes at a scan rate of 100 mVs<sup>-1</sup>. (B) DPVs of glucose at (1) GC/PDMA/Cu(cube) electrode and (2) GC/PDMA/Cu(pyramid). The electrolyte solution contains 10.0 mM glucose and 0.1 M NaOH.

**4.5** (A) Amperometric responses to a successive addition of 0.1  $\mu\text{M}$  glucose in phase I, 1.0  $\mu\text{M}$  glucose in phase II and 10.0  $\mu\text{M}$  glucose in phase III, (B) The current response vs. glucose concentration, (C) amperometric responses to additions of glucose (1 mM), UA (0.1 mM), DA (0.1 mM) and AA (0.1 mM). The supporting electrolyte is 0.1 M NaOH and the modified electrode was GC/PDMA/Cu (cube). The applied potential is 0.3 V.

5.1 The ASV response of  $\text{Cd}^{2+}$  changed with the addition of sulfide. 0.1 M PH 4.5 NaAc-HAc(---base line) buffer solution at  $3.6 \times 10^{-6}$  M; a-h:  $\text{C}_s^{*2-} = 0, 0.7, 1.4, 2.2, 2.9, 3.6, 4.3, 5.0 \times 10^{-6}$  M. Insert: plot of the relation between the peak current of  $\text{Cd}^{2+}$  and the concentration of sulfide added.

**5.2** Amperometric response of CIP biosensor for different concentrations of sulfide at -150 mV vs. Ag/ AgCl in 0.1 M phosphate buffer (PH 6.5) solution containing 0.6mM  $\text{H}_2\text{O}_2$  and 1.25 mM of hydroquinone. Inset (a): calibration curve for sulfide determination with CIP inhibition sensor.

**5.3** (A) Chronoamperometric response of sulfide at the FeCN-PIL-SPCE in pH 7, 0.1 M PBS at a detection potential of 0.0 V vs. Ag/ AgCl. The insert graph is the calibration curve with a linear concentration range of 1  $\mu\text{M}$  to 3 mM. (B) The results at the FeCN-PIL-SPCE for 10 continuous additions of 3  $\mu\text{M}$ , 50  $\mu\text{M}$  and 300  $\mu\text{M}$  sulfide, respectively.

**5.4** (A) Cyclic voltammograms of RGSs/GC electrode in 0.2 M PBS (pH 7.4) containing different concentrations of sulfide of (a)  $5 \times 10^{-3}$ , (b)  $1.0 \times 10^{-2}$ , (c)  $2.0 \times 10^{-2}$ , (d)  $4.0 \times 10^{-2}$ , (e)  $8.0 \times 10^{-2}$ , (f) 0.16, (g) 0.25, (h) 0.35, (i) 0.45, (j) 0.54, (k) 0.74, (l) 0.98, (m) 1.47, (n) 1.95, (o) 2.9, (p) 4.7, (q) 7.4 mM. (B) The changes of  $I_{pa}$  versus concentrations



of sulfide ranging from  $5 \times 10^{-3}$  to 7.4 mM. Inset: Plot of changes of  $I_{pa}$  versus concentration of sulfide ranging from  $5 \times 10^{-3}$  to 0.45 mM.

**5.5** (A) Image of CE-AD microchip showing microchannel engraved in PDMS mold, sample reservoirs, silicon tubes carrying sample and NaOH solution into the microchannel, gold microelectrodes (W1-3=working; C1-3=counter; R1-3=reference; S1-4= separation electrodes). (B) Schematics for electronic circuit and the operation of the in-house built dual potentiostat.

**LIST OF APPENDICES**

- Appendix A**            Copyright Releases Electroanalysis
- Appendix B**            Copyright Releases ECS Electrochemistry Letter
- Appendix C**            Copyright Releases Reviews in Analytical Chemistry

**LIST OF ABBREVIATIONS/SYMBOLS**

AC	Acetaminophen
AD	Amperometric detection
AFM	Atomic Force Microscopy
ASV	Anodic Stripping Voltammetry
AuNP	Au Nanoparticles
BDD	Boron-Doped Diamond
BiEFs	Bismuth-film Glassy Carbon Electrode
CE	Capillary Electrophoresis
CIP	Coprinus Cinereus Peroxidase
CNTs	Carbon Nanotubes
CoPCNF	Cobalt Pentacyanonitrosylferrate
CS	Chitosan
CV	Cyclic Voltammetry
CVD	Chemical Vapor Deposition
Cys	Cysteine
DA	Dopamine
DC	Constant Potential Amperometric Detection
DGA	D-Glutamic Acid
DLAA	DL-Aspartic
DLS	Dynamic Light Scattering
DMPD	<i>N,N</i> -Dimethyl- <i>p</i> -Phenylenediamine
DPV	Differential Pulse Voltammetry
EB	Emeraldine
EDX	Energy Dispersive X-ray spectroscopy

EIS	Electrochemical Impedance Spectroscopic
EP	Epinephrine
ES	Protonated Emeraldine Salt
FA	Folic Acid
FeCN-PIL-SPCE	Fe(CN) <sub>6</sub> <sup>3-</sup> -Immobilized Polymeric Ionic Liquid-Modified Electrode
FETs	Field Effect Transistors
GC	Glassy Carbon
GSH	Glutathione
GSSG	Glutathione Disulfide
GOD	Glucose Oxidase
Hcys	Homocysteine
HDVs	Hydrodynamic Voltammograms
HPLC-ECD	HPLC Coupled to Electrochemical Detection
LAA	L-Aspartic Acid
LBL	Layer-By-Layer
LE	Leucoemeraldine
LGA	L-Glutamic Acid
LOD	Limit of Detection
MWCNTs	Multi-Walled Carbon Nanotubes
NADH	Nicotinamide Adenine Dinucleotide Phosphate
NPs	Nanoparticles
NTA	NP-Tracking Analysis
PA	D-Penicillamine
PAD	Pulsed-Potential Amperometric Detection
PANI	Polyaniline
PBA	Poly(4-Bromoaniline)
PDMA	Poly-2,5-dimethoxyaniline

PDMS	Polydimethylsiloxane
PE	Pernigraniline
PNH	2, 2'-[1, 4-phenylenediyl-bis (nitrilomethyl-idene)]-bis (4-hydroxyphenol)
RGS	Reduced Graphene Sheets
RSD	Relative Standard Deviation
SAM	Self-Assembled
SCE	Saturated Calomel Electrode
SEM	Scanning Electron Microscopy
SPE	Screen Printed Electrode
SWCNTs	Single-Walled Carbon Nanotubes
TEM	Transmission Electron Microscopy
UA	Uric Acid
XRD	X-Ray Diffraction

## Chapter 1. Introduction

### 1.1 Overview of Electrochemical Sensor

An electrochemical sensor is a device which detects a variable quantity and then transfers the measurement into electrochemical signals to be recorded elsewhere [1]. The development of electrochemical sensor has gathered a great deal of attention in the last 3 decades as an inexpensive and simple means to sensitively detect a variety of chemical and biological analytes [1], and have found a wide range of applications in physical chemistry, materials science, biochemistry, solid-state physics, micro-device fabrication, electrical engineering, clinical diagnostics, medical engineering, process measuring engineering, and environmental analysis [2,3]. Today there are numerous literatures focusing on two branches of electrochemical sensing: (1) sensors with a great specificity and (2) sensors capable of simultaneous/multiplex determination [2]. Our group have developed, for example, a low cost modified carbon electrodes that can simultaneously determine 1,4-hydroquinone and pyrocatechol with the limit of 2.0  $\mu\text{M}$  and 5.0  $\mu\text{M}$ , respectively [4]. Besides that stability, activity and selectivity are of paramount importance in electrochemical sensing, low cost, miniaturization, reproducibility must also be considered when developing new sensors. Meanwhile, depending on the instruments, a range of detection modes such as potentiometric, voltammetric, conductimetric and impedimetric can be used for electrochemical detection.

In recent development of electrochemical sensors, nanomaterials have been extensively explored for signal amplification due to their large specific surface area [5].

Indeed, nano-size particles of less than 100 nm in diameter are currently attracting increasing attention for the wide range of new applications in various fields including industrial production [6]. Those being actively investigated in electrochemical sensing has roughly been focused on three categories, specifically including carbon nanotubes (CNTs), noble metal nanoparticles and conductive polymers. Firstly, CNTs will be discussed in this thesis, for it is one of the most exciting materials because of its unique electronic, chemical, and mechanical properties.

## **1.2 Electrochemical Sensing with Carbon Nanotubes**

CNTs are built from  $sp^2$  carbon units with a few nanometers in diameter and many microns in length [2, 7-9]. There are two groups of CNTs, say multi-walled (MW) and single-walled (SW) [10, 11] (Figure 1.1), which can be synthesized by various methods [12], such as, arc discharge [13, 14], laser ablation/vaporization [15, 16], and carbon vapor deposition (CVD) [17, 18]. CNTs have unique mechanical and electronic properties, and can behave electrically as a metal or semiconductor, depending on the diameter and the degree of helicity [1, 19-21]. Combined with chemical stability, CNTs have many advantages for sensing applications, such as small ratio between the size and surface area [11], outstanding electron transfer promoting ability [22]. When being used as electrodes modifier in electrochemical reactions for purposes such as easy protein immobilization [23, 24] etc., they are suitable for the modification of various electrodes due to high electronic conductivity for the electron transfer reactions, better electrochemical and chemical stabilities in both aqueous and non-aqueous solutions and the promotion of electron-transfer reaction in several small biologically important molecules and large biomolecules [1, 25].

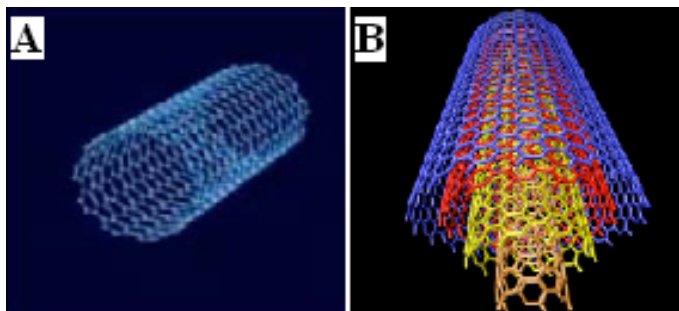


Figure 1.1 Schematics of an individual (A) SWCNT and (B) MWCNT. Ref [11]

Studies have shown that carbon atoms of CNTs at the sidewall and the end of the tubes are not the same, and the electroactive sites on CNTs are located at the tube ends [26, 27]. In other words, electrochemistry of CNTs is dominated by the ends of CNTs. In addition, both the orientation and length of the aligned CNTs have significant influence on the electron transfer rate. More specifically, according to the research by Gooding et al. electron transfer between the gold electrode and the ferrocene moiety has been found 40 times slower through randomly dispersed nanotubes than through vertically aligned nanotubes [27]. A theory has been proposed by the same group to account for the observation that the inverse of the apparent electron transfer rate constant ( $K_{app}$ ) is related to length of nanotubes [27].

Various electrochemical techniques such as voltammetry, amperometry, potentiometry, impedemetry and conductometry were reported to investigate CNTs-based electrodes as chemical sensors or biosensors. For example, an electrochemical sensor based on SWCNTs modified glassy carbon electrode has been developed by Chen and co-workers for the sensitive detection of valacyclovir, a substance that is the choice for the treatment of herpes zoster and cold sores. The results of cyclic voltammetry (CV) and differential pulse voltammetry (DPV) showed that the modified electrode possessed high



## Chapter 1. Introduction

activity, a wide linear response range and very low detection limit toward the electrochemical oxidation of valacyclovir, highlighting that this electrochemical sensor has strong potential to be applied in the quality control testing of pharmaceutical products and also for therapeutic drug monitoring in hospitals [28]. Mohammad et al. recently reported that an electrochemical sensor based on CNTs could be employed for selective determination of dopamine (DA) in the presence of uric acid (UA), folic acid (FA) and acetaminophen (AC). Their sensor was developed on a carbon paste electrode modified by Schiff base (2, 2'-[1, 4-phenylenediyl-bis (nitrilomethyl-ylene)]-bis (4-hydroxyphenol) (PNH)) and CNTs. The electrochemical properties of such modified electrodes were studied by CV and DPV of DA, which displayed two linear dynamic ranges with a detection limit of 0.42  $\mu\text{M}$  [29]. Another example of biocompatible electrochemical sensor was developed by Thomas et al., which can selectively determine epinephrine (EP) in the presence of 1000-fold excess of ascorbic acid (AA) and uric acid (UA). The electrochemical sensor was fabricated by modifying the carbon paste electrode (CPE) with multi-walled carbon nanotubes (MWCNTs) using a casting method. Both CV and electrochemical impedance spectroscopic (EIS) methods were employed to study the characters of the electrode, which reveal that the current sensitivity of EP was increased five times upon modification. The modified electrode is highly reproducible and stable with anti fouling effects [30].

Recently, there are attempts to combine CNTs with polymers or metal-nanoparticles to develop new platforms for electrochemical sensing. For examples, Zhai et al. developed a multilayer film of MWCNTs and chitosan (CS) to detect Nicotinamide adenine dinucleotide phosphate (NADH), whose direct oxidation needs a high

## Chapter 1. Introduction

overpotential at a bare electrode. The multilayer film of MWCNTs and CS was obtained by the layer-by-layer (LBL) method which takes advantage of the interaction between a positively charged CS and the negatively charged MWCNTs. This assembled {CHIT/MWCNTs}/ GC electrode exhibited a wide linear response, a rapid response time and a low detection limit for the detection of NADH, also, it is highly stable [31]. CNTs-polymer composite can also be used for the fabrication of DA sensor. Wang and co-workers [32] and Zhang group [33] have respectively reported poly (3-methylthiophene) modified glassy carbon electrode coated with Nafion/SWCNTs and a poly(styrenesulfonic acid) sodium salt/SWCNTs electrodes for highly selective and sensitive determination of DA.

GC electrode combining Au nanoparticles (AuNP) with multi-walled carbon nanotubes has also been made into a biosensor by cross-linking glucose oxidase (GOD) with glutaraldehyde, where MWCNTs were dispersed in AuNP-doped CS solution (AuNP-CS), which is prepared by treating the CS solution followed by chemical reduction of Au (III) with  $\text{NaBH}_4$ . Several electrochemical methods such as CV, EIS and amperometry were employed to investigate the synergistic effect between AuNP and CNTs of the AuNP-CNTs-CS material. The modified electrode was applied to detect  $\text{H}_2\text{O}_2$  at low potential. With the immobilization of GOD, the electrode could determine glucose in human serum samples [34].

Despite of the earlier promising results, there are still numerous challenges remaining in order to develop CNTs into active chemical and biochemical sensors that can be widely used. Firstly, impurities in manufacture and imperfections in processing [35], lead to undesirable properties of CNTs which are difficult to overcome. It is hard to

develop a cost-effective method for separating different types of CNTs [36]. The structure of CNTs determines the electronic state, which varies between individual nanotubes. For CNT-field effect transistors (FETs) different electronic states can lead to inhomogeneity between devices and it may also disturb other sensors as well [10, 12, 37]. Additionally, the difficulty in the miniaturization of sensors [38], possible toxicity of nanotubes [39], and the technological difficulty in fabrication [40] also limited the application of CNTs. The disadvantage also includes that the adsorbed acid moieties during purification and acid- treatment processes can decrease the electrocatalytic activity of CNTs in electroanalysis [1, 41]. Those suggest that more research needs to be done in this area.

### **1.3 Metal Nanoparticle in Electrochemical Sensing**

Over the past few decades, metal nanoparticles (NPs) have attracted much attention due to their fascinating physical and chemical properties, such as, size- and shape-dependent interatomic bond distances [42,43], optical and electronic properties [42, 44, 45], nanoscale electrochemical processes to be probed [46-49], which are significantly different from those of the bulk materials. One of the many applications of NPs is in electrocatalysis, as the small size of nanoparticles has allowed electric double layer effects on interfacial electron-transfer reaction and charge can transfer at the interface between a solid catalyst and an electrolyte [50]. In general, controlling the size of nanoparticles is a key factor in the development of electrochemical sensing systems [51]. The mass-transport rates of reactants, products and intermediates depend on the nanoparticles size and coverage on the support of an electrode [52, 53]. In other words, a high surface area to mass ratio that can be tailored to promote particular reaction

pathways are key advantages of nanoparticles in electrochemical sensing system [52]. It is important to note, however, that the catalytic activity does not scale linearly with the nanoparticle surface area and the ultrasmall nanoparticles may become non-metal-like [54] and be more prone to poisoning [55].

The supporting material of a solid sensor where nanoparticles are dispersed also plays a number of important roles in sensing performance, including acting as a conductive bridge, limiting agglomeration of the nanoparticles to maintain the high surface-to-volume ratio as well as interacting with nanoparticles to modify the electrocatalytic activity of those nanoparticles [52, 56]. The most commonly used supporting materials are carbon [57, 58], gold [59, 60], titania [56, 61] and doped tin oxides [62, 63] that are typically desired as optically transparent electrodes. According to the order of the formation and immobilization of nanoparticles, methods of making nanoparticulate electrodes can be roughly divided into three groups, i.e., (1) simultaneous, (2) immobilization followed by the formation of metal nanoparticles, and (3) synthesis of metal nanoparticles followed by their immobilization on the surface of support electrode [52]. Specifically, in the simultaneous approach the formation and immobilization of nanoparticles on a supporting electrode took place in a single step. This method usually is connected to the electrodeposition of nanoparticles onto a bare electrode [64, 65] or a supporting electrode that has been modified with a polymer film [66, 67] etc. Since there are many parameters that can be adjusted, such as current, potential, time, temperature, electrolyte composition, concentration of the metal ion, and the pH, electrodeposition is one of the most popular methods to synthesize modified electrode with variable size, shape and spatial distribution of nanoparticles.

However, the size of nanoparticles in electrochemical deposition is not easy to control, which often leads to deposited nanoparticle with a wide size distribution [64]. The reasons for this include progressive nucleation [64, 68], depletion effects [69] and Ostwald ripening [70]. There are several approaches to circumvent the size dispersion, such as the double potential pulse method [62, 64, 65], or driving a gas evolving reaction in parallel with the electrodeposition reaction [71, 72]. To better control nanoparticle sizes, the second, two-step procedure was developed, which involves the immobilization of metal ions and their subsequent reduction. Through adjusting the density of metal ion immobilization sites, the spatial distribution and average size of the resulting nanoparticles can be controlled. A main drawback of this approach is that the hardly controlled coordination between functional groups and desired metal precursor on the supporting electrode surface. One option to address this problem is to encapsulate the nanoparticles within the polyelectrolyte film which deposited onto the substrate electrode [73, 74]. The other option is diazonium coupling, which is most commonly applied on carbon electrode, such as highly oriented pyrolytic graphite [75], or CNTs [76, 77].

The third approach seems to provide the best way to control the size and shape of nanoparticle of an electrochemical sensor, which involves synthesizing metal nanoparticles separately, followed by their immobilization. Colloidal synthesis [78, 79], an empirical method, for example, offers excellent shape and size control of nanoparticles, which follows straightforward principle and requires simple equipment. An alternative method to fabricate nanoparticle is called “cathodic corrosion”, which is a novel electrochemical method [80, 81]. This method is achieved at very negative potential of about -5 or -10 V to the metal in an aqueous electrolyte containing a strong nonreducible

cation. According to the adjustment of several parameters, such as the electrolyte concentration, the electrical current and the voltage, the size and the shape of nanoparticles can be controlled. However, a challenge in the third approach is how to satisfactorily immobilize those nanoparticles on the supporting electrode and avoid interference with the nanoparticle reactivity. The most straightforward method is drop-casting, but may lead to inhomogeneous deposition with severe particle aggregation [82, 83]. The other way to tether nanoparticles is to functionalize the support electrode to obtain specific anchoring sites, through diazonium grafting, or a self-assembled monolayer (SAM) [84]. In addition, depositing a charged polymer (polyelectrolyte) on the support electrode with a charge opposite to that of the nanoparticles [85] is also a good way to tether nanoparticles.

The shape, size as well as the total surface area of nanoparticles coated on a supporting electrode can be determined either through an electrochemical or non-electrochemical method. CV is a very powerful way to determine both the exposed surface area and the dominant surface structure of the materials [86]. Recently, analysis of shape and structure of nanoparticles by electrochemical method has been extensively developed. Site-specific irreversible adsorption of adatoms can be achieved to identify the ratio of different species on shape-selected nanoparticles, and reveal quantitatively the amount of adsorption through the stripping after adsorption. The surface structure can be sensitively determined by the voltammetric signature for monolayer formation or monolayer “stripping” [87]. Thus, this technique can be applied to nanoparticulate electrodes, where an average nanoparticle shape can be determined by the relative number of surface facets. Moreover, electrochemical method can be applied to

## Chapter 1. Introduction

characterize the surface domains on nanoparticles detail by measuring the hydrogen adsorption and desorption region, as well as the oxidation of CO on the nanoparticles surface [87].

The size and/or shape of nanoparticles, on the other hand, can be determined through other non-electrochemical method, such as atomic force microscopy (AFM) [88], X-ray diffraction (XRD) [89], dynamic light scattering (DLS) [90], NP-tracking analysis (NTA) [91], scanning electron microscopy (SEM) [92] and transmission electron microscopy (TEM) [89].

As one of the most important chemical application of metal-nanoparticles, electrocatalysis has been extensively discussed lately. In 1990s, Chiou [94] and co-workers have deposited nano-gold particles uniformly on the carbon black supports, and developed this dispersed catalyst gas-diffusion electrode for SO<sub>2</sub> sensing. Because gold nanoparticles catalyze the electrochemical oxidation of SO<sub>2</sub>, the current is proportional to the concentration of SO<sub>2</sub> when the reaction controlling step is the diffusion of SO<sub>2</sub>. Additionally, this SO<sub>2</sub> sensor showed excellent stability, reproducibility, sensitivity and the response time was fast. In the same year, Casella [95] et al. introduced the second method that was mentioned above (i.e. immobilization of metal ions followed by reduction) to synthesize gold nanoparticles dispersed on the electrode surface. They also achieved an amperometric sensor for glucose sensing, based on a bimetallic electrode composed of copper nanoparticles dispersed onto a gold surface [96]. Constant-potential amperometric detection (DC) and in pulsed-potential amperometric detection (PAD) have been assessed for the stability, background current, sensitivity and linear range of the modified electrode. Natan and collaborators demonstrated that it was important of

nanometer-scale morphology in protein voltammetry, and proposed that well-defined Au colloid-based substrates hold promise as substrates for biological measurements at metal surfaces [97].

In 2000s, many researchers focused on the gold nano particles modified ITO electrode, which can be developed in electroanalysis as protein-based biosensors and sensitively determining guanosine and epinephrine. Also, Cui et al. displayed that seed-mediated growth of gold nanoparticles on glassy carbon (GC) surfaces was developed to electrochemically determine nitrite in a real wastewater sample, showing excellent stability and anti-interference ability [98]. Recently, metallic nanoparticles with organic shell encapsulation obtained attentions because of the potential technological application in many field. The core-shell structure gold nanoparticles have been demonstrated for the first time by Zheng et al., which can be utilized to construct network architectures that impart biomimetic ion-gating properties. According to the noncovalent head-to-head hydrogen-bonding linkages at the carboxylic shells, the nanoconstruction is formed and can be effectively tuned by pH between a neutral “close” and an ionic “open” or “close” state to exhibit electrochemical ion-gating properties [99].

## **1.4 Polymer-based Electrochemical Sensors**

### **1.4.1 Historical Development**

The word ‘polymer’ was derived from two classical Greek words ‘poly’ and ‘meres’, which mean ‘many’ and ‘parts’, respectively. The whole story began from 1862, since camphor was in fact discovered as an efficient plasticizer for cellulose nitrate by Alexander Parkes. However, the independent discovery of celluloid by John Wesley



Hyatt, which was the first time to take out patents, was recognized as the beginnings of plastics industry. Whereas cellulose nitrate is still derived from a natural polymer—cellulose, the first truly man-made plastic was phenol-formaldehyde plastics, which was developed by Leo Hendrick Baekeland. Other polymers—cellulose acetate, urea-formaldehyde, poly (vinyl chloride), and nylon followed in the 1920s. Later, the polymeric products achieved commercial success after a better understanding of the character of polymer in the period between 1925 and 1950. In 1950s, professors Karl Ziegler and Giulio Natta dedicated to develop catalysts that enabled polymerization at room temperature and normal atmospheric pressure and exactly controlled the positioning of atoms attached to the polymer chains. They had polymerized ethylene and propylene catalytically, resulting eventually in the long-sought goal of a synthetic rubber that is molecularly identical with natural rubber. Due to their important contribution in the polymer science and technology, Ziegler and Natta were awarded the Nobel Prize in 1963. New materials including thermoplastic polyesters, high-barrier nitrile resins and so-called high-temperature plastics were introduced between 1960s and 1970s [100].

In the period 1970 to 2000, scientists focused on the methods to make highly oriented polymers, which have provided tremendous stimulus to both basic polymer science and industrial developments. There are three methods that were discovered to enhance the properties, i.e., hydrostatic extrusion, die-drawing and hot compaction of oriented fibres and tapes [100]. Nowadays, polymer has permeated every field of our life, such as clothes, computer, glasses, chairs, toothbrush and so forth. As discussed above there are two types of polymers, one class is natural polymers, consisting of wool, hair, rubber, etc., and another are synthetic polymers which include nylon, synthetic rubber,

polyester, Teflon. Though polymers have been with us for long time, their applications in electrochemical sensing have not been fully explored in comparison to other materials.

### 1.4.2 Conducting Polymer

When we talk about conductive materials, we usually think of metals, not of synthetic polymers, such as plastics. But in the 1970s, three scientists collaborating at the University of Pennsylvania— Alan G. MacDiarmid, Alan J. Heeger, and Hideki Shirakawa—developed special ‘polymers’ of oxidized iodine-doped polyacetylene[101]. Their work, which earned them the Nobel Prize in chemistry in 2000, has opened up possibilities for the development of a new class of materials known as conducting polymers. In traditional polymers, such as polyethylenes, the valence electrons are bound in  $sp^3$  hybridized covalent bonds, which lead to low mobility and insulation or semiconductivity. However, in conjugated materials, polymers have backbones of contiguous  $sp^2$  hybridize carbon centers, which have high mobility when the material is “doped” by oxidation [102].

Conductive polymers can be prepared by chemical and/or electrochemical methods. Most redox conductive polymers are prepared by oxidative coupling of monocyclic precursors, while electrochemical method synthesizes polymer film on a working electrode. Comparing these two methods, electrochemical polymerization is preferable due to the rapid process, low cost and environmentally benign, especially if the polymeric product is required for using as a polymer film electrode, thin-layer sensor, in microtechnology. In addition, conducting polymer can be reversibly doped and undoped

using electrochemical method accompanied by significant changes in conductivity [103]. However the chemical approach is recommended if large amounts of polymer are needed.

Due to the straightforward preparation procedure, unique properties, and stability in air, conducting polymers have been developed as significant candidates for electrochemical sensors and biosensors [104, 105]. Most of the applications of conducting polymers as sensors include gas and vaporous sensors, pH sensor, ion selective electrodes, glucose sensor and so forth. For example, numerous publications have studied that polypyrrole could be applied as weak acid vaporous sensors such as  $\text{H}_2\text{S}$  and  $\text{CH}_3\text{COOH}$  due to the proton transfer [106]. Bulhoes and Faria have reported poly (1-aminoanthracene) film that was electropolymerized on platinum electrode could be used as a pH sensor [107]. The polymer electrode showed an apparent Nernstian response in the 1-12 pH range, with a slope of 52.5 mV/decade and no interference of alkaline ions was observed. Sommerdijk et al. have developed poly (3,4-ethylenedioxythiophene) used as the conducting component for amperometric glucose sensor, which demonstrated superior electrochemical stability [108].

### 1.4.3 Polyaniline

Among conducting polymers, polyaniline (PANI) has attracted interest due to its high specific capacitance, inexpensive monomer, good environmental stability, electroactivity and doping-dedoping chemistry. According to its multiple redox states, PANI can be controlled to reversibly change the oxidation state of their main chain by protonation of the imine nitrogen atoms. The literature dealing with the synthesis of PANI by different methods is sufficient but the comparison always between the chemical

and electrochemical polymerization. In terms of chemical polymerized method, polymeric stabilizers or variety of template can assemble and synthesize different morphologies of PANI, such as spherical shapes [109], needle-like shapes [110], nanowires [111, 112], nanotubes [113, 114], hollow microspheres [114] and so forth. (Figure 1.2)

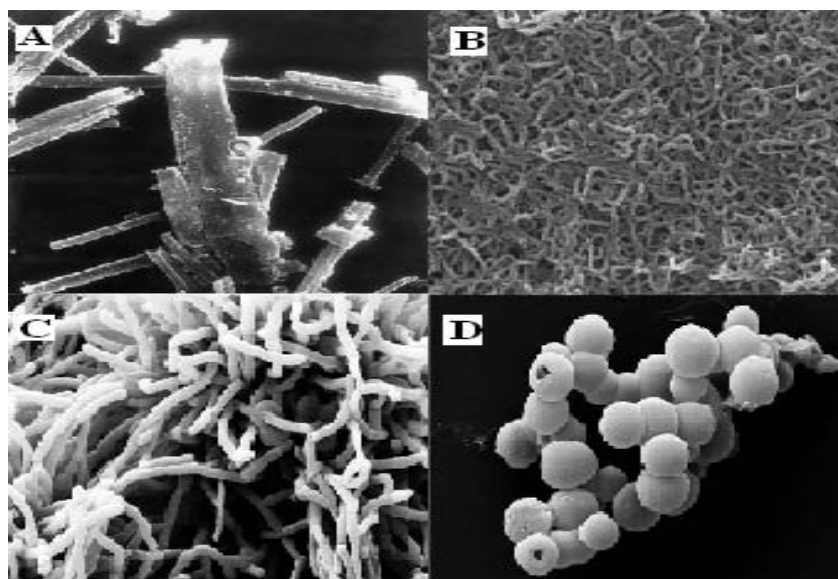


Figure 1.2 SEM images of different morphologies of PANI: (A) Needle-like shapes Ref [110] (B) Nanowires Ref [112] (C) Nanotubes Ref [114] (D) Hollow Microsphere Ref [114]

Manohar et al. have introduced an extremely simple “nanofiber seeding” method to chemically synthesize bulk quantities of PANI nanofibers in one step without the need for large organic dopants, surfactants, and/or large amounts of insoluble templates [115]. However, comparing with chemical synthesis of PANI, the electrochemical polymerization seems the preferred approach, due to: 1. The polymer film can be easily prepared by the electrochemical deposition route, which can be directly used for electrochemical studies [116]. 2. Many control parameters can be easily adjusted in order

**Chapter 1. Introduction**

to obtain different redox states. 3. It gives cohesive films which have been reported to show a fairly smooth featureless topography by scanning electron microscopy (SEM) [117].

The wide range of associated electrical, electrochemical, and optical properties makes PANI potentially attractive for using as an electronic material in a variety of application, such as solar energy conversion, rechargeable batteries, supercapacitors [116] and pseudocapacitors. Also, PANI can be used as a glucose sensor. Wu and Yin have reported that a new type of amperometric glucose sensor used PANI-wrapped boron nitride nanotubes decorated with Pt nanoparticles as the electrode material [118]. Ramya and Sangaranarayanan have developed a PANI nanofiber dendrites modified electrode using electrochemical synthesis method with p-toluenesulfonic acid, which can be applied to detect glucose in the presence of interference species such as AA, UA, and DA [119].

Although PANI has obtained great progress as sensors, there are several limitations and challenges must be addressed in order to making further advancement. The first limitation of PANI is the loss of conductivity in neutral and high pH environment. It has very poor conductivity when the pH is greater than 5, due to that PANI requires a large amount of protons attached to the polymer to be electrically conducting. Secondly, the conductivity of PANI is known to possess hysteresis, which can be observed in CV curves that the current response to the potential sweep in the positive direction is different from that to the reverse sweep of the potential. Last but not the least, the PANI based electrochemical sensors always have relatively slow response

time. Obviously, these concerns must be addressed in the near future before any realistic commercial development can be made.

In my thesis, electrochemical synthesis and applications of PANI and its derivatives will be discussed hereinafter.

## References

- [1] Ahammad, A.J.S.; Lee, J.; Rahman, M. A. Electrochemical Sensors Based on Carbon Nanotubes. *Sensors-basel* **2009**, 9, 2289-2319.
- [2] Power, A. C.; Morrin, A. Electroanalytical Sensor Technology, In *Electrochemistry*; Khalid, M., Ed.; Intech: Croatia, **2013**;141-178.
- [3] Tamaddon, A.; Amiri, R.; Hazini, F. Novel Lu<sup>3+</sup> Carbon Paste Electrode Based on Functionalized Multiwalled Carbon Nanotubes. *Electroanal.* **2014**, 26, 612-617.
- [4] Hu, X.; Li, J.; Wang, J. Structural Transformation of Carbon Electrodes for Simultaneous Determination of Dihydroxybenzene Isomers. *Electrochem Commun.* **2012**, 21, 73-76.
- [5] Wu, L.; Xiong, E.; Zhang, X.; Zhang, X. H.; Chen, J. H. Nanomaterials as Signal amplification elements in DNA-Based Electrochemical Sensing. *Nano Today* **2014**, <http://dx.doi.org/10.1016/j.nantod.2014.04.002>.
- [6] Vijayakumar, M.; Priya, K.; Nancy, F. T.; Noorlidah, A.; Ahemd, A. B. A. Biosynthesis, Characterisation and Anti-Bacterial Effect of Plant-Mediated Silver Nanoparticles Using Artemisia Nilagirica. *Ind Crop Prod.* **2013**, 41, 235-240.

- [7] Carbon Nanotubes: *A New Alternative For Electrochemical Sensors*; Rivas, G. A., Rubianes, M. D., Pedano, M. L., Ferreyra, N. F., Luque, G., Miscoria, S. A., Eds.; Nanotechnology Science and Technology Series: New York, **2009**.
- [8] Caglar, B. *Production of Carbon Nanotubes by PECVD and Their Applications to Supercapacitors*. <http://hdl.handle.net/2445/11122> (accessed Feb 10, **2010**)
- [9] Sathyanarayana, S., Hubner, C. *Thermoplastic Nanocomposites with Carbon Nanotubes*. Njuguna, J., Eds.; Structural Nanocomposites, Engineering Materials; Springer-Verlag, Berlin Heidelberg, **2013**.
- [10] Bandaru, P. R. Electrical Properties and Applications of Carbon Nanotube Structures. *J. Nanosci. Nanotechno.* **2007**, 7, 1-29.
- [11] Merkoci, A.; Pumera, M.; Llopis, X.; Perez, B.; Valle, M.; Alegret, S. New Materials for Electrochemical Sensing VI: Carbon Nanotubes. *Trends in Analytical Chemistry*, **2005**, 24, 826-838.
- [12] Jacobs, C. B.; Peairs, M. J.; Venton, B. J. Review: Carbon Nanotube Based Electrochemical Sensors for Biomolecules. *Anal. Chim Acta.* **2010**, 662, 105-127.
- [13] Iijima, S.; Ichihashi, T. Single-Shell Carbon Nanotubes of 1-Nm Diameter. *Nature* **1993**, 363, 603-605.
- [14] Bethune, D. S.; Kiang, C. H.; De Vries, M. S.; Gorman, G.; Savoy, R.; Vazquez, J.; Beyers, R. Cobalt-Catalysed Growth of Carbon Nanotubes with Single-Atomic-Layer Walls. *Nature* **1993**, 363, 605-607.

- [15] Scott, C. D.; Arepalli, S.; Nikolaev, P.; Smalley, R. E. Growth Mechanisms for Single-Wall Carbon nanotubes in a laser-ablation process. *Appl. Phys. A* **2001**, *72*, 573-580.
- [16] Poretzky, A. A.; Geohegan, D. B.; Fan, X.; Pennycook, S. J. Dynamics of Single-Wall Carbon Nanotube Synthesis by Laser Vaporization. *Appl. Phys. A* **2000**, *70*, 153-160.
- [17] Yacaman, M. J.; Yoshida, M. M.; Rendon, L.; Santiesteban, J. G. Catalytic Growth of Carbon Microtubules with Fullerene Structure. *Appl. Phys. Lett.* **1993**, *62*, 202-204.
- [18] Rafique, M. M. A.; Iqbal, J. Production of Carbon Nanotubes by Different Routes- A Review. *Journal of Encapsulation and Adsorption Science*, **2011**, *1*, 29-34.
- [19] Marinkovic, S. N. Carbon nanotubes. *J. Serb. Chem. Soc.* **2008**, *73*, 891-913.
- [20] Dadrasnia, E.; Puthukodan, S.; Lamela, H. Terahertz Electrical Conductivity and Optical Characterization of Composite Nonaligned Single- and Multiwalled Carbon Nanotubes. *J. Nanophoton.* **2014**, *8*, 083099.
- [21] Tahhan, M. Carbon Nanotubes and Conducting Polymer Composites. Ph. D Dissertation, University of Wollongong, **2004**.
- [22] Varghese, S. H.; Yoshida, Y.; Maekawa, T.; Sakthikumar, D. Enhancement of Glucose Sensing Behavior of Cobalt Tetraphenylporphyrin Thin Film Using Single-Wall Carbon Nanotubes. *Sensor. Mater.* **2011**, *23*, 335-345.



[23] Jiang, K.; Schadler, L. S.; Siegel, R. W.; Zhang, X.; Zhang, H.; Terrones, M. Protein Immobilization on Carbon Nanotubes via a Two-step process of Diimide-Activated Amidation. *J. Mater. Chem.* **2004**, 14, 37-39.

[24] Gao, Y.; Kyratzis, I. Covalent Immobilization of Proteins on Carbon Nanotubes Using the Cross-linker 1-ethyl-3-(3-dimethylaminopropyl)carbodiimide-a Critical Assessment. *Bioconjug. Chem.* **2008**, 19, 1945-1950.

[25] Balasubramanian, K.; Burghard, M. Chemically Functionalized Carbon Nanotubes. *Small* **2005**, 1, 180-192.

[26] Liu, Z.; Jiao, L.; Yao, Y.; Xian, X.; Zhang, J. Aligned, Ultralong Single-Walled Carbon Nanotubes: From Synthesis, Sorting, to Electronic Devices. *Adv. Mater.* **2010**, 22, 1-26.

[27] Gooding, J. J.; Chou, A.; Liu, J.; Losic, D.; Shapter, J. G.; Hibbert, D. B. The Effect of the Lengths and Orientations of Single-Walled Carbon Nanotubes on the Electrochemistry of Nanotube-Modified Electrodes. *Electrochem. Commun.* **2007**, 9, 1677-1683.

[28] Shah, B.; Lafleur, T.; Chen, A. Carbon Nanotube Based Electrochemical Sensor for the Sensitive Detection of Valacyclovir, *Faraday Discuss.* **2013**, 164, 135-146.

[29] Mazloun-Ardakani, M.; Naser-Sadrabadi, A.; Sheikh-Mohseni, M. A.; Benvidi, A.; Naeimi, H.; Karshenas, A. An Electrochemical Sensor Based on Carbon Nanotubes and A New Schiff Base for Selective Determination of Dopamine in the Presence of Uric Acid, Folic Acid, and Acetaminophen. *Ionics* **2013**, 19, 1663-1671.

- [30] Thomas, T.; Mascarenhas, R. J.; Martis, P.; Mekhalif, Z.; Swamy, B. E. Multi-Walled Carbon Nanotube Modified Carbon Paste Electrode as An Electrochemical Sensor for the Determination of Epinephrine in the Presence of Ascorbic Acid and Uric Acid. *Mater. Sci. Eng. C Mater. Biol. Appl.* **2013**, 33, 3294-3302.
- [31] Zhai, X.; Wei, W.; Zeng, J.; Gong, S.; Yin, J. Layer-by-Layer Assembled Film Based on Chitosan/Carbon Nanotubes, and its Application to Electrocatalytic Oxidation of NADH. *Microchim. Acta* **2006**, 154, 315-320.
- [32] Wang, H.; Li, T.; Jia, W.; Xu, H. Highly Selective and Sensitive Determination of Dopamine Using A Nafion/ Carbon Nanotubes Coated poly (3-methylthiophene) Modified Electrode. *Biosens. Bioelectron.* **2006**, 22,664-669.
- [33] Zhong, Y.; Cai, Y.; Su, S. Determination of Dopamine in the presence of ascorbic Acid by Poly(Styrene Sulfonic Acid) Sodium Salt/Single-Wall Carbon Nanotube Film Modified Glassy Carbon Electrode. *Anal. Biochem.*, **2006**, 350,285-291.
- [34] Kang, X.; Mai, Z.; Zou, X.; Cai, P.; Mo, J. Electrochemical Biosensor Based on Multi-Walled Carbon Nanotubes and Au Nanoparticles Synthesized in Chitosan. *J. Nanosci. Nanotechnol.* **2007**, 7, 1618-1624.
- [35] Thostenson, E. T.; Ren, Z.; Chou, T. Advances in the Science and Technology of Carbon Nanotubes and Their Composites: A Review. *Compos. Sci. Technol.* **2001**, 1899-1912.

- [36] Ma, P.; Siddiqui, N. A.; Marom, G.; Kim, J. Dispersion and Functionalization of Carbon Nanotubes for Polymer-Based Nanocomposites: A Review. *Composites: Part A* **2010**, 41, 1345-1367.
- [37] Cha, M.; Jung, S.; Cha, M.; Kim, G.; Ihm, J.; Lee, J. Reversible Metal-semiconductor Transition of ssDNA-Decorated Single-Walled Carbon Nanotubes. *Nano Lett.* **2009**, 9, 1345-1349.
- [38] Kumar, B.; Castro, M.; Feller, J. F. Quantum Resistive Vapour Sensors Made of Polymer Coated Carbon Nanotubes Random Networks For Biomarkers Detection. *Chemical Sensors*, **2013**, 3, 1-7.
- [39] Firme, C. P.; Bandaru, P. R. Toxicity Issues in the Application of Carbon Nanotubes to Biological Systems. *Nanomed-Nanotechnol.* **2010**, 6, 245-256.
- [40] Castro Neto, A. H.; Guinea, F.; Peres, N. M. R.; Novoselov, K. S.; Geim, A. K. The Electronic Properties of Graphene, *Rev. Mod. Phys.* **2009**, 81, 110-155.
- [41] Goyal, R. N.; Bishnoi, S. Surface Modification in Electroanalysis: Past, Present and Future. *Indian J Chem.* **2012**, 51A, 205-225.
- [42] Sun, C. Q.; Tay, B. K.; Zeng, X. T.; Li, S.; Chen, T. P.; Zhou, J.; Bai, H. L.; Jiang, E. Y. Bond-Order-Bond-Length-Bond-Strength (bond-OLS) Correlation Mechanism for the Shape-and-Size Dependence of a Nanosolid. *J. Phys.: Condens. Matter* **2002**, 14, 7781-7795.

[43] Zanchet, D.; Tolentino, H.; Martins Alves, M. C.; Alves, O. L.; Ugarte, D. Inter-Atomic Distance Contraction in Thiol-Passivated Gold Nanoparticles. *Chem. Phys. Lett.* **2000**, 323, 167-172.

[44] Link, S.; El-Sayed, M. A. Size and Temperature Dependence of the Plasmon Absorption of Colloidal Gold Nanoparticles, *J. Phys. Chem. B* **1999**, 103, 4212-4217.

[45] Fu, H.; Yao, Y. Size Effects on the Optical Properties of Organic Nanoparticles. *J. Am. Chem. Soc.*, **2001**, 123, 1434-1439.

[46] Zhang, B.; Fan, L.; Zhong, H.; Liu, Y.; Chen, S. Graphene Nanoelectrodes: Fabrication and Size-Dependent Electrochemistry. *J. Am. Chem. Soc.* **2013**, 135, 10073-10080.

[47] Watkins, J. J.; White, H. S. The Role of the Electrical Double Layer and Ion Pairing on the Electrochemical Oxidation of Hexachloroiridate(III) at Pt Electrodes of Nanometer Dimensions. *Langmuir*, **2004**, 20, 5474-5483.

[48] Smith, C. P.; White, H. S. Theory of the Voltammetric Response of Electrodes of Submicron Dimensions. Violation of Electroneutrality in the Presence of Excess Supporting Electrolyte. *Anal. Chem.* **1993**, 65, 3343-3353.

[49] He, R.; Chen, S.; Yang, F.; Liang, B. Dynamic Diffuse Double-Layer Model for the Electrochemistry of Nanometer-Sized Electrodes. *J. Phys. Chem. B* **2006**, 110, 3262-3270.

[50] Belding, S. R.; Campbell, F. W.; Dickinson, E. J. F.; Compton, R. G. Nanoparticle-Modified Electrodes, *Phys. Chem. Chem. Phys.* **2010**, 12, 11208-11221.

[51] Hernandez-Santos, D.; Gonzalez-Garcia, M. B.; Garcia, A. C. Metal-Nanoparticles Based Electroanalysis. *Electroanal.* **2002**, 14, 1225-1235.

[52] Kleijn, S. E. F.; Lai, S. C. S.; Koper, M. T. M.; Unwin, P. R. Electrochemistry of Nanoparticles. *Angew, Chem. Int. Ed.* **2014**, 53, 3558-3586.

[53] Yang, H.; Kumar, S.; Zou, S. Electroreduction of O<sub>2</sub> on Uniform Arrays of Pt Nanoparticles. *J. Electroanal. Chem.* **2012**, 688, 180-188.

[54] Wertheim, G. K. *Small Particles and Inorganic Clusters*; Chapon, C., Gillet, M., Henry, C., Eds.; Springer, Berlin/Heidelberg, **1989**, 319-326.

[55] Proch, S.; Wirth, M.; White, H. S.; Anderson, S. L. Strong Effects of Cluster Size and Air Exposure on Oxygen Reduction and Carbon Oxidation Electrocatalysis by Size-Selected Pt<sub>n</sub> (n<11) on Glassy Carbon Electrodes. *J. Am. Chem. Soc.* **2013**, 135, 3073-3086.

[56] Hayden, B. E.; Pletcher, D.; Suchsland, J. P. Enhanced Activity for Electrocatalytic Oxidation of Carbon Monoxide on Titania-Supported Gold Nanoparticles. *Angew. Chem.* **2007**, 119, 3600-3602.

[57] McCreery, R. L. Advanced Carbon Electrode Materials for Molecular Electrochemistry. *Chem. Rev.* **2008**, 108, 2646-2687.

- [58] Salazar-Banda, G. R.; Eguiluz, K. I. B.; Avaca, L. A. Boron-Doped Diamond Powder as Catalyst Support for Fuel Cell Applications. *Electrochem Commun.* **2007**, *9*, 59-64.
- [59] Vidal-Iglesias, F. J.; Solla-Gullon, J.; Rodriguez, P.; Herrero, E.; Montiel, V.; Feliu, J. M.; Aldaz, A. Shape-Dependent Electrocatalysis: Ammonia Oxidation on Platinum Nanoparticles with Preferential (100) Surface. *Electrochem Commun.* **2004**, *6*, 1080-1084.
- [60] Solla-Gullon, J.; Rodriguez, P.; Herrero, E.; Aldaz, A.; Feliu, J. M. Surface Characterization of Platinum Electrode. *Phys. Chem. Chem. Phys.* **2008**, *10*, 1359-1373.
- [61] Hayden, B. E.; Pletcher, D.; Suchsland, J. P.; Williams, L. J. The Influence of Support and Particle Size on the Platinum Catalysed Oxygen Reduction Reaction. *Phys. Chem. Chem. Phys.* **2009**, *11*, 9141-9148.
- [62] Sandmann, G.; Dietz, H.; Plieth, W. Preparation of Silver Nanoparticles on ITO Surfaces by a Double-Pulse Method. *J. Electroanal. Chem.* **2000**, *491*, 78-86.
- [63] Minami, T. Transparent Conducting Oxide Semiconductors for Transparent Electrodes. *Semicond. Sci. Technol.* **2005**, *20*, S35-S44.
- [64] Penner, R. M. Mesoscopic Metal Particles and Wires by Electrodeposition. *J. Phys. Chem. B.* **2002**, *106*, 3339-3353.
- [65] Bayati, M.; Abad, J. M.; Nichols, R. J.; Schiffrin, D. J. Substrate Structural Effects on the Synthesis and Electrochemical Properties of Platinum Nanoparticles on Highly Oriented Pyrolytic Graphite. *J. Phys. Chem. C.* **2010**, *114*, 18439-18448.

[66] Patten, H. V.; Ventosa, E.; Colina, A.; Ruiz, V.; Lopez-Palacios, J.; Wain, A. J.; Lai, S. C. S.; Macpherson, J. V.; Unwin, P. R. Influence of Ultrathin Poly-(3,4-Ethylenedioxythiophene) (PEDOT) Film Supports on the Electrodeposition and Electrocatalytic Activity of Discrete. *J. Solid State Electrochem.* **2011**, 15, 2331-2339.

[67] Giacomini, M. T.; Ticianelli, E. A.; McBreen, J.; Balasubramanian, M. Oxygen Reduction on Supported Platinum/Polythiophene Electrocatalysts. *J. Electrochem. Soc.* **2001**, 148, A323-S329.

[68] Scharifker, B.; Hills, G. Theoretical and Experimental Studies of Multiple Nucleation. *Electrochim. Acta* **1983**, 28, 879-889.

[69] Garcia-Pastoriza, E.; Mostany, J.; Scharifker, B. R. Spatial Distribution of Nuclei Inhibition of Local Nucleation Rates by the Most Influential Neighbours. *J. Electroanal. Chem.* **1998**, 441, 13-18.

[70] Dudin, P. V.; Unwin, P. R.; Macpherson, J. V. Electrochemical Nucleation and Growth of Gold Nanoparticles on Single-Walled Carbon Nanotubes: New Mechanistic Insights. *J. Phys. Chem. C* **2010**, 114, 13241-13248.

[71] Zach, M. P.; Penner, R. M. Nanocrystalline Nickel Nanoparticles. *Adv. Mater.* **2000**, 12, 878-883.

[72] Lai, A. C. S.; Dudin, P. V.; Macpherson, J. V.; Unwin, P. R. Visualizing Zeptomole (Electro) Catalysis at Single Nanoparticles within an Ensemble. *J. Am. Chem. Soc.* **2011**, 133, 10744-10747.

[73] Dai, J.; Bruening, M. L. Catalytic Nanoparticles Formed by Reduction of Metal Ions in Multilayered Polyelectrolyte Films. *Nano Lett.* **2002**, 497-501.

[74] Joly, S.; Kane, R.; Radzilowski, L.; Wang, T.; Wu, A.; Cohen, R. E.; Thomas, E. L.; Rubner, M. F. Multilayer Nanoreactors for Metallic and Semiconducting Particles. *Langmuir* **2000**, 16, 1354-1359.

[75] Bayati, M.; Abad, J. M.; Bridges, C. A.; Rosseinsky, M. J.; Schiffrin, D. J. Size Control and Electrocatalytic Properties of Chemically Synthesized Platinum Nanoparticles Grown on Functionalised HOPG. *J. Electroanal. Chem.* **2008**, 623, 19-28.

[76] Waje, M. M.; Wang, X.; Li, W.; Yan, Y. Deposition of Platinum Nanoparticles on Organic Functionalized Carbon Nanotubes Grown *In Situ* on Carbon Paper for Fuel Cells. *Nanotechnology* **2005**, 16, S395-400.

[77] Guo, D.; Li, H. Electrochemical Synthesis of Pd Nanoparticles on Functional MWNT Surface. *Electrochem. Commun.* **2004**, 6, 999-1003.

[78] Niu, Y.; Crooks, R. M. Dendrimer-Encapsulated Metal Nanoparticles and their Applications to Catalysis. *C. R. Chim.* **2003**, 6, 1049-1059.

[79] Grohn, F.; Bauer, B. J.; Akpalu, Y. A.; Jackson, C. L.; Amis, E. J. Dendrimer Templates for the Formation of Gold Nanoclusters. *Macromolecules* **2000**, 33, 6042-6050.



[80] Yanson, A.; Rodriguez, P.; Garcia-Araez, N.; Mom, R. V.; Tichelaar, F. D.; Koper, M. T. M. Cathodic Corrosion: A Quick, Clean, and Versatile Method for the Synthesis of Metallic Nanoparticles. *Angew, Chem. Int. Ed.* **2011**, 50, 6346-6350.

[81] Rodriguez, P.; Tichelaar, F. D.; Koper, M. T. M.; Yanson, A. I. Cathodic Corrosion as a Facile and Effective Method to Prepare Clean Metal Alloy Nanoparticles. *J. Am. Chem. Soc.* **2011**, 133, 17626-17629.

[82] Deegan, R. D.; Bakajin, O.; Dupont, T. F.; Huber, G.; Nagel, S. R.; Witten, T. A. Capillary Flow as the Cause of Ring Stains from Dried Liquid Drops. *Nature.* **1997**, 389, 827-829.

[83] Nguyen, T. A. H.; Hampton, M. A.; Nguyen, A. V. Evaporation of Nanoparticle Droplets on Smooth Hydrophobic Surfaces: The Inner Coffee Ring Deposits. *J. Phys. Chem. C.* **2013**, 117, 4707-4716.

[84] Freeman, R. G.; Grabar, K.C.; Allison, K. J.; Bright, R. M.; Davis, J. A.; Guthrie, A. P.; Hommer, M. B.; Jackson, M. A.; Smith, P. C.; Walter, D. G.; Natan, M. J. Self-Assembled Metal Colloid Monolayers: An Approach to SERS Substrates. *Science* **1995**, 267, 1629-1632.

[85] Tang, Y.; Cheng, W. Nanoparticle-Modified Electrode with Size- and Shape-Dependent Electrocatalytic Activities. *Langmuir* **2013**, 29, 3125-3132.

[86] Trasatti, S.; Petrii, O. A. Real Surface Area Measurements in Electrochemistry. *Pure Appl. Chem.* **1991**, 63, 711-734.

[87] Vidal-Iglesias, F. J.; Aran-Ais, R. M.; Solla-Gullon, J.; Herrero, E.; Feliu, J. M. Electrochemical Characterization of Shape-Controlled Pt Nanoparticles in Different Supporting Electrolytes. *ACS Catal.* **2012**, *2*, 901-910.

[88] Klapetek, P.; Valtr, M.; Necas, D.; Salyk, O.; Dzik, P. Atomic Force Microscopy Analysis of Nanoparticles in Non-ideal Conditions. *Nanoscale Res. Lett.* **2011**, *6*, 514-523.

[89] Borchert, H.; Shevchenko, E. V.; Robert, A.; Mekis, I.; Kornowski, A.; Grubel, G.; Weller, H. Determination of Nanocrystal Sizes: A Comparison of TEM, SAXS, and XRD Studies of Highly Monodisperse CoPt<sub>3</sub> Particles. *Langmuir*, **2005**, *21*, 1931-1936.

[90] Liu, X.; Dai, Q.; Austin, L.; Coutts, J.; Knowles, G.; Zou, J.; Chen, H.; Huo, Q. A One-Step Homogeneous Immunoassay for Cancer Biomarker Detection Using Gold Nanoparticle Probes Coupled with Dynamic Light Scattering. *J. Am. Chem. Soc.* **2008**, *130*, 2780-2782.

[91] Filipe, V.; Hawe, A.; Jiskoot, W. Critical Evaluation of Nanoparticle Tracking Analysis (NTA) by NanoSight for the Measurement of Nanoparticles and Protein Aggregates. *Pharm. Res.* **2010**, *27*, 796-810.

[92] Qu, L.; Dai, L.; Osawa, E. Shapes/Size-Controlled Syntheses of Metal nanoparticles for Site-Selective Modification of Carbon Nanotubes. *J. Am. Chem. Soc.* **2006**, *128*, 5523-5532.

[94] Chiou, C. Y.; Chou, T. C. Amperometric Sulfur Dioxide Sensors Using the Gold Deposited Gas Diffusion Electrode. *Electroanal.* **1996**, *8*, 1179-1182.

[95] Casella, I. G.; Destradis, A.; Desimoni, E.; Colloidal Gold Supported onto Glassy Carbon Substrates as an Amperometric Sensor for Carbohydrates in Flow Injection and Liquid Chromatography. *Analyst* **1996**, 121, 249-254.

[96] Casella, I. G.; Gatta, M.; Guascito, M. R.; Cataldi, T. R. I. Anal. Highly-Dispersed Copper Microparticles on the Active Gold Substrate as an Amperometric Sensor for Glucose. *Chim. Acta* **1997**, 357, 63-71.

[97] Brown, K. R.; Fox, A. P.; Natan, M. J. Morphology-Dependent Electrochemistry of Cytochrome c at Au Colloid Modified SnO<sub>2</sub> Electrodes. *J. Am. Chem. Soc.* **1996**, 118, 1154-1157.

[98] Cui, Y.; Yang, C.; Zeng, W.; Oyama, M.; Pu, W.; Zhang, J. Electrochemical Determination of Nitrite Using a Gold Nanoparticles-Modified Glassy Carbon Electrode Prepared by the Seed-Mediated Growth Technique. *Anal. Sci.* **2007**, 23, 1421-1425.

[99] Zheng, W.; Maye, M. M.; Leibowitz, F. L.; Zhong, C. Imparting Biomimetic Ion-Gating Recognition Properties to Electrodes with a Hydrogen-Bonding Structured Core-Shell Nanoparticle Network. *Anal. Chem.* **2000**, 72, 2190-2199.

[100] Ebewele, R. O. Polymer Science and Technology. CRC Press: Boca Raton, New York, **2000**.

[101] Shirakawa, H.; Louis, E.J.; MacDiarmid, A.G.; Chiang, C.K.; Heeger, A.J. Synthesis of electrically conducting organic polymers: Halogen derivatives of polyacetylene, (CH)<sub>x</sub>. *J. Chem. Soc. Chem. Commun.* **1977**, 1977, 578-580.

[102] Park, S.-M. *Electrochemistry of  $\pi$ -Conjugated Polymers*. In: *Handbook of Organic Conductive Molecules and Polymers*, Nalwa, H. S., Ed., Chichester, Wiley, **1997**, 3, 429-469.

[103] Lee, J.; Park, D.; Shim, Y. Electrochemical Characterization of Poly(1,8-diaminonaphthalene): A Functionalized Polymer. *J. Electrochem. Soc.* **1992**, 139, 3507-3514.

[104] Lange, U.; Roznyatovskaya, N. V.; Mirsky, V. M. Conducting Polymers in Chemical Sensors and Arrays. *Anal. Chim. Acta* **2008**, 614, 1-26.

[105] Hoa, D. T.; Suresh Kumar, T. N.; Puneekar, N. S.; Srinivasa, R. S.; Lal, R.; Contractor, A. Q. A Biosensor Based on Conducting Polymers. *Anal. Chem.* **1992**, 64, 2645-2646.

[106] Krivan, E.; Visy, C.; Dobay, R.; Harsanyi, G.; Berkesi, O. Irregular Response of the Polypyrrole Films to H<sub>2</sub>S. *Electroanal.* **2000**, 12, 1195-1200.

[107] Faria, R. C.; Bulhoes, L. O. S. Hydrogen Ion Selective Electrode Based on Poly(1-aminoanthracene) Film. *Anal. Chim. Acta* **1998**, 377, 21-27.

[108] Kros, A.; Van Hovell, S. W. F. M. Poly(3,4-ethylenedioxythiophene)-Based Glucose Biosensors. *Adv. Mater.* **2001**, 13, 1555-1557.

[109] Landfester, K.; Montenegro, R.; Scherf, U.; Guntner, R.; Asawapirom, U.; Patil, S.; Neher, D.; Kietzke, T. Semiconducting Polymer Nanospheres in Aqueous Dispersion Prepared by a Miniemulsion Process. *Adv. Mater.* **2002**, 14, 651-655.

- [110] Jung, W.; Lee, Y. M.; Jo, N.; Lee, J. Control of Polyaniline Particle Shapes. *Macromol. Chem. Phys.* **2008**, 209, 1083-1093.
- [111] Huang, J.; Kaner, R. B. A General Chemical Route to Polyaniline Nanofibers. *J. Am. Chem. Soc.* **2004**, 126, 851-855.
- [112] Zhong, W.; Deng, J.; Yang, Y.; Yang, W. Synthesis of Large-Area Three-Dimensional Polyaniline Nanowire Networks Using a “Soft Template”. *Macromol. Rapid Commun.* **2005**, 26, 395-400.
- [113] Ruez, J.; Barjovanu, R.; Massey, J. A.; Winnik, M. A.; Manners, I. Self-Assembled Organometallic Block Copolymer Nanotubes. *Angew. Chem. Int. Ed.* **2000**, 39, 3862-3865.
- [114] Tavandashti, N. P.; Ghorbani, M.; Shojaei, A. The Morphology Transition Control of Polyaniline from Nanotubes to Nanospheres in a Soft Template Method. *Polym. Int.* **2014** [Accepted Article]
- [115] Zhang, X.; Goux, J.; Manohar, S. K. Synthesis of Polyaniline Nanofibers by “Nanofiber Seeding”. *J. Am. Chem. Soc.* **2004**, 126, 4502-4503.
- [116] Mondal, S. K.; Barai, K.; Munichandraiah, N. High Capacitance Properties of Polyaniline by Electrochemical Deposition on a Porous Carbon Substrate. *Electrochem. Acta* **2007**, 52, 3258-3264.
- [117] Huang, W.; Humphrey, B. D. Mac Diarmid, A. G. Polyaniline, a Novel Conducting Polymer. *J. Chem. Soc., Faraday Trans. 1*, **1986**, 82, 2385-2400.

[118] Wu, J.; Yin, L. Platinum Nanoparticle Modified Polyaniline-Functionalized Boron Nitride Nanotubes for Amperometric Glucose Enzyme Biosensor. *ACS Appl. Mater. Interfaces*, **2011**, 3, 4354-4362.

[119] Ramya, R.; Sangaranarayanan, Electrochemical Sensing of Glucose Using Polyaniline Nanofiber Dendrites-Amperometric and Impedimetric Analysis, *J. Appl. Polym. Sci.* **2013**, 129, 735-747.

## Chapter 2 Electrochemical Synthesis of Poly-(4-bromoaniline) for the recognition of Chiral Molecules

### 2.1 Introduction

The recognition of chiral molecules represents an important task in many areas [1-5]. For example, in the development of chiral drugs, normally only one enantiomer tends to be physiologically active while the other is inactive or even toxic. Recently, D-penicillamine (PA) has been used to treat rheumatoid arthritis and hepatitis [6,7], but in contrast L-PA could induce several adverse reactions such as neuritis and osteomyelitis [8]. A key step in sensing chiral molecules is to build a chiral surface that can identify the minute differences between the enantiomers [9-13]. A variety of methods such as coating, covalent bonding and self-assembly have been applied to prepare the chiral surface or directly utilize gold chiral surfaces [14-17].

To develop low cost and sensitive chiral sensors, conductive organic materials have recently been investigated as the promising candidates [18-28], where chiral polymers were synthesized in the presence of chiral substituents or chiral dopant anions [29]. When the chiral dopants were removed from the polymer, the remaining polymer matrix attained the capability of recognizing a single enantiomer. Chiral polyaniline (PANI), for example, has been prepared in 1994 by Havinga and co-workers through electropolymerization of aniline in the presence of enantiomeric HCSA ((+)- or (-)-camphorsulfonic acid) or by the acid doping of preformed emeraldine base [30]. Recently Kong and co-workers synthesized a molecularly imprinted PANI electrode column by reversibly doping/undoping chiral amino acids and applied such PANI electrode column

as a chiral sensor for enantioselective recognition of various amino acids [27]. They also employed poly(aniline-co-m-aminophenol) to create an electrode column for the recognition of glutamic acid enantiomers [28].

So far, the success of polymer based electrochemical chiral sensing has largely relied on the doping of probe chiral molecules during the fabrication process. The complicated fabrication procedure hinders their broad applications. To overcome the need of making probing chiral molecules and directly exploit the asymmetric structure of polymer chains in chiral sensing, in this work poly(4-bromoaniline) (PBA) was electrochemically synthesized on a gold electrode without the presence of any doping agents. As shown in the following, the as-prepared Au/PBA electrode exhibits very different behaviors in the electrochemical oxidation of L- and D-glutamic acids and L- and D-aspartic acids, in which not only their anodic peak currents are different, but also the oxidation waveforms are qualitatively different, providing an intuitive way to recognize these chiral amino acids.

## **2.2 Experimental**

Nitric acid (60-70%), D-glutamic acid (DGA) (>99%) and potassium ferricyanide (III) (99%) were purchased from Aldrich. Sodium hydroxide was purchased from Merck KGaA (Germany). L-glutamic acid (LGA) (>99%) and L-aspartic acid (LAA) (>99%) were purchased from Fluka A.G. Switzerland. 4-bromoaniline (>98%) was obtained from the British Drug Houses Ltd. DL-aspartic acid (DLAA) was purchased from J.T. Baker. Scanning electron microscopy (SEM) images and Energy-dispersive X-ray spectroscopy (EDX) were taken on a Quanta 200 FEG microscope (FEI, Inc.). All electrochemical



experiments were performed at room temperature ( $22 \pm 2^\circ\text{C}$ ) with a CHI660D electrochemical workstation (CHInstrument, USA).

A three-electrode system was employed, using a bare or PBA modified Au electrode (with a 2.0 mm diameter) as the working electrode, a Pt wire as the auxiliary electrode, and a saturated calomel electrode (SCE) as the reference electrode. Before the polymerization, the Au electrode was polished with 0.05  $\mu\text{M}$  alumina powder (CHInstrument), then cleaned by ultrasonic cleaner (Branson 1510, USA), and finally rinsed with double distilled water. The scan rate used in the cyclic voltammetry (CV) was 50 mV/s, unless otherwise stated in the context. Parameters used in the differential pulse voltammetry (DPV) measurements were 10 mV increment, 50 mV pulse amplitude, 200 ms pulse width and 500 ms pulse period. Electrochemical impedance spectroscopy (EIS) was measured at the formal redox potential of  $\text{Fe}(\text{CN})_6^{4-}/\text{Fe}(\text{CN})_6^{3-}$  (i.e., 0.262 V vs SCE) in the frequency range of 100 kHz to 0.1 Hz with an amplitude of 5 mV. There are 12 points per frequency decade. The electrolyte solution for the EIS measurements consisted of 5.0 mM  $\text{K}_3\text{Fe}(\text{CN})_6$  and 0.1 M NaCl.

### 2.3 Results and Discussion

Figure 2.1a presents CVs collected during the electrochemical polymerization of 4-bromoaniline on a Au electrode. The electrolyte solution consisted of 0.05 M 4-bromoaniline and 1.0 M  $\text{HNO}_3$ . For the first forward scan from -0.2 to 1.0 V, there was only one anodic peak at above 0.8V (vs SCE), which corresponded to the oxidation of 4-bromoaniline. On the reverse scan, a cathodic peak emerged at around 0.47 V, which arose from the reduction of the intermediates from 4-bromoaniline oxidation. Another

notable change is that after the first cycle a new anodic peak emerged at the potential of 0.5 V, presumably due to the products generated through the preceding reduction reactions. The amplitude of this anodic peak increased initially and then started decreasing after 5 cycles. Our following experiments indicate that if the electrochemical synthesis was stopped right after 5 cycles, the as-prepared PBA film would exhibit the best selectivity in the detection of glutamic acid chiral molecules. We have therefore used this turning point as a reference to fabricate PBA in this study. As shown in the following, Phenomenologically, the yellow Au electrode turned into orange color after 5 CV scans, indicating the formation of a polymer film. Electrochemical polymerization of 4-bromoaniline has been investigated earlier by Nagy and co-workers [31] and by Sari and Talu [32]. The suggested electropolymerization mechanisms include the polymerization at an ortho-position as well as at the para-position that is followed by the bromination of the aniline polymers. Our study suggests that the newly formed anodic peak at  $V = 0.5$  can provide a visible guidance to optimize PBA film for chiral sensing.

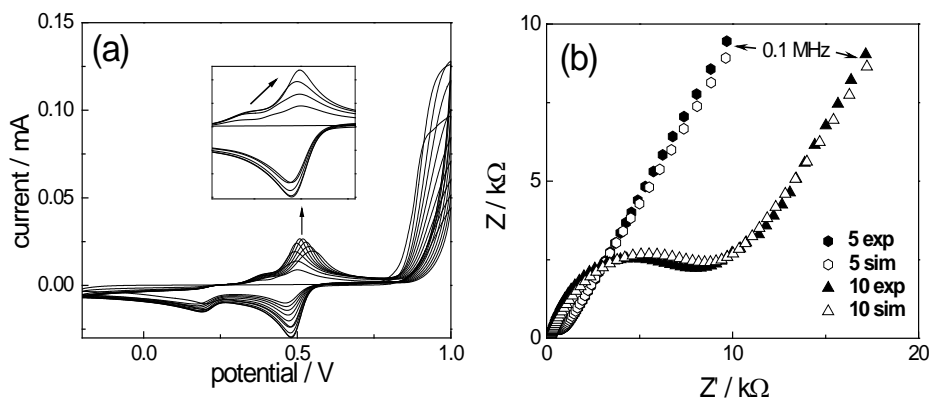


Figure 2.1 CVs of 4-bromoaniline (a), EIS of the PBA films (b), Electrolyte used in (b) consists of 5.0 mM  $K_3Fe(CN)_6$  and 0.1M NaCl, (5 and 10 means CV cycles for PBA film; sim means simulated EIS and exp means experimental EIS, in which 12 data points were recorded per frequency decade at 0.262 V).

Electrochemical properties of two PBA films fabricated respectively with 5 and 10 CV cycles were examined with EIS, using  $\text{Fe}(\text{CN})_6^{3-}/\text{Fe}(\text{CN})_6^{4-}$  as the redox marker. The EIS spectra shown in Figure 2.1b illustrate that the film prepared with 5 cycles has a much smaller charge transfer resistance ( $550 \Omega$  vs.  $9200 \Omega$  for 10 cycles), which is a desired property for electrochemical reactions. Simulated EIS was carried out in a modified Randles circuit by using constant phase element (CPE) instead of capacitance.

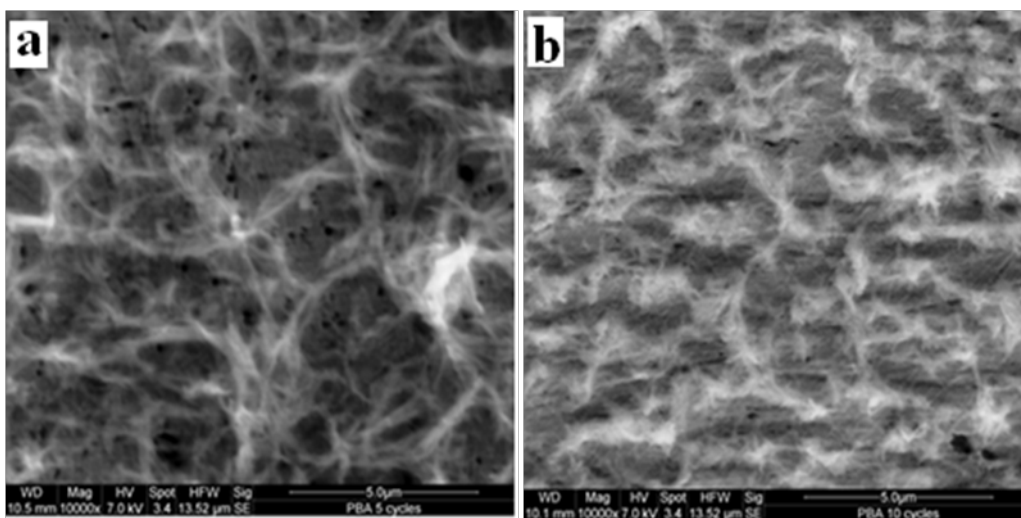


Figure 2.2 SEMs of the PBA films fabricated with 5 cycles (a) and 10 cycles (b).

Figure 2.2 presents SEM images of the PBA films on Au electrodes. Both films look like a porous matrix being made up of a large number of nanofibers. As the number of CV cycles was increased from 5 to 10, the film became a lot denser due to the continuous growth of the PBA polymer. This accounts for the observed increase of electrochemical impedance in Figure 2.1b. EDX data shows that the atomic ratio of Br/N for both films is a lot smaller than 1, as opposed to the 1/1 in its monomers, suggesting that some bromine have lost during the electropolymerization [32]. In other words, the above electrochemical synthesis of PBA in acidic solution is likely a combination of meta-

position and para-position polymerization, in which the meta-position polymerization is due to the para-position bromide inhibition. The para-position polymerization is accompanied with the bromine lost [32,33]. As the polymer grew denser and thicker, the Br/N ratio increased slightly.

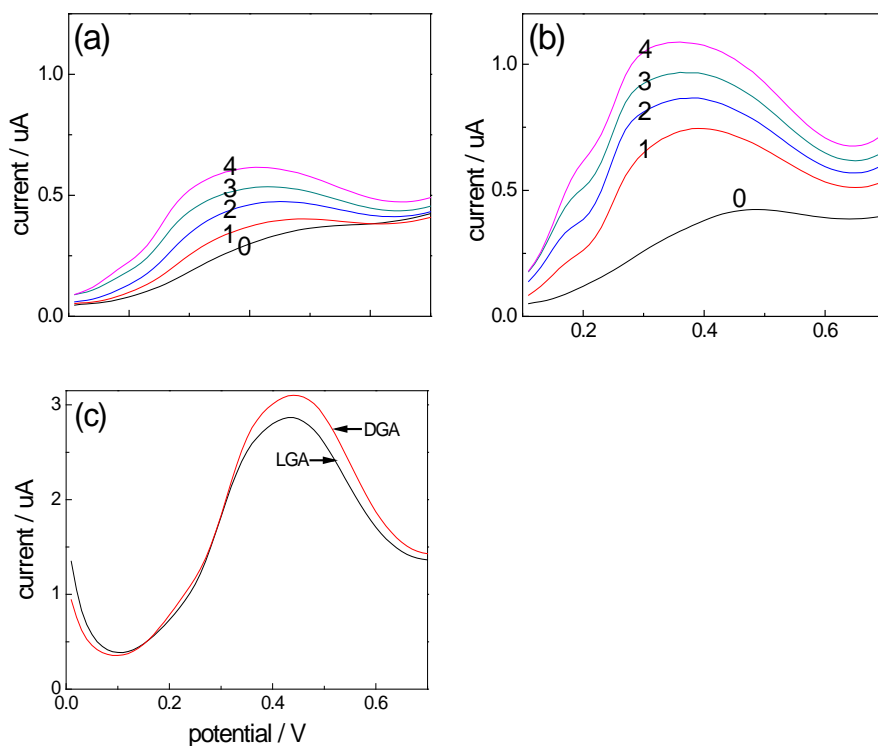


Figure 2.3 DPVs of DGA (a) and LGA (b) at the Au-PBA Au electrode, (c) DPVs of DGA and LGA at a bare Au electrode. The concentration of LGA and DGA in (c) is 15.0 mM.

The selectivity of the above prepared PBA films on the electrochemical oxidation of LGA and DGA was investigated with DPV in a 0.1 M NaOH solution. The Au-PBA film was prepared with 5 cycles. DPV spectra in Figure 2.3a illustrate that as the DGA concentration was increased from 0 (curve 0) to 5 mM (curve 1), 10 mM (curve 2), 15 mM (curve 3) and then 20 mM (curve 4), the amplitude of the anodic peak, centred around 0.4 V, increased accordingly. The corresponding anodic peaks of LGA in Figure

2.3b are greatly higher than that of DGA, indicating that the PBA film favors the oxidation of LGA over DGA. Such a conclusion is further supported by the negative shift of peak potential. Another more pronounced difference is that there is a shoulder at 0.2 V in the LGA spectrum, accompanying the sharp increase of the anodic current. This shoulder became more and more obvious as the LGA concentration was increased from 5 to 20 mM. Such a qualitative change in the DPV spectrum provides an intuitive way to recognize chiral glutamic acids. To demonstrate the essential role of PBA film in the above experiments, DPVs of the LGA and DGA at a bare Au electrode were presented in Figure 2.2c. Here, the only difference is their amplitude. It is interesting to point out that, as opposed to the Au-PBA electrode, here the oxidation peak of DGA is actually slightly higher than that of LGA. The peak current at the bare Au electrode is higher than that achieved at the Au-PBA electrode. Such a decrease is due to that the partial coverage of the Au surface by PBA film reduces the number of active sites.

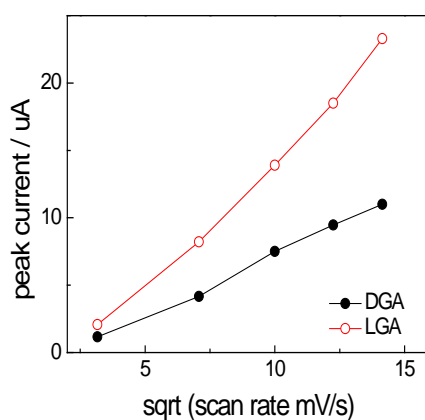


Figure 2.4 The relationship between the peak current and the scan rate in the cyclic voltammetry experiments. The concentration of LGA and DGA used in these experiments is 15.0 mM, The scan rate was adjusted between 5 and 200 mV/s.

In Figure 2.4 the peak current of glutamic acids at the Au-PBA electrode was examined as a function of scan rate, where the square root of the scan rate has a linear relationship with the peak current, suggesting that the electro-oxidation process is diffusion-controlled. The PBA film was fabricated with 5 CV cycles.

Figure 2.5 shows the electro-oxidation behavior of chiral aspartic acid at the Au-PBA electrode. As the concentration of LAA was increased from 0 to 30 mM in Figure 2.5a, the DPVs display only a smooth current peak with an increasing magnitude. The commercial L-/D- aspartic acid mixture, on the other hand, produced DPVs that have a broad shoulder at around 0.4 V, while the current density is much higher than that of equivalent amount of LAA. The qualitative change in the DPV spectra from Figure 2.5a to 2.5b, including the negative shift of the peak potential, is clearly due to the presence of DAA.

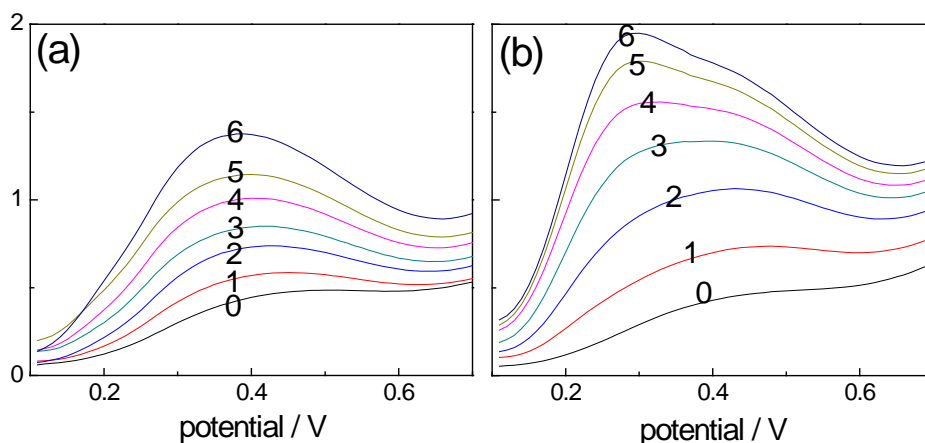


Figure 2.5 DPVs of (a) LAA and (b) DLAA at the Au-PBA electrode. The aspartic concentration was increased from 0 (curve 0) to 30.0 mM (curve 6) with an increment of 5.0 mM.

The electrochemical measurements in Figure 2.3 and 2.5 illustrate that L-aspartic acid and D-glutamic acid have similar electrochemical oxidation behavior at the PBA modified Au electrode. In terms of their molecular structures, due to the zigzag carbon chain and one -CH<sub>2</sub> group difference between the DGA and LAA molecules, DGA has indeed the same steric structure as LAA, in which planes of the two carboxyl groups are in opposite phase with one faces into the paper while the other faces outside the paper. The above analysis suggests that rapidly synthesized PBA film has attained the desired enantiomeric surface for recognizing chiral amino acids.

## 2.4 Conclusions

A facile method was established to fabricate optimized Au-PBA electrodes for electrochemically recognizing chiral amino acids. Notably, this approach does not require the doping of chiral molecules. To gain insights into the positive results achieved with PBA, we have repeated the above experiments with aniline and found that the polyaniline film electropolymerized on Au electrode could not produce similar results, which led us to suggest that the asymmetric structure of the PBA polymer chain is essential in the chiral sensing. Meanwhile, when glassy carbon electrodes were used as the substrate, no such distinguishable DPV responses could be obtained either, implicating that above enantioselective recognition arises from the synergistic interactions between gold and PBA film. This approach may be extended to conductive polymers from meta-/ortho-substituted monomers for developing new low cost chiral sensors.

## References

- [1] Stinson, S.C. Chiral pharmaceuticals. *Chemical & Engineering News* **2001**, 79, 45-57.
- [2] Trojanowicz, M.; Kaniewska, M. Electrochemical Chiral Sensors and Biosensors . *Electroanal.* **2009**, 21, 229-238.
- [3] Han, Q.; Chen, Q.; Wang, Y. H.; Zhou, J.; Fu, Y. Z. Enantioselective Recognition of Dopa Enantiomers in the Presence of Ascorbic Acid or Tyrosine. *Electroanal.* **2012**, 24, 332-337.
- [4] Wang, Y. H.; Zhou, J.; Han, Q.; Chen, Q.; Guo, L. J.; Fu, Y. Z. Chiral Recognition of Penicillamine Enantiomers Based on DNA-MWNT Complex Modified Electrode. *Electroanal.* **2012**, 24, 1561-1566.
- [5] Qin, H. X.; Liu, J. Y.; Chen, C. G.; Wang, J. H.; Wang, E. K. An Electrochemical Aptasensor for Chiral Peptide Detection using Layer-by-Layer Assembly of Polyelectrolyte-Methylene Blue/Polyelectrolyte-Graphene Multilayer. *Anal. Chim. Acta* **2012**, 712, 127-131.
- [6] Junker, P. D-Penicillamine in Rheumatoid Arthritis. *Ind. J. Pediatr.* **1986**, 53, 625-628.
- [7] Jacobs, J.W. G.; Van der Weide, F. R.; Kruijssen, M. W. M. Fatal Cholestatic Hepatitis Caused By D-Penicillamine. *Rheumatology* **1994**, 8, 770-773.
- [8] Kean, W. F.; Howard-Lock, H. E.; Lock, C. J. L. Chirality in Antirheumatic Drugs. *The Lancet* **1991**, 338, 1565-1568.
- [9] Knight, P. D.; Scott, P. Predetermination of Chirality at Octahedral Centres with Tetradentate Ligands: Prospects for Enantioselective Catalysis. *Coordi. Chem. Rev.* **2003**, 242, 125-143.



- [10] Knof, U.; von Zelewsky, A. Predetermined Chirality at Metal Centers. *Angew. Chem. Int. Ed.* **1999**, 38, 302-322.
- [11] Biscarini, P.; Benedetti, M.; Kuroda, R.; Ferranti, F. Transfer of Chirality in Complexes with  $D_3$  Symmetry: Kinetics of the Formation Reaction of Chiral Tris[ $O,O'$ -bis(2-methylbutyl)dithiophosphato]chromium(III) Complexes ( $\Lambda,\Delta$ )-[Cr{( $\pm$ )-Mebdtp} $_3$ ],  $\Delta$ -(+) $_{589}$ - and  $\Lambda$ -(-) $_{589}$ -[Cr{(+)-( $S$ )( $S$ )-Mebdtp} $_3$ ]. *Eur. J. Inorg. Chem.* **2006**, 16, 3167-3176.
- [12] Sheridan, E. M.; Breslin, C. B. Enantioselective Detection of D- and L-Phenylalanine Using Optically Active Polyaniline. *Electroanal.* **2005**, 17, 532-537.
- [13] Feng, J. M.; Yang, P. J.; Wang, S.; Wang, J. Photoelectrochemical Chiral Sensing on the Basis of TiO $_2$ -Metal Complex Hybrid Film. *J. Electroanal. Chem.* **2012**, 674, 97-102.
- [14] Wang, Y. X.; Yin, X. L.; Shi, M. H.; Li, W.; Zhang, L.; Kong, J. L. Probing Chiral Amino Acids at Sub-Picomolar Level Based on Bovine Serum Albumin Enantioselective Films Coupled With Silver-Enhanced Gold Nanoparticles. *Talanta* **2006**, 69, 1240-1245.
- [15] Xu, M.H.; Lin, J.; Hu, Q.S.; Pu, L. Fluorescent Sensors for the Enantioselective Recognition of Mandelic Acid: Signal Amplification by Dendritic Branching. *J. Am. Chem. Soc.* **2002**, 124, 14239-14246.
- [16] Mirceski, V.; Quentel, F.; L'her, M. Chiral Recognition Based on the Kinetics of Ion Transfers Across Liquid/Liquid Interface. *Electrochem. Commun.* **2009**, 11, 1262-1264.
- [17] Yashima, E.; Maeda, K.; Nishimura, T. Detection and Amplification of Chirality by Helical Polymers. *Chem. Eur. J.* **2004**, 10, 42-51.

- [18] Patil, D. S.; Shaikh, J. S.; Pawar, S. A.; Devan, R. S.; Ma, Y. R.; Moholkar, A. V.; Kim, J. H.; Kalubarme, R. S.; Park, C. J.; Patil, P. S. Investigations on Silver/Polyaniline Electrodes for Electrochemical Supercapacitors. *Phys. Chem. Chem. Phys.* **2012**, *14*, 11886-11895.
- [19] Li, Q. H.; Wu, J. H.; Tang, Q. W.; Lan, Z.; Li, P. J.; Lin, J. M.; Fan, L. Q. Application of Microporous Polyaniline Counter Electrode for Dye-Sensitized Solar Cells. *Electrochem. Commun.* **2008**, *10*, 1299-1302.
- [20] Meng, C. Z.; Liu, C.H.; Fan, S.S. Flexible Carbon Nanotube/Polyaniline Paper-Like Films and Their Enhanced Electrochemical Properties. *Electrochem. Commun.* **2009**, *11*, 186-189.
- [21] Bian, C. Q.; Yu, A. S.; Wu, H. Q. Fibriform Polyaniline/Nano-TiO<sub>2</sub> Composite as an Electrode Material for Aqueous Redox Supercapacitors. *Electrochem. Commun.* **2009**, *11*, 266-269.
- [22] Ma, X. F.; Wang, M.; Chen, H. Z.; Li, G.; Sun, J. Z.; Bai, R. Preparation of Water Soluble Poly(aniline) and Its Gas-Sensitivity. *Green Chemistry* **2005**, *7*, 507-513.
- [23] Chen, L.; Su, Z. H.; He, X. H.; Liu, Y.; Qin, C.; Zhou, Y. P.; Li, Z.; Wang, L. H.; Xie, Q. J.; Yao, S. Z. Square Wave Anodic Stripping Voltammetric Determination of Cd and Pb Ions at a Bi/Nafion/Thiolated Polyaniline/Glassy Carbon Electrode. *Electrochem. Commun.* **2012**, *15*, 34-37.
- [24] Basozabal, I.; Gomez-Caballero, A.; Unceta, N.; Aranzazu Goicolea, M.; Barrio, R. J. Voltammetric Sensors with Chiral Recognition Capability: The Use of A Chiral Inducing

Agent in Polyaniline Electrochemical Synthesis for the Specific Recognition of the Enantiomers of the Pesticide Dinoseb. *Electrochimica Acta* **2011**, 58, 729-735.

[25] Yin, X.L.; Ding, J.J.; Zhang, S.; Kong, J.L. Enantioselective sensing of Chiral Amino Acids by Potentiometric Sensors Based on Optical Active Polyaniline Films. *Biosens. Bioelectron.* **2006**, 21, 2184.

[26] Huang, J.X.; Egan, V.M.; Guo, H.L.; Yoon, J.Y.; Briseno, A.L.; Rauda, I.E.; Garrell, R.L.; Knobler, C.M.; Zhou, F.M.; Kaner, R.B. Enantioselective Discrimination of D- and L-Phenylalanine by Chiral Polyaniline Thin Films. *Adv. Mater.* **2003**, 15, 1158-1161.

[27] Kong, Y.; Ni, J. H.; Wang, W. C.; Chen, Z. D. Enantioselective Recognition of Amino Acids Based on Molecularly Imprinted Polyaniline Electrode Column. *Electrochim. Acta* **2011**, 56, 4070-4074.

[28] Kong, Y.; Li, X.Y.; Ni, J.H.; Yao, C.; Chen, Z.D. Enantioselective Recognition of Glutamic Acid Enantiomers Based on Poly(Aniline-co-m-Aminophenol) Electrode Column. *Electrochem. Commun.* **2012**, 14, 17-20.

[29] Kane-Maguire, L.A.P.; Wallace, G.G. Chiral Conducting Polymers. *Chem. Soc. Rev.* **2010**, 39, 2545-2576.

[30] Havinga, E.E.; Bouman, M.M.; Meijer, E.W.; Pomp, A.; Simenon, M.M.J. Large Induced Optical Activity in The Conduction Band of Polyaniline Doped With (1S)-(+)-10-Camphorsulfonic Acid. *Synth. Metals* **1994**, 66, 93-97.

[31] Kadar, M.; Nagy, Z.; Karancsi, T.; Farsang, G. The Electrochemical Oxidation of 4-Bromoaniline, 2,4-Dibromoaniline, 2,4,6-Tribromoaniline and 4-Iodoaniline in

Acetonitrile Solution. *Electrochim. Acta* **2001**, *46*, 3405-3414.

[32] Sari, B.; Talu, M. Electrochemical Polymerization and Analysis of Some Aniline Derivatives. *Turkish J. of Chem.* **1998**, *22*, 301-307.

## Chapter 3 Controlled Synthesis of Polyaniline on Glassy Carbon Electrodes for Improved pH sensing

### 3.1 Introduction

Polyaniline (PANI) is a unique conducting polymer [1,2] and has shown its own tunable organic nature. Its ability to form various micro/nanostructures [3-7] has opened up further dimensions to the design and development of new electronic devices and biosensors on the basis of conductive polymers [8-13]. In recent decades, in-situ electrochemical polymerization has become an attractive approach in the fabrication of PANI, as it yields a reproducible film thickness and stability [14-16]. PANI-coated electrodes have been utilized successfully in numerous electrochemical sensing applications, such as the detection of nitrite [17],  $\text{H}_2\text{O}_2$  [18-19] and pH [20-26], etc. In one of our very recent works presented in chapter 2 [13], Poly (4-bromoaniline) (PBA) film has been in-situ synthesized on a gold electrode, which demonstrates promising ability for enantioselective recognition of amino acids. Notably, the differential pulse voltammograms of L and D-glutamic acid not only have very different current density at the same concentration, but also show different shapes, providing an intuitive way to probe the chiral molecules.

It is generally agreed that PANI has a variety of oxidation states that are both pH and potential dependent: leucoemeraldine (LE, fully reduced), emeraldine (EB, partially-oxidised) and pernigraniline (PE, fully oxidised) [22]. This makes PANI a potential candidate in pH sensing. As a pH sensor, PANI-coated electrodes overcome some limitations of the conventional glass electrode, such as high ohmic resistance, the need

for internal solution and fragility of the glass. Due to that the amine group in PANI can be protonated or deprotonated, PANI-coated electrodes can be served as either optical pH sensors [20-22] or potential-based pH sensors [23-26]. Of particular relevance to the optical pH sensors is the equilibrium between the two partially oxidized forms --- the deprotonated emeraldine base (EB) and protonated emeraldine salt (ES). ES form of PANI displays two characteristic absorbance ranging at 390-450 nm or above 700 nm [23]. EB form of PANI shows a single absorbance at 640-650 nm [23]. The largest spectral change due to deprotonation of ES is obtained between pH 5 and pH 8, whereas only small changes are observed between pH 2 and pH 5 due to the hysteresis in the transfer between EB and ES forms. This leads to the limitation of the pH range of such sensors. Such limitation not only happens in optical PANI pH sensors, but also exists in the potential-based pH sensing.

The main goal of the present study is to controllably synthesize PANI through introducing additives to the electrolyte. Through controlling the final chemical state of the PANI polymer, their pH sensing performance such as range and response time may be improved. We found that it is possible to improve the hysteresis in the transfer between EB and ES forms by having bromide ions present in the solution during the preparation of PANI. Impressively, the synthesized PANI polymer also displays a broad linear response to pH, i.e. between 1 and 13. Such potential-based pH sensor is very stable whether it is stored in water or exposed to air.

## 3.2 Experimental

Aniline (>98%), Nitric acid (60-70%) and potassium ferricyanide (III) (99%) were purchased from Aldrich. Sodium hydroxide was purchased from Merck KGaA

(Germany). All aqueous solutions were prepared with double distilled water. A wide range of buffers covering pH from 1 to 13 were prepared with phosphate buffer. Hydrochloric acid (0.1 M) and sodium hydroxide (0.1 M) were used to adjust the pH to the desired value. Scanning electron microscopy (SEM) images and Energy-dispersive X-ray spectroscopy (EDX) were taken on a Quanta 200 FEG microscope (FEI, Inc.). All electrochemical experiments were performed at room temperature ( $22 \pm 2^\circ\text{C}$ ) with a CHI660D electrochemical workstation (CHInstrument, USA).

A three-electrode system was employed, using a modified glassy carbon electrode (with a 2.0 mm diameter) as the working electrode, a Pt wire as the auxiliary electrode, and a saturated calomel electrode (SCE) as the reference electrode. Before the polymerization of aniline, the glassy carbon electrode was polished with  $0.05 \mu\text{m}$  alumina powder (CHInstrument), then cleaned by ultrasonic cleaner (Branson 1510, USA), and finally rinsed with double distilled water. The scan rate used in the cyclic voltammetry was 100 mV/s, unless otherwise stated in the context. Electrochemical impedance spectroscopy was measured at the formal redox potential of  $\text{Fe}(\text{CN})_6^{4-}/\text{Fe}(\text{CN})_6^{3-}$  in the frequency range from 100 kHz to 0.1 Hz with an amplitude of 5 mV. The electrolyte solution for the EIS measurements consisted of 5.0 mM  $\text{K}_3\text{Fe}(\text{CN})_6$  and 0.1 M  $\text{KNO}_3$ .

### 3.3 Results and Discussion

Cyclic voltammograms recorded during the electrochemical synthesis of polyaniline were presented in Figure 3.1, where the electrolyte consists of 1.0 M  $\text{HNO}_3$  and 0.05 M aniline in the absence (Figure 3.1a) and presence (Figure 3.1b) of bromide ions. The sweep rate used here was 50 mV/s. There is a well-defined anodic peak around 1.0 V in

both Figures 3.1a and 3.1b, which decreases drastically from the first to the second loop. Without the presence of bromide ions it can be seen in Figure 3.1a that there are four pairs of redox peaks with growing magnitudes. This is a typical behavior of the synthesis of polyaniline on an electrode. The oxidation peak around 200 mV (peak A) is obviously enhanced the most among four peaks and is attributed to the transition of leucoemeraldine to emeraldine. Redox peaks B/B' and C/C' correspond to the redox of the benzoquinone/ hydroquinone couple and the redox of head-to-tail dimer, respectively. The oxidation peak D is attributed to the transition of emeraldine to pernigraniline, which is the fully oxidized form. The fabricated PANI film at a GC electrode after 10 cycles of CV is green, which is the color of PANI in the ES form.

After 0.05M NaBr was added into the electrolyte solution, however, the oxidation peak at 200 mV was dramatically reduced and shifted positively by about 0.05 V (see the results shown in Figure 3.1b). The main pair of redox peaks in Figure 3.1b become D/ D', which is due to the transition of emeraldine to pernigraniline. The color of the film in Figure 3.1b is violet, which is very different from that seen in Figure 3.1a. The violet color corresponds to PANI in a fully oxidized form. This result highlights that the additive bromide ions have significant influence on the electrochemical polymerization of PANI and can manifest the final chemical state of the synthesized PANI polymer, i.e. pushing the final product to PE form. As a comparison, we have also tested other halogen ions, specifically, adding 0.05 M NaCl into the solution. Quantitatively the same CV curves as shown in Figure 3.1a were achieved. The observation that chloride ions have no similar effect as bromide ions may arise from the fact that bromide ions were easier to adsorb/reduce at the electrode surface and then occupied the active spots of LE at the low



potential.

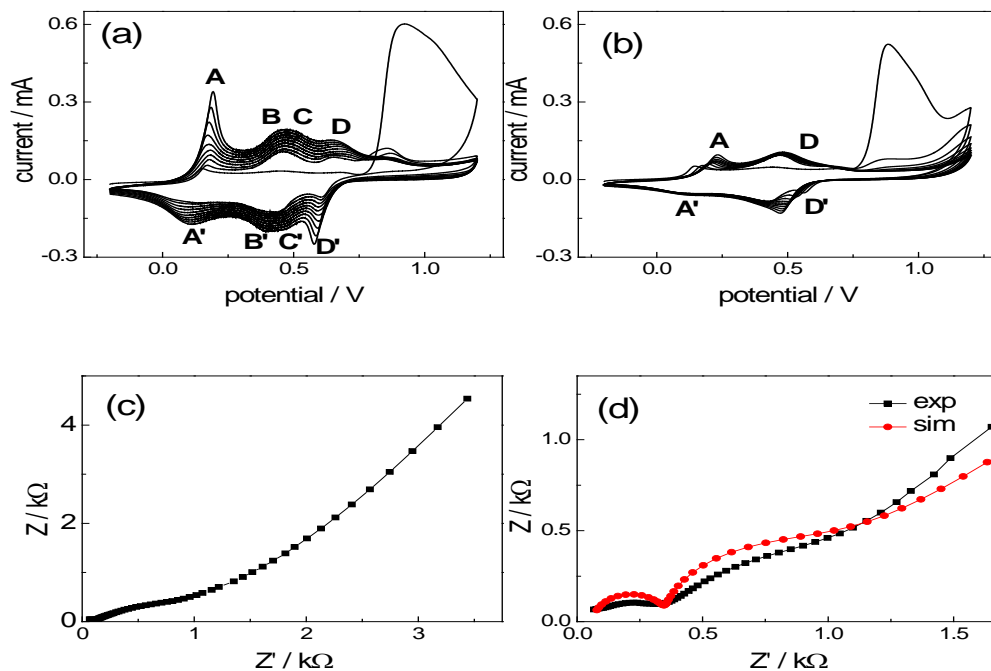
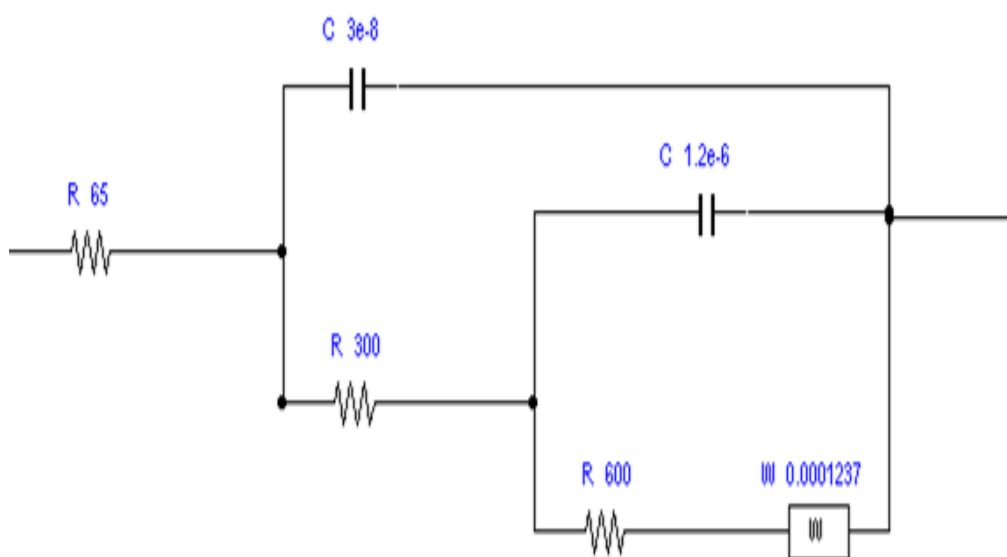


Figure 3.1 Cyclic voltammogram ( $50 \text{ mV s}^{-1}$ ) of electrochemically synthesized PANI in  $0.05 \text{ M}$  aniline and  $1 \text{ M HNO}_3$  at glassy carbon electrode in the absence (a) and presence (b) of  $0.05 \text{ M NaBr}$ ; (c) EIS measurements of polymer film (a) in  $5 \text{ mM K}_3\text{Fe(CN)}_6$  with the electrolyte  $0.1 \text{ M NaCl}$  solution within the range from  $100 \text{ mHz}$  to  $100 \text{ kHz}$ , with an amplitude of  $5 \text{ mV rms}$ , the fixed potential of the film corresponded to the anodic potential; (d) Experimental and simulated EIS curves of polymer film (b) under the same condition in (c).

EIS was employed to characterize properties of the PANI film synthesized without (Figure 3.1c) and with (Figure 3.1d) the presence of bromide ions in the electrolyte solution. Here,  $\text{K}_3\text{Fe(CN)}_6$  was employed as the redox mark. In general, a semicircle is expected to occur in EIS, in which the radius of the semicircle reflects the charge transfer rate at the interface. Figure 3.1c shows a distorted half circle, whereas in Figure 3.1d there appears to be two half cycles. Such a difference in the electrochemical property is likely due to that in the case of Figure 3.1c, the film was predominantly the ES form of

PANI, while in the later case the PANI film consists of two major forms (ES and PE). Again, the EIS spectra further confirm the bromide effects on the electrochemical synthesis of PANI. The EIS spectrum seen in Figure 3.1d can be reproduced with a general model shown in the following (see model 1). The outer circuit represents the small half cycle with 0.3 k $\Omega$  resistance, and the inner circuit represents the large half cycle with 0.6 k $\Omega$  resistance. The simulated spectrum is overlap in Figure 3.1d.



Model 1

PE form is the most  $\pi$  conjugated conducting form and therefore would facilitate the electron transfer through it. As a result, it may favor the oxidation of  $K_3Fe(CN)_6$ , in comparison to the other two forms of PANI film. Therefore, the small half circuit seen in Figure 3.1d is suggested here to arise from the PE form, whereas the larger half cycle is derived from the ES form.

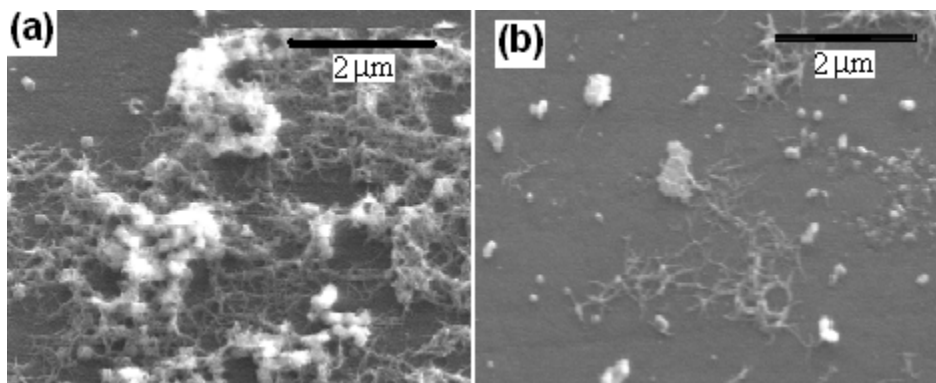


Figure 3.2 SEM images for 10 cycles of bromide-absence PANI (a) and bromide-presence PANI (b) on glassy carbon electrode, the conditions of electropolymerization of PANI were the same as Figure 1a and 1b, respectively.

Figure 3.2 shows SEM images of the PANI films prepared with (a) and without (b) the presence of bromide ions in the electrolyte solution. While fiber structures can be seen in both images, a noticeable difference is the quantity of those polymers, despite that they were prepared through the identical protocol with the same reaction time. The decrease in the amounts of fibers seen in Figure 3.2b is consistent with the CV spectrum presented in Figure 3.1b, where the peak current is clearly lower than that seen in Figure 3.1a. The decrease may be attributed to the fact that the additive bromide ions may occupy some active sites on the glassy carbon electrode, making the effective surface area for the oxidation of aniline monomer smaller. EDX data shows no bromine atom neither in Figure 3.2(a) nor Figure 3.2(b), suggesting that bromide ions can significantly impact the polymerization of PANI, but didn't dope into the backbone structure of polymer.

The ability of using the above prepared PANI film on a glassy carbon electrode as a pH sensor was explored by using open circuit potential (OCP) method [26]. As shown in Figure 3.3, the OCP of both films decreases with the increase of the solution pH value.

For the PANI film synthesized without adding bromide ions, its OCP decreases about 12 mV/ pH within the pH range of 1 to 4 and 39 mV/ pH for pH between 4 and 13. The smaller potential variation in strong acidic pH range could be due to the hysteresis in the transfer from EB to ES form by big clusters aggregation. A notable difference is that for the film fabricated in the presence of bromide ions, its response to pH change is linear over the range of 1 to 13, making it a better candidate in applications of pH sensing. The plot shows that the pH linear range was between 1 and 13 with the slope of -29 mV/ pH.

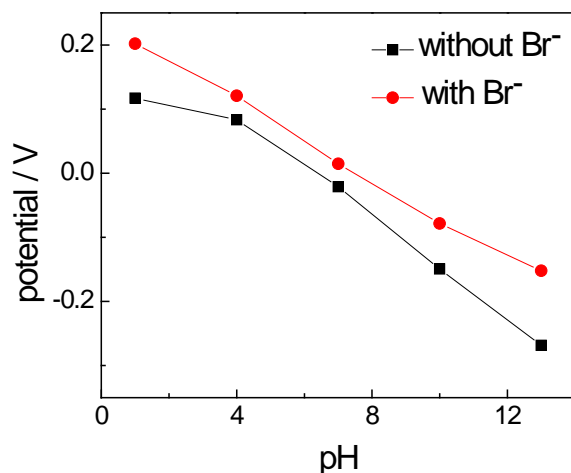


Figure 3.3 pH vs. OCP (open circuit potential) curve tested by bromide-free PANI (square) and bromide-added PANI (circle) modified GC electrode. pH buffered solution was prepared by pH = 7 phosphate buffer, hydrochloric acid (0.1 M) and sodium hydroxide (0.1 M) were used to adjust the pH to the desired value.

A possible explanation for the results presented in Figure 3.3 is that leucoemeraldine base  $[-(\text{C}_6\text{H}_4)-\text{N}(\text{H})-(\text{C}_6\text{H}_4)-\text{N}(\text{H})]_{4x}$  displays a hydrophobic character unfavorable for molecular adsorption, but pernigraniline base  $[-(\text{C}_6\text{H}_4)-\text{N}=(\text{C}_6\text{H}_4)=\text{N}-]_{4x}$  is hydrophilic enabling the formation of differently charged surface groups like  $\text{C}-\text{NH}_2$ ,  $\text{C}-\text{NH}_3^+$ , by a protonation-deprotonation mechanism, depending on the proton concentration in solution. Thus protonation is more favored for pernigraniline base, which subsequently broadens

the linear potential response to pH values.

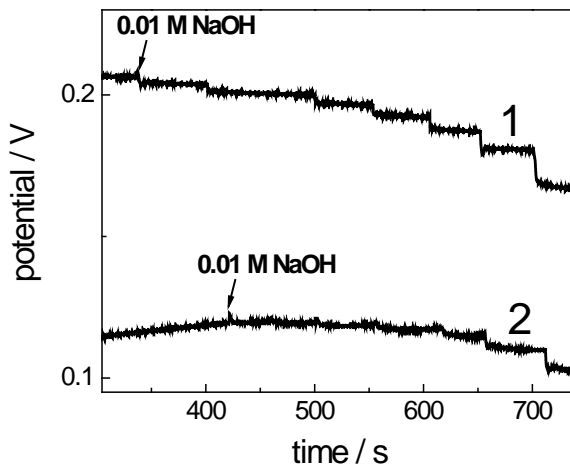


Figure 3.4 Open circuit potential responses to a successive addition of 0.01 M NaOH in pH = 1 phosphate buffer, curve 1 and 2 represent bromide-added PANI and bromide-free PANI modified GC electrode, respectively.

Figure 3.4 shows the potential responses of the two films to a series of consecutive addition of 0.01 M NaOH to the sample solution. Both curves 1 and 2 were started at the same pH = 1 phosphate buffer. The response time for the PANI film prepared in the presence of bromide ions (curve 1) is less than 8 s, i.e. the time required by the system to reach a steady open circuit potential upon the addition of NaOH. However, the potential response time of curve 2, where the PANI film prepared without bromide ions, was much longer (i.e., between 15-25 seconds for each addition). Within the strong acid range, the curve 2 does not exhibit obvious decrease. Results of Figure 3.3 and 3.4 clearly demonstrate that PANI prepared in the presence of bromide ions does not only a broad linear potential response, but also exhibits a shorter response time. Further tests indicate that the bromide-controlled PANI film has good consistency and accuracy with the values detected in the reverse direction from base to acid. The film can be stored in air or

distilled water for one month without losing its performance.

### 3.4 Conclusions

Knowing that PANI polymer can exist at three different oxidation states, where each chemical state may have different electrochemical properties, this research explored a way to control the synthesis of PANI for potential applications in electrocatalysis and chemical sensing. The preliminary data indicate that the addition of bromide ions in the monomer solution could greatly affect the synthesized PANI film. As indicated by the CV voltammograms, the PE and ES become the dominant constituents of the as-prepared PANI polymer. Other physical observations such as the color of the as-prepared film support the above conclusion. When the synthesized PANI films were applied in pH sensing, the film obtained under the influence of bromide ions exhibits distinct advantages with regard to large linear potential response range to pH, a short response time, high accuracy and stability. As discussed earlier, such a change is likely due to that amine groups in PANI are more favored in protonation, making the potential response more sensitive in acidic pH range. Notably, this bromide controlled approach is relatively simple and inexpensive and provides a promising means of developing a new kind of potential chemical sensors for in situ monitoring. No similar effect was obtained with chloride ions. This may come from the fact that bromide ions can be oxidized into bromine atoms/molecules within the potential applied, whereas chloride cannot be oxidized. The bromine subsequently oxidizes the EB form of PANI polymer, making that PE and ES the dominant components of the final PANI product.

## References

- [1] MacDiarmid, A. G. "Synthetic Metals": A Novel Role for Organic Polymers (Nobel Lecture). *Angew. Chem., Int. Ed.* **2001**, 40, 2581-2590.
- [2] Heeger, A. J. Semiconducting and Metallic Polymers: The Fourth Generation of Polymeric Materials (Nobel Lecture). *Angew. Chem., Int. Ed.* **2001**, 40, 2591-2611.
- [3] Han, J.; Fang, P.; Dai, J.; Guo, R. One-Pot Surfactantless Route to Polyaniline Hollow Nanospheres with Incontinuous Multicavities and Application for the Removal of Lead Ions from Water. *Langmuir* **2012**, 28, 6468-6475.
- [4] Huang, L. M.; Wang, Z. B.; Wang, H. T.; Cheng, X. L.; Mitra, A.; Yan, Y. S. Polyaniline Nanowires by Electropolymerization from Liquid Crystalline Phases. *J. Mater. Chem.* **2002**, 12, 388-391.
- [5] Olejnik, P.; Gniadek, M.; Palys, B. Layers of Polyaniline Nanotubes Deposited by Langmuir-Blodgett Method. *J. Phys. Chem. C* **2012**, 116, 10424-10429.
- [6] Liu, Z.; Zhang, X. Y.; Poyraz, S.; Surwade, S. P.; Manohar, S. K. Oxidative Template for Conducting Polymer Nanoclips. *J. Am. Chem. Soc.* **2010**, 132, 13158-13159.
- [7] Choi, S. J.; Park, S. M. Electrochemical Growth of Nanosized Conducting Polymer Wires on Gold Using Molecular Templates. *Adv. Mater.* **2000**, 12, 1547-1549.
- [8] Jiang, H.; Ma, J.; Li, C. Z. Polyaniline-MnO<sub>2</sub> Coaxial Nanofiber with Hierarchical Structure for High-Performance Supercapacitors. *J. Mater. Chem.* **2012**, 22, 16939-16942.

- [9] Patil, D. S.; Shaikh, J. S.; Pawar, S. A.; Devan, R. S.; Ma, Y. R.; Moholkar, A. V.; Kim, J. H.; Kalubarme, R. S.; Park, C. J.; Patil, P. S. Investigations on Silver/Polyaniline Electrodes for Electrochemical Supercapacitors. *Phys. Chem. Chem. Phys.* **2012**, *14*, 11886-11895.
- [10] Wei, X. L.; Wang, Y. Z.; Long, S. M.; Bobeczko, C.; Epstein, A. J. Synthesis and Physical Properties of Highly Sulfonated Polyaniline. *J. Am. Chem. Soc.* **1996**, *118*, 2545-2555.
- [11] Basozabal, I.; Gomez-Caballero, A.; Unceta, N.; Aranzazu Goicolea, M.; Barrio, R.J. Voltammetric Sensors with Chiral Recognition Capability: The Use of A Chiral Inducing Agent in Polyaniline Electrochemical Synthesis For the Specific Recognition of the Enantiomers of the Pesticide Dinoseb. *Electrochim. Acta* **2011**, *58*, 729-735.
- [12] Ma, X. F.; Wang, M.; Chen, H. Z.; Li, G.; Sun, J. Z.; Bai, R. Preparation of Water Soluble Poly(Aniline) and its Gas-Sensitivity. *Green Chem.* **2005**, *7*, 507-513.
- [13] Li, J.; Hu, X. F.; Wang J. Electrochemical Recognition of Chiral Molecules With Poly-(4-Bromoaniline) Modified Gold Electrode. *Electroanalysis* **2013**, *25*, 1975-1980.
- [14] Grennan, K.; Strachan, G.; Porter, A. J.; Killard, A. J.; Smyth, M. R. Atrazine Analysis Using An Amperometric Immunosensor Based on Single-Chain Antibody Fragments and Regeneration-Free Multi-Calibrant Measurement. *Anal. Chim. Acta* **2003**, *500*, 287-298.
- [15] Myler, S.; Collyer, S. D.; Davis, F.; Gornall, D. D.; Higson, S. P. J. Sonochemically Fabricated Microelectrode Arrays for Biosensors Part III. AC Impedimetric Study of



Aerobic and Anaerobic Response of Alcohol Oxidase Within Polyaniline. *Biosens.*

*Bioelectron.* **2005**, 21, 666-671.

[16] Oliveira, M.; Viswanathan, S.; Morais, S.; Delerue-Matos, C. Development of Polyaniline Microarray Electrodes for Cadmium Analysis. *Chemical Papers* **2012**, 66, 891-898.

[17] Kazimierska, E.; Smyth, M. R.; Killard, A. J. Size-Dependent Electrocatalytic Reduction of Nitrite at Nanostructured Films of Hollow Polyaniline Spheres and Polyaniline-Polystyrene Core-Shells. *Electrochim. Acta* **2009**, 54, 7260-7267.

[18] Luo, X. L.; Vidal, G. D.; Killard, A. J.; Morrin, A.; Smyth, M. R. Nanocauliflowers: A Nanostructured Polyaniline-Modified Screen-Printed Electrode with a Self-Assembled Polystyrene Template and Its Application in an Amperometric Enzyme Biosensor. *Electroanal.* **2007**, 19, 876-883.

[19] Ngamna, O.; Morrin, A.; Moulton, S. E.; Killard, A. J.; Smyth, M. R.; Wallace, G. G. An HRP Based Biosensor Using Sulphonated Polyaniline. *Synthetic Metals* **2005**, 153, 185-188.

[20] Jin, Z.; Su, Y. X.; Duan, Y. X. An Improved Optical pH Sensor Based on Polyaniline. *Sensors and Actuators: B* **2000**, 71, 118-122.

[21] Kaempgen, M.; Roth, S. Transparent and Flexible Carbon Nanotube/Polyaniline pH sensors. *J. Electroanal. Chem.* **2006**, 586, 72-76.

[22] Ge, C. H.; Armstrong, N. R.; Saavedra, S. S. pH-Sensing Properties of Poly(aniline)

Ultrathin Films Self-Assembled on Indium-Tin Oxide. *Anal. Chem.* **2007**, 79, 1401-1410.

[23] Lindfors, T.; Ivaska, A. pH Sensitivity of Polyaniline and its Substituted Derivatives.

*J. Electroanal. Chem.* **2002**, 531, 43-52.

[24] Pandey, P. C.; Singh, G. Electrochemical Polymerization of Aniline in Proton-Free Nonaqueous Media. *J. Electrochem. Soc.* **2002**, 149, D51-D56.

[25] Gao, W.; Song, J. F. Polyaniline Film Based Amperometric pH Sensor Using A Novel Electrochemical Measurement System. *Electroanal.* **2009**, 21, 973-978.

[26] Zhang, X. J.; Ogorevc, B.; Wang, Solid-State pH nanoelectrode Based on Polyaniline Thin Film Electrodeposited Onto Ion-Beam Etched Carbon Fiber. *J. Anal. Chim. Acta* **2002**, 452, 1-10.

## Chapter 4 Designed Electrodeposition of Copper Nanoparticles inside/on Conductive Polymers and Applications as Non-enzymatic Glucose Sensor

### 4.1 Introduction

The fact that the selectivity and sensitivity of existing nonenzymatic glucose sensors [1,2] are still not as good as those of enzyme-based sensors [3,4] has fueled the constant search for new types of sensing materials and platforms for glucose detection. In the past two decades, sensors based on carbon nanotubes (CNTs)-inorganic hybrids including Pt/CNT [5,6], PtPb/CNT [7], Pd/Single walled CNT [8], NiO/Multi walled carbon nanotubes (MWCNT) [9], NiCu/MWCNTs [10], Cu/MWCNTs [11], Cu<sub>2</sub>O/MWCNT [12] have been developed for the direct electrochemical detection of glucose. Those nonenzymatic glucose CNT-biosensors have shown promising results such as a faster response time and a higher stability than their enzyme counterparts. The cupric oxide modified MWCNT electrode, for example, has successfully detected glucose with a limit of detection (LOD) of 50 nM and a sensitivity of  $6.5 \mu\text{A} \cdot \mu\text{M}^{-1}$  and displayed only 9% current reduction after 30 days of storage at room temperature [12]. Many kinds of Cu/Cu<sub>2</sub>O/CuO nanoparticles with different morphology and sizes have been synthesized on various substrates and the related study has led to better understanding on influences of nano-shapes and sizes on the sensitivity and selectivity [13-16]. However, seldom can reach to the level of facets' influences is due to the difficulty in fabricating nanoparticles enclosed with a specific facet.

To improve the performance, a large surface area is sought when preparing electrochemical sensors. Porous polymers in general have a large specific area, making

them an attractive candidate as the substrate [17-20]. Indeed there are increasing interests in the last decade to deposit metallic or semiconductor nanoparticles on conductive polymer matrices such as polypyrrole and polyaniline [21-25]. The polymer matrix can also be used for stabilizing the growth of nanoparticles and avoiding the agglomeration process, where the stabilized nanoparticles can be studied for their catalytic, optical, magnetic, and electrical properties [26]. Meanwhile, the nanoparticles deposited into polymer matrices can also modify the electronic, mechanical, and electrical properties of the polymer matrix [27]. The synergistic interactions have made the study of incorporating nanosized metal particles into polymer matrices current interests for many applications.

From existing reports, however, the formation of electrodeposited particles on or inside the conducting polymers appears to occur randomly [28]. When the deposition only takes place on the surface of a polymer matrix, the large specific surface area from the porous micro structure of the substrate is wasted. This study aims to design a convenient technique that copper nanoparticles can be deposited inside a conductive polymer matrix. The approach employed here is through the addition of chloride ions to the electrolyte solution. Studies have demonstrated that halogen ions preferentially adsorb on a specific face of metal crystals, providing a way to develop facet-controlled synthesis of nanocrystals [29-32]. A very recent study, using custom-build in situ high-speed electrochemical STM, found the reduction of the critical Cu nucleus size in the presence of  $\text{Cl}^-$ , which could lead to a lower nucleation barrier [32]. In other words, chloride could be introduced to the electrolyte solution to make more sites on the polymer chains suitable for the nucleation, which shall in turn favor the uniform deposition of

copper nanoparticles inside a three-dimensional polymer matrix. Here, we electrochemically synthesized a conducting polymer, poly-2,5-dimethoxyaniline (PDMA), on a glassy carbon electrode and used it as a solid template for preparing Cu nanoparticles with and without  $\text{Cl}^-$ . Pulsed deposition was employed to allow ions diffuse into the matrix during the “off” period. As shown in the following, the presence of  $\text{Cl}^-$  not only increased the nucleus density and thus reduced the size of Cu nanoparticles, but also exhibited significant effects on their morphology. Electrochemical experiments further demonstrate that the Cu/polymer composite film fabricated in the presence of chloride ion have better electroactivity in the detection of glucose.

## 4.2 Experimental

2,5-dimethoxyaniline ( $\geq 98\%$ ), sulfuric acid (95-98%), D(+)-Glucose, dopamine hydrochloride (DA) were purchased from Aldrich. L-ascorbic acid (AA) was obtained from the British Drug Houses Ltd. and uric acid (UA) was purchased from Fisher Scientific Company. Sodium hydroxide was purchased from Merck KGaA (Germany). Both copper sulfate ( $\geq 98\%$ ) and potassium chloride ( $\geq 99\%$ ) were obtained from ACP Chemicals Inc. All solutions were prepared with double distilled water.

Scanning electron microscopy (SEM) and Energy-dispersive X-ray spectroscopy (EDX) were performed with a Quanta 200 FEG microscope (FEI, Inc.). All electrochemical experiments were carried at room temperature ( $22 \pm 2^\circ\text{C}$ ) with a CHI660D electrochemical workstation (CHInstrument, USA). A three-electrode system was employed, using a bare or modified glassy carbon electrode (with a 3.0mm diameter) as the working electrode, a Pt wire as the auxiliary electrode, and a saturated calomel electrode (SCE) as the reference electrode. All electrochemical experiments were

performed at room temperature ( $22 \pm 2^\circ\text{C}$ ) with a CHI660D electrochemical workstation (CHIInstrument, USA). Before the *in situ* electrochemical polymerization of 2,5-dimethoxyaniline (PDMA), glassy carbon electrode was polished with  $0.05 \mu\text{M}$  alumina powder (CHIInstrument USA), then cleaned by ultrasonic cleaner (Branson 1510, USA) for 2 minutes, and finally rinsed with double distilled water. The polymer and copper products were characterized with SEM and EDX.

The poly(2,5-dimethoxyaniline) (PDMA) was synthesized with a cyclic voltammetry technique scanned between  $-0.2$  and  $1.0$  V (vs SCE) at a rate of  $100$  mV/s. Pulsed current was used to electrochemically deposit copper nanoparticles into the conducting poly(2,5-dimethoxyaniline) matrix. There are four main parameters in the pulsed deposition method: the off time, the on time, the number of cycles and the applied current: the off time was 10 seconds, the on-time was 10 seconds, the applied cathodic current was  $200$  mA for 20 cycles. After the deposition, the films were washed with double-distilled water and allowed to dry in nitrogen stream.

### **4.3 Results and Discussion**

Figure 4.1(A) presents cyclic voltammograms (CVs) of 2,5-dimethoxyaniline at a GC electrode, performed at  $100$  mV/s for 20 cycles. The electrolyte solutions contains  $20.0$  mM 2,5-dimethoxyaniline and  $0.5$  M sulfuric acid. For the first forward scan from  $-0.2$  to  $1.0$  V, only one anodic peak was observed at above  $0.65$  V, which corresponded to the oxidation of 2,5-dimethoxyaniline. On the reverse scan, a cathodic peak emerged at around  $0.25$  V, which arose from the reduction of the intermediates produced from 2,5-dimethoxyaniline oxidation. Another notable change is that after the first cycle a new anodic peak emerged at the potential of  $0.3$  V, presumably due to the products generated

#### Chapter 4 Designed Electrodeposition of Copper Nanoparticles in side/on Conductive Polymers and Applications as Non-enzymatic Glucose Sensor

through the preceding redox reactions. The amplitude of this anodic peak increased gradually with the number of cycles. Phenomenologically, the gray GC electrode turned into blue after 20 CV cycles, indicating the formation of polymer film on its surface. Earlier study has shown that poly(2,5-dimethoxyaniline) is highly conductive [33].

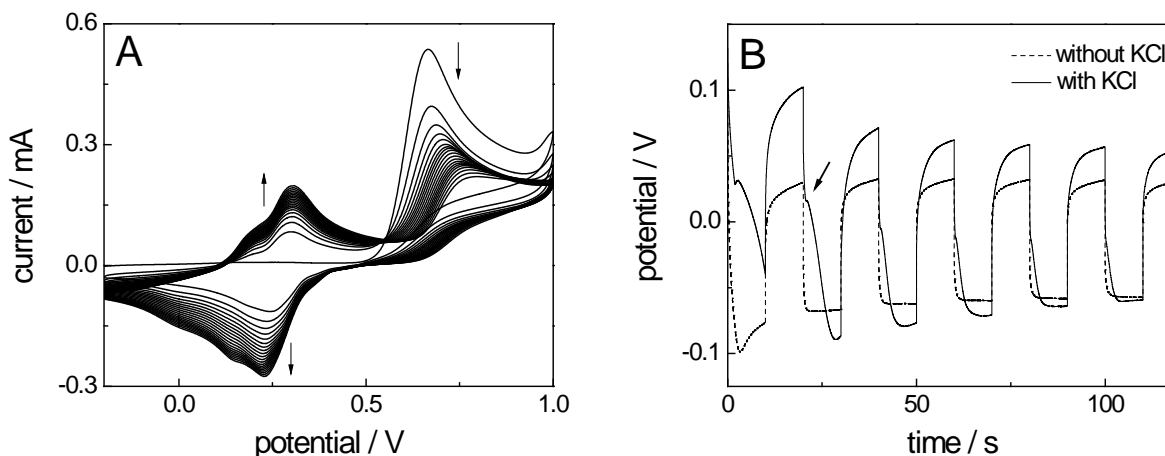


Figure 4.1 (A) CVs of 20.0 mM 2,5-dimethoxyaniline in 0.5 M  $\text{H}_2\text{SO}_4$  solution at a scan rate of 100 mV/s. (B) pulsed deposition of Cu in 0.1 M  $\text{CuSO}_4$  solution with or without KCl additives. The number of cycles is 20 in both (A) and (B).

In Figure 4.1(B) pulsed current was employed to deposit Cu using the GC/PDMA as the substrate. The following parameters were used in this synthesis: the off-time was 10 seconds, the on-time was 10 seconds, the applied cathodic current was 0.2 mA for 20 cycles. The electrolyte solution composed of 0.10 M  $\text{CuSO}_4$  adjusted with sulfuric acid to pH = 4.5. The dashed and solid lines correspond to the synthesis in the absence and in the presence of 20.0 mM KCl in the reaction solution, where quite different potential profiles were observed. In the absence of  $\text{Cl}^-$ , as soon as the current is on, the potential dropped sharply to a negative value in order to maintain the desired cathodic current density. After the initial drop, the potential stayed flat during the on-period. Upon turning

**Chapter 4 Designed Electrodeposition of Copper Nanoparticles in side/on Conductive Polymers and Applications as Non-enzymatic Glucose Sensor**

off the current, the potential gradually relaxes to the zero-current potential, which is described by the Nernst equation. In the presence of  $\text{Cl}^-$  in the reaction solution, after the initial sharp potential drop to near 0 upon turning on the current, the potential stayed at the near 0 briefly and then gradually decreased toward more negative values. This behavior suggests that the system does not require a large negative overpotential to maintain the present current density. In other words, the reactant became easily reduced. This is in agreement with earlier observation on the accelerated reduction of copper ions because of the formation of  $\text{Cu-Cl}^-$  complexes. Near the end of the on period, the potential became more negative, presumably due to that extensive consumption of copper ions, where larger overpotential is needed to maintain the current density. The electrochemical system in the presence of  $\text{Cl}^-$  has a larger zero-current potential, which indicates that copper ion concentration rapidly regains a higher concentration in comparison to the case of without  $\text{Cl}^-$ . This phenomenon is likely determined by the structure of the PDMA/Cu composite films (i.e., porous matrix vs surface blocked matrix).

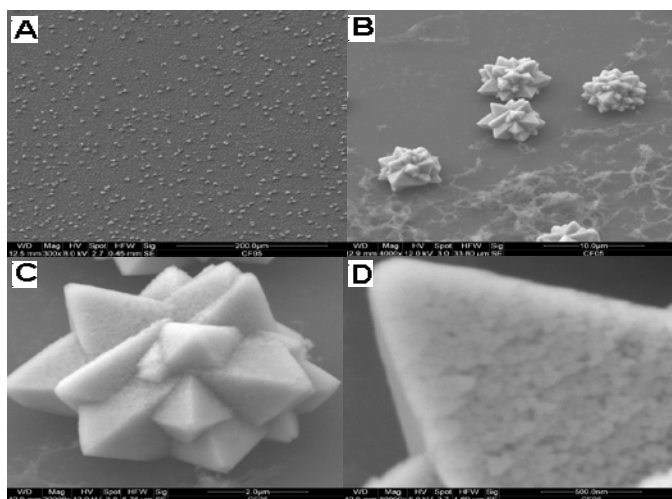


Figure 4.2 SEM images of the PDMA film after the Cu deposition. No additive such as KCl was added to the electrolyte solution.



**Chapter 4 Designed Electrodeposition of Copper Nanoparticles in side/on Conductive Polymers and Applications as Non-enzymatic Glucose Sensor**

Figure 4.2 presents SEM images of the PDMA film after the pulsed electrodeposition of copper particle in a 0.1 M  $\text{CuSO}_4$  solution that does not contain any other additives such as KCl. Figure 4.2(A) indicates that there are many micro-sized particles scattered almost uniformly on the surface of the PDMA film. EDX measurement confirms that those particles are copper. The size and morphology of those copper particles can be better identified from Figures 4.2(B) and 4.2(C), which indicate that each copper crystal is made up of many small pyramids. This microstructure is qualitatively the same as those obtained when copper was directly electrodeposited on a glassy carbon electrode [34]. Detailed examination on the surface morphology of those pyramids (see Figure 4.2(D)) indicates that those surfaces are not smooth, where dark colored regions indicate the presence of many steps and kinks.

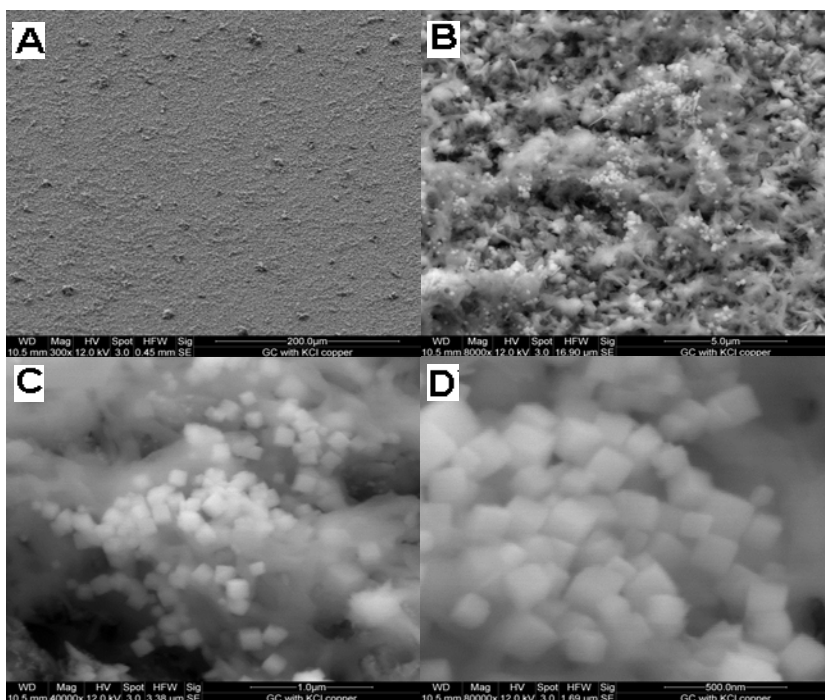


Figure 4.3 SEM images of the PDMA file after the Cu deposition. The pulsed electrodeposition of copper took place in the presence of 20.0 mM KCl in the electrolyte.

Figure 4.3 shows SEM images of the PDMA film taken after copper deposition in a 0.1 M  $\text{CuSO}_4$  solution that also contains 20.0 mM KCl. The current pulse protocol and number of cycles used here are the same as those used in Figure 4.2. The flat surface in Figure 4.3(A) (in relative to Figure 4.2(A)) suggests that most of the deposition activity took place inside the PDMA matrix. SEM in Figure 4.3(B) confirms that there are various nanoparticles inside the porous PDMA polymer. The magnified SEM images in Figures 4.3(C) and 4.3(D) indicate that those copper deposits are nanocubes, which is different from the assembled pyramids formed in Figure 4.2. The above results clearly indicate that the additive  $\text{Cl}^-$  not only greatly increases the total number of particles (i.e., the number of nucleation sites), but also controls the crystal morphology of the final products. Increasing number of particles causes the significant decrease of the particle size, which provides a larger surface area and more edges to facilitate catalytic reactions. Similar copper nanocubes were obtained in the electrodeposition of copper on the vertically aligned MWCNTs from  $\text{CuCl}_2$  electrolyte [35]. Together with what are seen in Figures 4.2 and 4.3, it is logical to conclude that  $\text{Cl}^-$  is an effective additive to affect the crystal growth and to obtain copper nanocubes. Another significant result is that the presence of  $\text{Cl}^-$  allows the copper deposition to mainly take place inside the polymer matrix, i.e., offering a controllable approach to make the composites of metal nanoparticles and conducting polymers. The response potential profile in Figure 4.1(B) suggests that the presence of  $\text{Cl}^-$  complexes, likely through forming complexes with copper ions, makes the reduction of copper favored. The accelerated reduction, together with the pulse deposition technology, could be responsible for the deposition inside the polymer matrix. A very recent study suggests that the adsorption of  $\text{Cl}^-$  on copper lowered nucleation

energy barrier [32], which subsequently makes more sites on the PDMA chain qualified to support copper nucleation. This factor may also contribute to the observed electrochemical behavior.

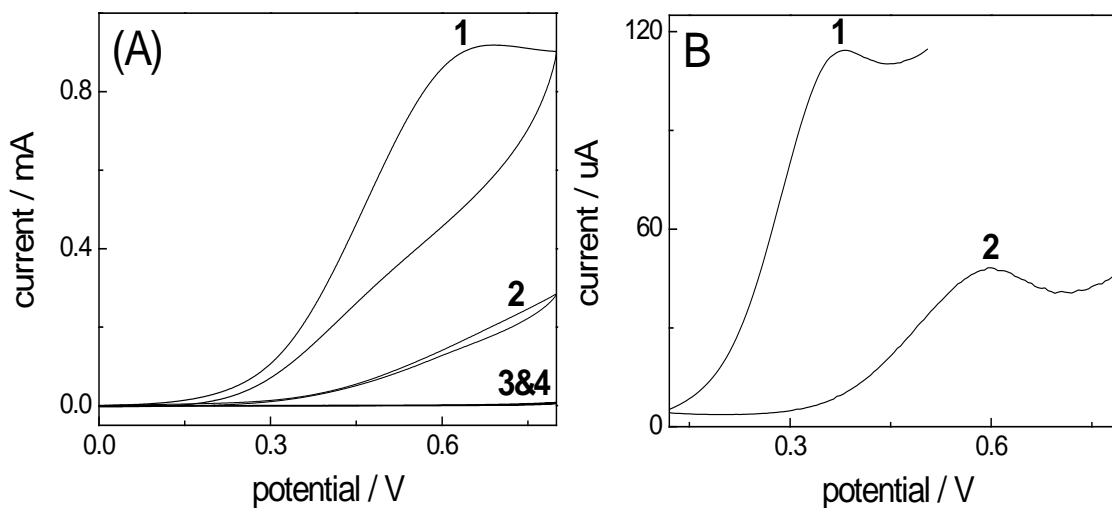


Figure 4.4 (A) CVs of glucose at (1) GC/PDMA/Cu(cube), (2) GC/PDMA/Cu(pyramid), (3) GC/PDMA and (4) bare GC electrodes at a scan rate of  $100 \text{ mVs}^{-1}$ . (B) DPVs of glucose at (1) GC/PDMA/Cu(cube) electrode and (2) GC/PDMA/Cu(pyramid). The electrolyte solution contains 10.0 mM glucose and 0.1 M NaOH.

The cyclic voltammograms of 10.0 mM glucose at a bare GC (curve 4), GC/PDMA (curve 3) GC/PDMA/Cu(pyramid, curve 2) and GC/PDMA/Cu(cube, curve 1) electrodes are depicted in Figure 4.4(A). The supporting electrolyte is 0.1 M NaOH. No oxidation peak is observed at the bare GC electrode, suggesting that GC electrode is inactive for the electro-oxidation of glucose. CV at the GC/PDMA electrode overlaps with curve 3, indicating that the conductive polymer does not catalyzed the electro-oxidation of

glucose either. With the GC/PDMA/Cu(pyramid) electrode, great electroactivity was achieved when the applied potential was increased to above 0.4 V (vs SCE), although there was no anodic peak. At the GC/PDMA/Cu(cube) electrode the response current increased dramatically starting from 0.2 V to 0.7 V and exhibited a well-developed anodic (i.e., oxidation) peak around 0.6 V. This result not only suggests that copper is responsible for the glucose oxidation, but also implies copper nanocubes, which have a higher aspect ratio and larger surface area, can give rise to higher current response.

In Figure 4.4(B) differential pulse voltammetry (DPV) was applied to detect glucose. The employed parameters are 5 mV increment, 50 mV pulse amplitude, 200 ms pulse width. Same as in Figure 4.4(A) the glucose concentration is 10.0 mM. It illustrates that at the GC/PDMA/Cu(pyramid) electrode there is an anodic peak with the peak potential around 0.6 V (curve 2). The peak potential decreased to near 0.3 V at the GC/PDMA/Cu(cube) electrode (curve 1). The negative shift in the oxidation peak suggests that the {100} cubic facet of the copper crystal favors the electro-oxidation of glucose [36]. The lower current intensity achieved at GS/PDMA/Cu(pyramid) electrode is likely due to that the Cu particle size there is too large, resulting in a low aspect ratio and small total surface area.

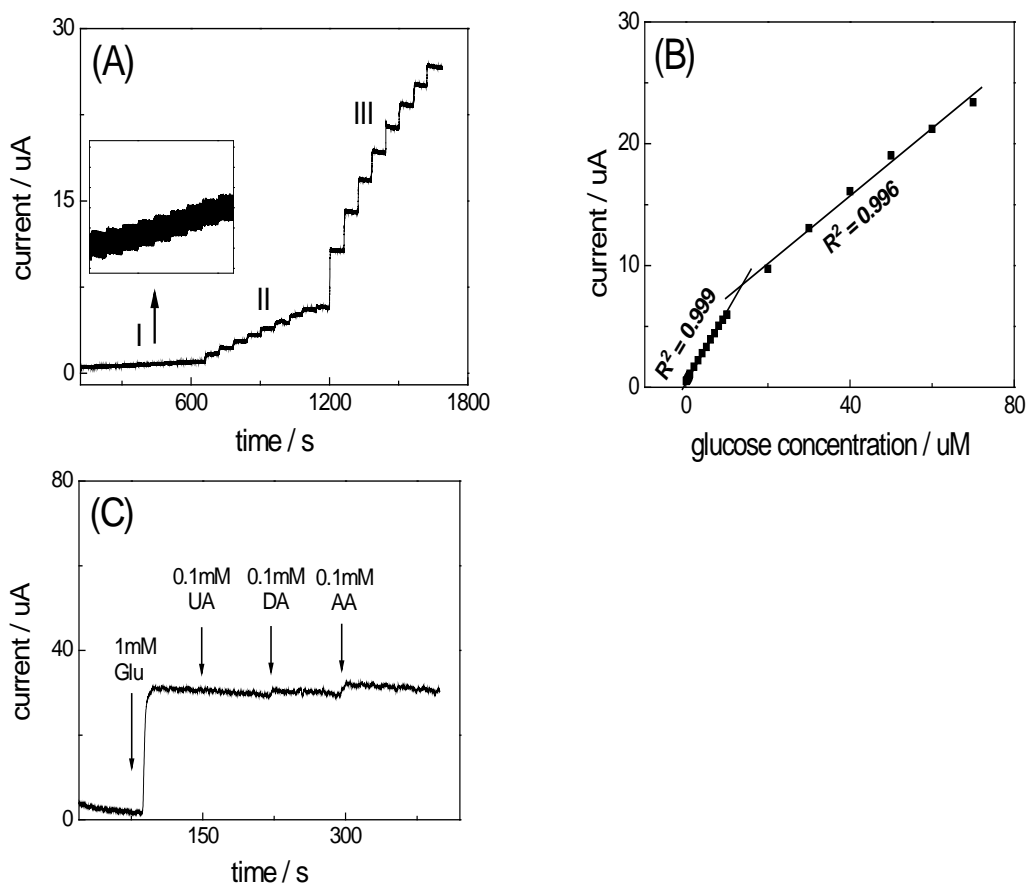


Figure 4.5 (A) Amperometric responses to a successive addition of 0.1 uM glucose in phase I, 1.0 uM glucose in phase II and 10.0 uM glucose in phase III, (B) The current response vs. glucose concentration, (C) amperometric responses to additions of glucose (1 mM), UA (0.1 mM), DA (0.1 mM) and AA (0.1 mM). The supporting electrolyte is 0.1 M NaOH and the modified electrode was GC/PDMA/Cu(cube). The applied potential is 0.3 V.

Amperometric responses of the GC/PDMA/Cu(cube) electrode to successive additions of glucose are shown in Figure 4.5(A), where 0.1 uM in phase I, 1.0 uM in phase II and 10.0 uM in phase III was added each time. The applied potential is 0.3V (vs SCE). The inset indicates that this modified glassy carbon electrode could detect glucose as low as  $10^{-7}$  M. Such a low detection limit shall be attributed to the high surface-to-

**Chapter 4 Designed Electrodeposition of Copper Nanoparticles in side/on Conductive Polymers and Applications as Non-enzymatic Glucose Sensor**

volume ratio of the small Cu nanocrystals and the favorite facet of nanocubes. The large noise seen in the inset is due to the influence of continuous stirring. The fast current response can be attributed to the fast diffusion of glucose molecules in the three dimensional porous framework of PDMA matrix and the great electron conductivity of the matrix. As shown in Figure 4.5(B), the response current has two linear regions with respect to glucose concentration, i.e., from 0.1  $\mu\text{M}$  to 10  $\mu\text{M}$  with a linear regression coefficient 0.999 and from 10  $\mu\text{M}$  up to 70  $\mu\text{M}$  with a linear regression coefficient 0.995. The sensitivity is higher within the low glucose concentration range. We also tested the sensitivity of the GC/PBMA/Cu(pyramid) electrode and found that only had one tenth of the responses plotted in Figure 4.5(B).

A number of oxidizable interfering species co-exist with glucose in many samples. Therefore, it is necessary to investigate whether such interferents could produce response current comparable to that corresponding to glucose. The normal physiological level of glucose in human blood is 3-8 mM compared to about 0.1 mM of interfering species, while the glucose/interferents ratio is even higher in food samples. The current response of several common interferents such as 0.1 mM L-ascorbic acid (AA), 0.1 mM uric acid (UA) and 0.1 mM dopamine (DA) were tested in Figure 4.5(C), along with 1.0 mM glucose in a supporting solution of 0.1 M NaOH. The applied potential was 0.3V. These results suggest that the as-prepared GC/PDMA/Cu electrode is highly specific to glucose even in the presence of several common interfering species found in human blood and biological samples. The above prepared glucose sensor also shows a good reproducibility and stability, with a loss of less than 10% in the current response after being kept in water for more than a week at room temperature.

## **4.4 Conclusions**

Chloride ions are found to be an effective additive to manifest the growth of copper crystals, leading to the formation of copper nanocubes instead of octahedrons. Such a morphology selection may arise from the preferential adsorption of halogen ions on a specific crystal face. Significantly, chloride also offers a convenient way to design whether the copper nanoparticles deposit inside the polymer matrix or at the outside of the matrix. This finding may be extended to fabricating composites of other metal nanoparticles and conductive polymers. According to a recent study, the above observed influences of chlorides may come from the reduction of the copper nucleation energy by chloride, which subsequently makes more sites on the polymer chains feasible for accommodating copper deposition [32]. The accelerated electroreduction of copper ions, as indicated by the response potential profile in Figure 4.1(b), could also contribute to the great increase in the total number of nucleation sites (i.e., number of particles) [35]. This study demonstrated that different morphology of Cu nanoparticles could give rise to distinctive peak potential for the electrochemical oxidation of glucose, in which glucose is greatly favored to be oxidized on the (100) cubic facet rather than on (111) octahedral facet.

## References

- [1] Holt-Hindle, P.; Nigro, S.; Asmussen, M.; Chen, A. Amperometric Glucose Sensor Based on Platinum-iridium Nanomaterials, *Electrochem. Commun.* **2008**,10, 1438-1441.
- [2] Toghiani, K. E.; Compton, R. G. Electrochemical Non-enzymatic Glucose Sensors: A Perspective and an Evaluation. *Int. J. Electrochem. Sci.* **2010**,5, 1246-1301.
- [3] Newman, J. D.; Turner, A. P. F.; Marrazza, G. Ink-Jet Printing for the Fabrication of Amperometric Glucose Biosensors. *Anal. Chim. Acta* **1992**,262, 13-17.
- [4] Scognamiglio, V. Nanotechnology in Glucose Monitoring: Advances and Challenges in the Last10 Years. *Biosens. Bioelectron.* **2013**, 47, 12-25.
- [5] Rong, L. Q.; Yang, C.; Qian, Q. Y.; Xia, X. H. Study of the Nonenzymatic Glucose Sensor Based on Highly Dispersed Pt Nanoparticles Supported on Carbon Nanotubes. *Talanta* **2007**, 72, 819-824.
- [6] Wen, Z. H. ; Ci, S. Q. ; Li, J. H. Pt Nanoparticles Inserting in Carbon Nanotube Arrays: Nanocomposites for Glucose Biosensors. *J. Phys. Chem. C.* **2009**, 113, 13482-13487.
- [7] He, B.; Hong, L. J.; Lu, J.; Hu, J .G.; Yang, Y. Y.; Yuan, J. H.; Niu, L. A Novel Amperometric Glucose Sensor Based on PtIr Nanoparticles Uniformly Dispersed on Carbon Nanotubes. *Electrochim. Acta* **2013**, 91, 353-360.
- [8] Meng, L.; Jin, J.; Yang, G. X.; Lu, T. H.; Zhang, H.; Cai, C. X. Nonenzymatic Electrochemical Detection of Glucose Based on Palladium-Single-Walled Carbon Nanotube Hybrid Nanostructures. *Anal. Chem.* **2009**, 81, 7271-7280.



- [9] Shamsipur, M.; Najafi, M.; Hosseini, M. R. M. Highly Improved Electrooxidation of Glucose at a Nickel(II) Oxide/Multi-Walled Carbon Nanotube Modified Glassy Carbon Electrode. *Bioelectrochemistry* **2010**, *77*, 120-124.
- [10] Lin, K. C.; Lin, Y. C.; Chen, S. M. A Highly Sensitive Nonenzymatic Glucose Sensor Based on Multi-Walled Carbon Nanotubes Decorated with Nickel and Copper Nanoparticles. *Electrochim. Acta* **2013**, *96*, 164-172.
- [11] Wu, H. X.; Cao, W. M.; Lin, Y.; Liu, G.; Wen, Y.; Yang, H. F.; Yang, S. P. In Situ Growth of Copper Nanoparticles on Multiwalled Carbon Nanotubes and Their Application as Non-Enzymatic Glucose Sensor Materials. *Electrochim. Acta* **2010**, *55*, 3734-3740.
- [12] Zhang, X.J.; Wang, G. F.; Zhang, W.; Wei, Y.; Fang, B. Fixure-Reduce Method for the Synthesis of Cu<sub>2</sub>O/MWCNTs Nanocomposites and its Application as Enzyme-Free Glucose Sensor. *Biosens. Bioelectron.* **2009**, *24*, 3395-3398.
- [13] Jin, M. S.; Zhang, H.; Wang, J. G.; Zhong, X. L.; Lu, N.; Li, Z. Y.; Xie, Z. X.; Kim, M. J.; Xia, Y. N. Copper Can Still Be Epitaxially Deposited on Palladium Nanocrystals to Generate Core Shell Nanocubes Despite their Large Lattice Mismatch. *ACS Nano* **2012**, *6*, 2566-2573.
- [14] Kuo, C.H.; Huang, M. H. Morphologically Controlled Synthesis of Cu<sub>2</sub>O Nanocrystals and their Properties. *Nano Today* **2010**, *5*, 106-116.
- [15] Jiang, F.; Wang, S.; Lin, J. J.; Jin, H. L.; Zhang, L. J.; Huang, S. M.; Wang, J. Aligned SWCNT-Copper Oxide Array As a Nonenzymatic Electrochemical Probe of Glucose. *Electrochem. Commun.* **2011**, *13*, 363-365.

- [16] Leng, M.; Yu, C.; Wang, C. Polyhedral Cu<sub>2</sub>O Particles: Shape Evolution and Catalytic Activity on Crosscoupling Reaction of Iodobenzene and Phenol. *Cryst. Eng. Comm.* **2012**, 14, 8454-8461.
- [17] Han, J.; Fang, P.; Dai, J.; Guo, R. One-Pot Surfactantless Route to Polyaniline Hollow Nanospheres with Incontinuous Multicavities and Application for the Removal of Lead Ions from Water. *Langmuir* **2012**, 28, 6468-6475.
- [18] Huang, L. M.; Wang, Z. B.; Wang, H. T.; Cheng, X. L.; Mitra, A.; Yan, Y. S. Polyaniline Nanowires by Electropolymerization from Liquid Crystalline Phases. *J. Mater. Chem.* **2002**, 12, 388-391.
- [19] Olejnik, P.; Gniadek, M.; Palys, B. Layers of Polyaniline Nanotubes Deposited by Langmuir–Blodgett Method. *J. Phys. Chem. C* **2012**, 116, 10424-10429.
- [20] Liu, Z.; Zhang, X. Y.; Poyraz, S.; Surwade, S. P.; Manohar, S.K. Oxidative Template for Conducting Polymer Nanoclips. *J. Am. Chem. Soc.* **2010**, 132, 13158-13159.
- [21] Shi, L.; Liang, R. P.; Qiu, J. D. Controllable Deposition of Platinum Nanoparticles on Polyaniline-Functionalized Carbon Nanotubes. *J. Mater. Chem.* **2012**, 22, 17196-17203.
- [22] Chen, S. G.; Wei, Z. D.; Qi, X. Q.; Dong, L. C.; Guo, Y. G.; Wan, L. J.; Shao, Z. G.; Li, L. Nanostructured Polyaniline-Decorated Pt/C@PANI Core-Shell Catalyst with Enhanced Durability and Activity. *J. Am. Chem. Soc.* **2012**, 134, 13252-13255.
- [23] Kalakodimi, R.P.; Nookala, M. Electrooxidation of Ascorbic Acid on a Polyaniline-Deposited Nickel Electrode: Surface Modification of a Non-Platinum Metal for an Electrooxidative Analysis. *Anal. Chem.* **2002**, 74, 5531-5537.

**Chapter 4 Designed Electrodeposition of Copper Nanoparticles in side/on Conductive Polymers and Applications as Non-enzymatic Glucose Sensor**

- [24] Pandey, R.K.; Lakshminarayanan, V. Electro-Oxidation of Formic Acid, Methanol, and Ethanol on Electrodeposited Pd-Polyaniline Nanofiber Films in Acidic and Alkaline Medium. *J. Phys. Chem. C* **2009**, 113, 21596-21603.
- [25] Valentini, F.; Galache Fernandez, L.; Tamburri, E.; Palleschi, G. Single Walled Carbon Nanotubes/Polypyrrole-Gox Composite Films to Modify Gold Microelectrodes for Glucose Biosensors: Study of the Extended Linearity. *Biosens. Bioelectron.* **2013**, 43, 75-78.
- [26] Leone, A.; Marino, W.; Scharifker, B.R. Electrodeposition and Electrochemical Behavior of Palladium Particles at Polyaniline and Polypyrrole Films. *J. Electrochem. Soc.* **1992**, 139, 438-443.
- [27] Qi, Z.; Shan, J.; Pickup Peter, G. in *Conducting Polymers and Polymer Electrolytes*. *Am. Chem. Soc.* **2002** pp.166-183.
- [28] Armel, V.; Winther-Jensen, O.; Kerr, R.; MacFarlane, D.R.; Winther-Jensen, B. Designed Electrodeposition of Nanoparticles Inside Conducting Polymers. *J. Mater. Chem.* **2012**, 22, 19767-19773.
- [29] Peng, H. C.; Xie, S. F.; Park, J.; Xia, X. H.; Xia, Y. N. Quantitative Analysis of the Coverage Density of Br<sup>-</sup> Ions on Pd{100} Facets and its Role in Controlling the Shape of Pd Nanocrystals. *J. Am. Chem. Soc.* **2013**, 135, 3780-3783.
- [30] Sneed, B. T.; Kuo, C. H.; Brodsky, C. N.; Tsung, C. K. Iodide-Mediated Control of Rhodium Epitaxial Growth on Well-Defined Noble Metal Nanocrystals: Synthesis, Characterization, and Structure-Dependent Catalytic Properties. *J. Am. Chem. Soc.* **2012**, 134, 18417-18426.

**Chapter 4 Designed Electrodeposition of Copper Nanoparticles in side/on Conductive Polymers and Applications as Non-enzymatic Glucose Sensor**

- [31] Niu, W. X.; Xu, G. B. Crystallographic Control of Noble Metal Nanocrystals. *Nano Today* **2011**, 6, 265-285.
- [32] Yanson, Y. I.; Rost, M. J. Structural Accelerating Effect of Chloride on Copper Electrodeposition. *Angew. Chem. Int. Ed.* **2013**, 52, 2454-2458.
- [33] Jain, S.; Surwade, S. P.; S. R. Agnihotra, Dua, V.; Eliason, P. A.; Morose, G. J.; Manohar, S. K. Green Chemistry Synthesis of Nanostructured Poly(2,5-Dimethoxyaniline). *Green Chem.* **2010**, 12, 585-589.
- [34] Grujicic, D.; Pesic, B. Electrodeposition of Copper: The Nucleation Mechanisms. *Electrochim. Acta* **2002**, 47, 2901-2912.
- [35] Yang, J.; Zhang, W. D.; Gunasekaran, S. An Amperometric Non-Enzymatic Glucose Sensor by Electrodepositing Copper Nanocubes onto Vertically Well-Aligned Multi-Walled Carbon Nanotube Arrays. *Biosens. Bioelectron.* **2010**, 26, 279-284.
- [36] Siegfried, M. J.; Choi, K. S. Electrochemical Crystallization of Cuprous Oxide with Systematic Shape Evolution. *Adv. Mater.* **2004**, 16, 1743-1746.

## Chapter 5 Electrochemical Detection of Sulfide: A Review

### 5.1 Introduction

The broad presence of sulfide in nature including biological systems has made the study of sulfide a great interest for chemists [1], biochemists [2], environmentalist [3,4], mineralogists [5] and geochemists [6]. There are two classes of sulfides, i.e., inorganic sulfides and organic sulfides. Many important metals are present in nature combined with sulfur as metal sulfides, such as: cadmium [7], cobalt [8], copper [9], lead [10], molybdenum [11], nickel [12], zinc [13] and iron [14]. For mineralogists and geochemists, determining the sulfides context is a key to understand the formation mechanism and the geological processes by which certain ore deposits have formed [15]. For chemical engineers, the sulfide within oil and gas reserves can pose problems throughout the petroleum industry [16]. The potential hazards faced by workers involved in the processing of sulfide contaminated feedstock has meant that there is a pressing need for the development of fast and sensitive detection technologies [17]. Over the centuries, there is widespread awareness of the toxicity of sulfide in its liberated hydrogen sulfide ( $\text{H}_2\text{S}$ ) form [18, 19]. Even at a low concentration,  $\text{H}_2\text{S}$  can lead to personal distress, while at a higher concentration it can result in loss of consciousness, permanent brain damage or even death due to the neurotoxic effect of the gas [20, 21].

In the last ten years, hydrogen sulphide has also been identified as an important endogenous signaling molecule [22], which has provided attractive opportunities for  $\text{H}_2\text{S}$  to be developed into an innovative class of drugs [23, 24]. Moreover, hydrogen sulfide was discovered as an oxygen sensor in trout gill chemoreceptors, where the balance between constitutive production and oxidation, tightly couples tissue [ $\text{H}_2\text{S}$ ] to  $\text{Po}_2$  and may provide an

exquisitely sensitive, yet simple, O<sub>2</sub> sensor in a variety of tissues [25]. In addition to inorganic sulfide, organic sulfide, such as biological thiols play crucial roles in biological systems for their biological activity [26]. In addition, the abnormal levels of sulfide in the human body have been implicated in the aetiology of several diseases [27, 28].

As a result, the detection of hydrogen sulfide has gained significant importance within the analytical community as both a consequence of its toxicity, its biological/physiological roles and its therapeutic potential [29].

## 5.2 Classical Detection Methods

Table 1. Different methods used in different periods

Time Range	Methods	Advantages	Disadvantages
1970s	Titration with iodine [29]	Simplicity	Significant limitations
1980s	Methylene blue test [30]	Simplicity Selectivity Sensitivity	Interferences from light and nitrogen dioxide
1990s	UV [37], Fluorescence [38], HPLC [40]	Selectivity Sensitivity	Time consuming Large scale instruments
2000s-now	Atomic spectroscopic [43], Chemiluminescent [44], Ion-chromatographic [47]	Sensitivity Selectivity	Time consuming Large scale instruments

In the last four decades, various techniques have been successfully developed to measure sulfide in a variety of media even down to nanomolar concentrations. Since the 1970s, for example, the titration of sulfide with iodine has become a classical approach to sulfide determination [30]. Unfortunately, the simplicity of this method comes with

limitations in terms of sensitivity and selectivity when dealing with real world samples. Then, in the late 1800's, the methylene blue test was developed as the most common approach to the analysis of sulfide [31, 32]. This basic test, which involves the reaction of aqueous sulfide with *N,N*-dimethylphenyl-1,4-diamine in the presence of a small quantity of ferric ions giving rise to a characteristic blue coloration, retains significant analytical value today in terms of simplicity, selectivity, and sensitivity [17]. However, the methylene blue method has some limitations due to interferences from photosensitivity, cross-reactivity with nitrogen dioxide, aggregate formation (dimer, trimers or *n*-mers) leading to deviations from Beer's law, as well as pH artifacts that erroneously affect absorbance readings [33-36]. After the 1990s, a number of investigation, such as, UV/visible absorption spectroscopy [37], fluorescence [38], and HPLC [40] techniques have led to substantial improvements in sensitivity. For example, with the fluorescence method the signal is linear over the range 0.75-15.0 mg l<sup>-1</sup> of injected sulfide, with a limit of detection of 0.08 mg l<sup>-1</sup> injected sulfide when 9.0 M H<sub>2</sub>SO<sub>4</sub> is used in the *N,N*-dimethyl-*p*-phenylenediamine (DMPD) carrier stream [39]. Infrared spectroscopy has also been applied to the quasi-direct determination of sulphide [41]. Over the past decade, a variety of analytical methods for determining sulfides have been reported [42]. Atomic spectroscopic techniques [43] and chemiluminescent [44] approaches have been investigated in the analysis of reduced sulfur species such as dimethylsulfide. Spectrophotometric method still played an important role in the detection of sulfide [45, 46]. Ion-chromatographic techniques were also developed as a useful method to determine sulfides such as hydrosulfuric acids [47]. In addition, Raman spectroscopy has also been used to measure sulphide. In the Raman studies, methemoglobin was bound to non-functionalized carbon nanotubes. The subsequent addition of H<sub>2</sub>S resulted in significant

changes to the Raman spectrum of the carbon nanotubes-hemoglobin complexes. These studies suggest that carbon nanotubes-hemoglobin complexes can potentially be utilized as biosensors to measure H<sub>2</sub>S in blood [48, 49]. More recently, our group introduced a method based on the selective permeability of polydimethylsiloxane (PDMS) to detect free H<sub>2</sub>S [50].

### 5.3 Electrochemical Methods

Notably, the above classical methods require complex instrumentation and are time-consuming. The electrochemical methods on the other hand offer distinct advantages of high sensitivity, rapidity, affordable instrumentation and relatively simpler procedures. As a result there has been renewed interest in developing new electrochemical methods to determine sulfides both in the inorganic and organic forms.

#### 5.3.1 Anodic Stripping Voltammetry

In 2011, Huang and co-workers introduced an indirect determination method for sulfide in water samples by anodic stripping voltammetry (ASV) [51]. Three-electrode system was used in their electrochemical experiment, utilizing a bismuth-film glassy carbon electrode (BiEFs) as the working electrode, saturated calomel as the reference electrodes (SCE) and platinum wire as the counter electrode. There are two steps in the operation. In the first step, the working electrode was deposited 120s under a preconcentration potential of -1.2 V while stirring in 25 mL of 0.1 M pH 4.5 NaAc-HAc containing a certain amount of Cd<sup>2+</sup>. Then, the linear sweep curve between -1.0 V and -0.5 V was performed in the same solution to get the modified working electrode. In the second step, different amount of S<sup>2-</sup> was added into above solution for ASV.



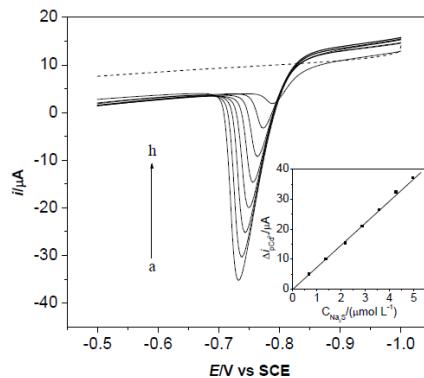


Figure 5.1 The ASV response of  $\text{Cd}^{2+}$  changed with the addition of sulfide. 0.1 M PH 4.5 NaAc-HAc(---base line) buffer solution at  $3.6 \times 10^{-6}$  M; a-h:  $C_{\text{S}^{2-}}^* = 0, 0.7, 1.4, 2.2, 2.9, 3.6, 4.3, 5.0 \times 10^{-6}$  M. Insert: plot of the relation between the peak current of  $\text{Cd}^{2+}$  and the concentration of sulfide added.

The principle for sulfide determination by ASV is based on the interaction between  $\text{Cd}^{2+}$  and  $\text{S}^{2-}$  to form CdS precipitate, therefore, the concentration of sulfide can be determined by the peak current of  $\text{Cd}^{2+}$ . As can be seen from Figure 5.1, the peak current of  $\text{Cd}^{2+}$  decreased while more  $\text{S}^{2-}$  added into the solution, and  $\Delta i_{\text{pCd}^{2+}}$  has a linear relationship with the concentration of sulfide. This proposed method can determine  $\text{S}^{2-}$  in the range of  $(0.7-5.0) \times 10^{-6}$  M (Figure 1) with a limit of detection (LOD) of  $2.1 \times 10^{-7}$  M and a relative standard deviation (RSD) of 3.6% for  $1.7 \times 10^{-6}$  M. The advantages of this method are affordable instrument and simple manipulation. It has been successfully applied to the determination of  $\text{S}^{2-}$  in different water matrices.

### 5.3.2 Amperometric Method

Amperometry is another attractive technique to obtain sensitive and fast-responsive results. Savizi et al. developed an amperometric inhibition biosensor for the determination of sulfide [52]. This biosensor was fabricated by immobilizing coprinus cinereus peroxidase (CIP) on the surface of screen printed electrode (SPE). Chitosan/acrylamide was applied for

the immobilization of peroxidase on the working electrode. The amperometric measurement was performed at an applied potential of  $-150$  mV versus Ag/AgCl in the presence of hydroquinone as an electron mediator and  $0.1$  M phosphate buffer solution of pH 6.5. Current inhibition with different concentrations of sulfide and a linear response of the elevation of sulfide concentration to the inhibition of current were shown in Figure 2. The determination range of sulfide can be achieved between  $1.09$   $\mu\text{M}$  and  $16.3$   $\mu\text{M}$  with a detection limit of  $0.3$   $\mu\text{M}$  (Figure 5.2). This biosensor has also been successfully tested for the analysis of environmental water samples.

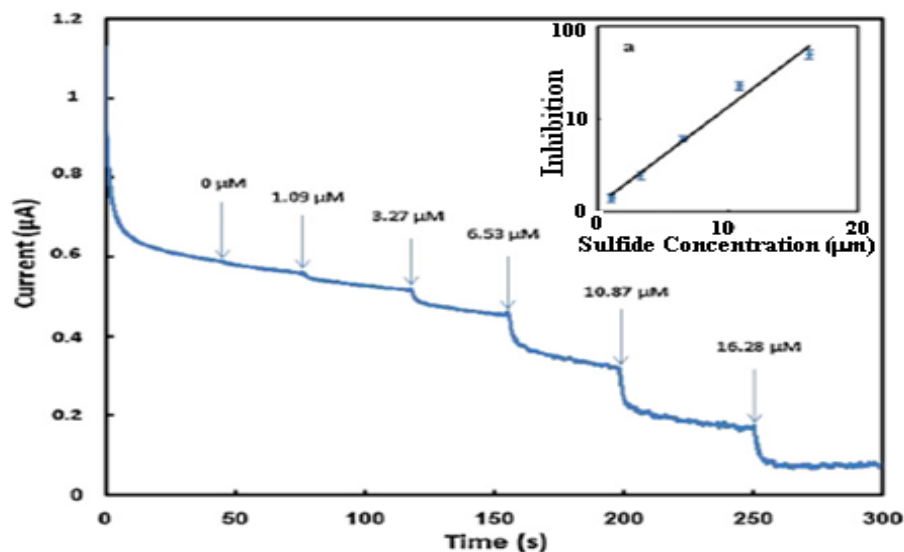


Figure 5.2 Amperometric response of CIP biosensor for different concentrations of sulfide at  $-150$  mV vs. Ag/AgCl in  $0.1$  M phosphate buffer (PH 6.5) solution containing  $0.6\text{mM}$   $\text{H}_2\text{O}_2$  and  $1.25$  mM of hydroquinone. Inset (a): calibration curve for sulfide determination with CIP inhibition sensor.

Though this method has the advantage of quicker response time against sulfide, the disadvantage is the poor selectivity.  $\text{Fe}^{3+}$  and  $\text{Cd}^{2+}$  have significant interference with the detection of sulfide and the error caused by  $\text{CN}^-$  is up to 43.25%.

Chang, etc. have reported that they have used hydrodynamic chronoamperometry to detection sulfide at a highly stable  $\text{Fe}(\text{CN})_6^{3-}$ -immobilized polymeric ionic liquid-modified electrode (designated as FeCN-PIL-SPCE) [53]. Under a detection potential of 0.0 V in pH 7 PBS buffer solution, a linear calibration in the range of 1  $\mu\text{M}$  up to 3 mM with a limit detection (S/N=3) of 12.9 nM was obtained (Figure 5.3A). As shown in Figure 3B, the relative standard deviations are all less than 5 % for various concentrations of sulfide, which demonstrate that the FeCN-PIL-SPCE electrode is stable and reproducible toward the detection of sulfide.

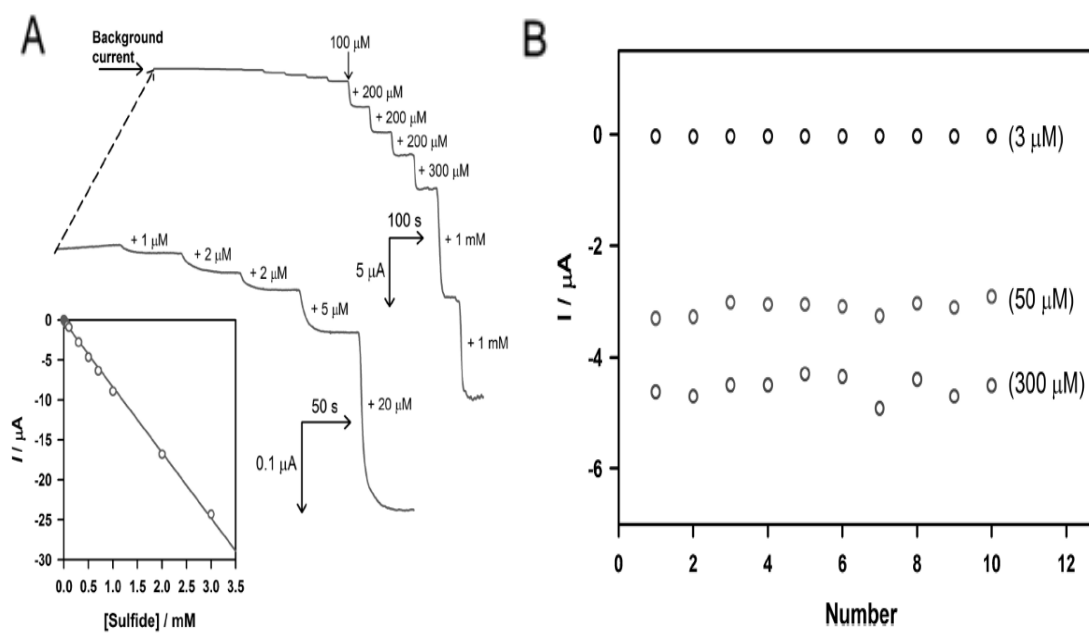


Figure 5.3 (A) Chronoamperometric response of sulfide at the FeCN-PIL-SPCE in pH 7, 0.1 M PBS at a detection potential of 0.0 V vs. Ag/ AgCl. The insert graph is the calibration curve with a linear concentration range of 1  $\mu\text{M}$  to 3 mM. (B) The results at the FeCN-PIL-SPCE for 10 continuous additions of 3  $\mu\text{M}$ , 50  $\mu\text{M}$  and 300  $\mu\text{M}$  sulfide, respectively.

The proposed system shows good selectivity in real sample analysis. Practical test of the above system include the determination of sulfide content in hot spring water and ground water.

### 5.3.3 Cyclic Voltammetry

Cyclic voltammetry (CV) is another useful and widely applied method in the field of electrochemical detection of sulfide [54]. Qi and co-workers have shown the rapid detection of sulfide on reduced graphene sheets (RGS) modified GC electrodes by CV in 2011 [55]. The morphology and electrochemical properties of the RGS were characterized by atomic force microscopy (AFM) and CV. The AFM results indicate that the fascinating electrical properties maybe due to the nanosized sheets which are single-layer sheets contained of a large amount of open graphitic edge planes [56, 57]. The CV detection at RGCs/GC electrodes with 0.5 mM sulfide at various scan rates indicated the adsorption-controlled kinetic of this system. The stability of the RGSs/GC electrodes was studied by repeating the determination of 0.5 mM sulfide at set intervals for 22 h with a scan rate of  $0.1 \text{ V s}^{-1}$  in a potential range of -0.6-0.8 V in 0.2 M PBS buffer solution (pH 7.4). The results showed good reproducibility for the detection of sulfide.

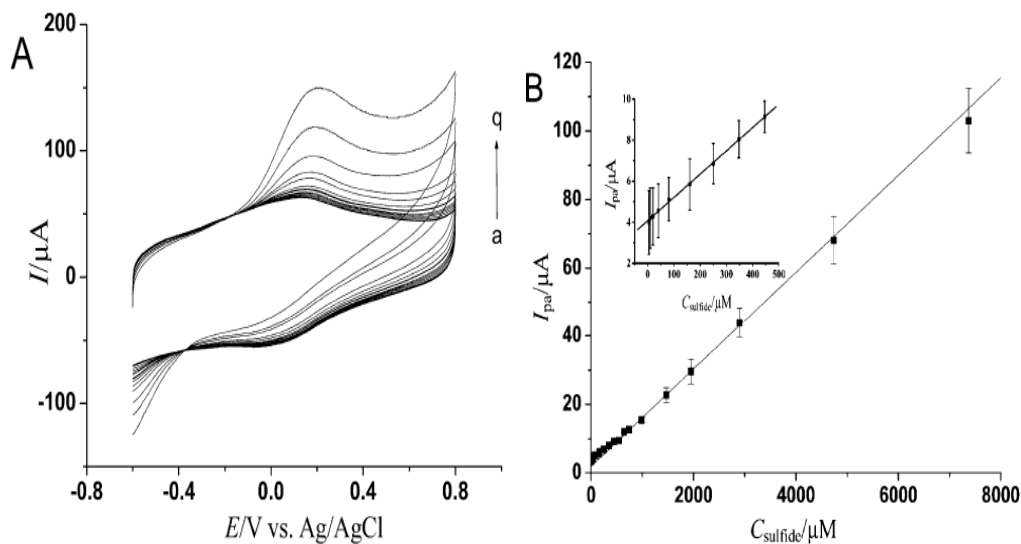


Figure 5.4 (A) Cyclic voltammograms of RGSs/GC electrode in 0.2 M PBS (pH 7.4) containing different concentrations of sulfide of (a)  $5 \times 10^{-3}$ , (b)  $1.0 \times 10^{-2}$ , (c)  $2.0 \times 10^{-2}$ , (d)  $4.0 \times 10^{-2}$ , (e)  $8.0 \times 10^{-2}$ , (f) 0.16, (g) 0.25, (h) 0.35, (i) 0.45, (j) 0.54, (k) 0.74, (l) 0.98, (m) 1.47, (n) 1.95, (o) 2.9, (p) 4.7, (q) 7.4 mM. (B) The changes of  $I_{pa}$  versus concentrations of sulfide ranging from  $5 \times 10^{-3}$  to 7.4 mM. Inset: Plot of changes of  $I_{pa}$  versus concentration of sulfide ranging from  $5 \times 10^{-3}$  to 0.45 mM.

It can be seen from Figure 5.4A that the oxidation peak current increases with the increase of sulfide concentration. Figure 5.4B showed the detection limit was  $4.2 \times 10^{-3}$  mM with a linear correlation coefficient of 0.999 and the detection range was between  $5 \times 10^{-3}$  and 7.4 mM. The analytical application has been assessed for the direct determination of sulfide in water samples. The recovery of sulfide was in the range of 97.62 % and 106.90 %, indicating that the sensor is sufficient for practical application.

Another study utilizing the CV method to detect sulfide was reported by Paim and Stradiotto [58]. They modified a glassy carbon electrode with cobalt pentacyanonitrosylferrate (CoPCNF) film. The redox couple of the CoPCNF film presented an electrocatalytic response to sulfide in aqueous solution and the analytical curve was linear

in the concentration range of  $7.5 \times 10^{-5}$  to  $7.7 \times 10^{-4}$  M with a detection limit of  $4.6 \times 10^{-5}$  M for sulfide ions in 0.5 M  $\text{KNO}_3$  solution. Compared with other electrochemical systems, a wide linear range was observed here. Furthermore, CV method can provide much more information than other electrochemical methods. For example, the anodic current might change linearly with the square root of the scan rate, indicating diffusion-controlled kinetics [59]. The transfer electron number, the redox potential and the surface coverage [60] can also obtain from the CV spectrum. However, the sensitivity and the detection limit of  $4.6 \times 10^{-5}$  M were not as good as other methods mentioned above.

#### 5.3.4 Photoelectrochemical Method

A facile and effective photoelectrochemical method has been developed for in situ determination of aqueous  $\text{H}_2\text{S}$  based on the deposition of CdS nanoclusters onto  $\text{TiO}_2$  nanotubes by Li [61]. Their article demonstrated that the photocurrent produced by bare  $\text{TiO}_2$  is negligible compared with that from CdS/  $\text{TiO}_2$  films. Moreover the photocurrent increased with the increasing amount of CdS nanoclusters which were deposited onto  $\text{TiO}_2$  nanotubes exposing in  $\text{CdSO}_4$  solution with the increased concentration of  $\text{Na}_2\text{S}$ . The good linearity of logarithm photocurrent intensity versus the logarithm concentration of  $\text{Na}_2\text{S}$  was also obtained. This work exhibited a broad linear range for  $\text{H}_2\text{S}$  detection from  $1 \times 10^{-8}$  to  $1 \times 10^{-3}$  M. The detection limit was 0.31 nM (~9.92 ppt), far lower than other methods. The most obvious advantages of this approach are high sensitivity, broad linear range and a low detection limit. In addition, because of the good selectivity, this method can be applied to detect sulfide in complex samples.

### 5.3.5 Electrochemical Detection Methods Coupled with Other Devices

Recently, increasing number of groups have attempted to couple electrochemical detection methods to other devices for the direct routine sensitive and simultaneous measurement of aminothiols, disulfides, and thioethers in either plasma or tissue homogenates [62-65].

As was mentioned before, the amperometric detection (AD) technique is a highly sensitive electrochemical method to detect sulfide. However, the capillary electrophoresis (CE) analysis combined with AD technique can achieve unparalleled sensitivity up to attomole levels. Particularly, recent advances in the microfabrication techniques make the development of on-chip CE devices coupled with electrochemical detection methods quicker. Recently, Chand and co-workers published an article dealing with separation, aliquot and detection of amino thiols on a microchip capillary electrophoresis with electrochemical detection in a microchannel [62]. The advantages of the modified microchannel are that it can collect the separated thiols in different reservoirs for further analysis and also ignore the need of electrode regeneration, which are totally different with conventional capillary electrophoresis. In Chand's work, the gold electrodes which were fabricated on glass wafers were used to separate and detect thiols, while microchannels were laid in PDMS. The microchannel had an inverted double Y-shaped structure which was required to easily store the separated analytes in different reservoirs. They also fabricated a potentiostat array to simultaneously detect analytes in different channels. The CE-AD microchip in Chand's work was fabricated by standard photolithographic procedures [66]. The chip was built on a single soda lime glass substrate with microchannel engraved in PDMS. There were three sets of a three-electrode system (working electrode, reference electrode and counter electrode) in the

CE-AD microchip and were used for electrochemical detection; in addition, electrodes for applying separation electric field were fabricated on the soda lime glass wafer using the vacuum thermal evaporation method [67]. After completion, the PDMS mold carrying microchannel was linked to the glass substrate containing Au microelectrodes by UV-ozone treatment. The configuration of the CE-AD microchip is shown in Figure 5.5.

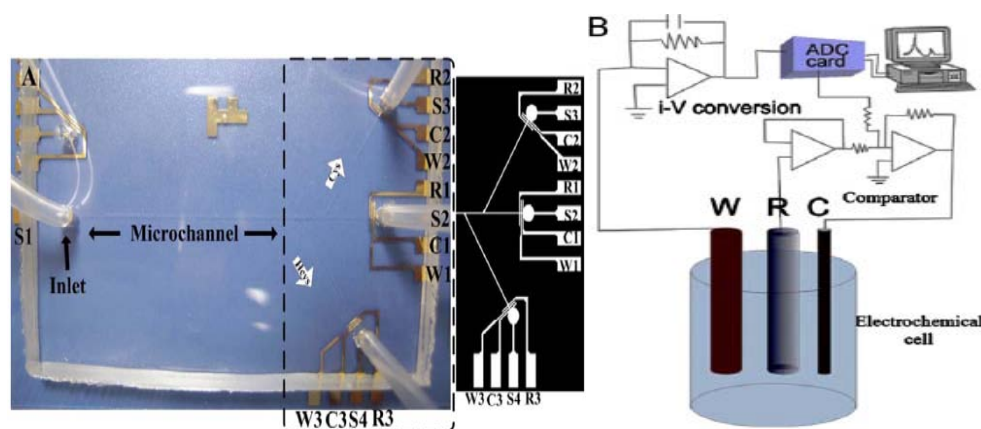


Figure 5.5 (A) Image of CE-AD microchip showing microchannel engraved in PDMS mold, sample reservoirs, silicon tubes carrying sample and NaOH solution into the microchannel, gold microelectrodes (W1-3=working; C1-3=counter; R1-3=reference; S1-4= separation electrodes). (B) Schematics for electronic circuit and the operation of the in-house built dual potentiostat.

Electrochemical measurements included cyclic voltammetry and chronoamperometry (*i-t* curve). The CV analysis of cysteine (Cys) and homocysteine (Hcys) was the pre-requisite in order to find the detection voltage to be applied in the CE-AD procedure, as well as the peak current range that the chemicals would generate. The CV experiments were employed separately in a 0.1 M NaOH solution with 100  $\mu$ M Cys and Hcys, respectively. A stable voltammogram demonstrated no sign of thiols depositing on the electrode surface. From the CV curves, Cys and HCys produced defined oxidation peaks in the anodic scan at 0.42 and



0.48 V, respectively. Hence, a detection voltage of 0.5 V was applied to detect the sample in straight microchannel. Then, a small volume of a 2  $\mu\text{L}$  mixture containing 5  $\mu\text{M}$  Cys and HCys each were injected into the reservoir and subsequently analyzed on the microfluidic chip at 0.5 V. The resulting electropherogram showed that the migration times of Cys and HCys were 280 s and 345 s, respectively. Thus, it proved the effectiveness of using such a device in the separation of Cys and HCys. For the simultaneous detection of both Cys and Hcys, they injected 2  $\mu\text{L}$  of an equiproportionate mixture of Cys and HCys into a fresh device filled with 1.5% (w/v) agarose gel and applied an initial separation voltage between the inlet and outlet reservoir of the straight channel. The electric field was switched in the direction of outlet of the branched channels after 230 s. Thereafter, the detection voltage was set to 0.42 V and 0.48V for Cys and HCys, respectively, which was obtained from CV figures. In order to accurately calibrate the system for quantitative analysis, the calibration plots which were obtained for each analyte over a concentration range of 0.1-5  $\mu\text{M}$  represented a typical sigmoidal correlation between peak current and concentration. A linear response was obtained for a range from 0.5  $\mu\text{M}$  to 3  $\mu\text{M}$  and the calculated limit of detection (LOD) for the sensor was 0.05  $\mu\text{M}$  ( $S/N=3$ ). Compared with other conventional CE or flow injection based detection procedures, the advantages of this method were the lower separation voltage [68], the lower limit of detection [69] and the higher peak resolution [70]. This CE-AD device has been successfully tested for the detection of amino thiols in real blood samples without the need of any sample pretreatments.

In addition, HPLC coupled to electrochemical detection (HPLC-ECD) is another sensitive approach that was recently developed for the direct measurement of thiols, disulfides and thioethers [63]. Bailey et al. introduced two different methods using reversed-

phase HPLC with the electrochemical detection on a boron-doped diamond (BDD) working electrode for the direct, routine, sensitive and simultaneous measurement of a number of aminothiols, disulfides, and thioethers, in either plasma or tissue.<sup>49b</sup> Firstly, the hydrodynamic voltammograms (HDVs) for aminothiols, thioethers, and disulfides were obtained to illustrate that the optimal applied potential for the detection of these compounds on BDD electrode was approximately +1500 mV (vs. palladium reference electrode). Then the analysis of various concentrations of aminothiols using HPLC with a BDD electrode produced a linear response curve, which showed the limit of detection (LOD) was about 0.66 nM (on column). The analysis of a typical plasma sample using the plasma chromatography method showed that the plasma levels of glutathione (GSH) and glutathione disulfide (GSSG) were 4.5 nM and 0.59 nM, respectively. The analysis of GSH and GSSG in rat brain and liver samples were also presented as 0.204  $\mu$ M, 9.04 nM, 3.659  $\mu$ M and 35.68 nM, respectively.

Table. 2 Different analytical characteristics by different electrochemical method

Electrochemical method	WE	LOD	Detection range	Real application
Anodic stripping voltammetry	BiEFs [51]	0.21 $\mu\text{M}$	0.7-5.0 $\mu\text{M}$	Sulfide in water
Amperometric method	CIP biosensor [52]	0.3 $\mu\text{M}$	1.09-16.3 $\mu\text{M}$	Sulfide in water
	FeCN-PIL-SPCE [53]	12.9 nM	1 $\mu\text{M}$ - 3 mM	Sulfide in water
Cyclic voltammetry	RGSs/GC [55]	4.2 $\mu\text{M}$	$5 \times 10^{-3}$ -7.4 mM	Sulfide in water
	CoPCNF/GC [58]	46 $\mu\text{M}$	75-770 $\mu\text{M}$	
Photoelectrochemical method	CdS/TiO <sub>2</sub> [61]	0.31 nM	$1 \times 10^{-8}$ - $1 \times 10^{-3}$ M	aqueous H <sub>2</sub> S in water
CE-AD	Gold [62]	0.05 $\mu\text{M}$	0.5 $\mu\text{M}$ to 3 $\mu\text{M}$	Aminothiols in real blood
HPLC-ECD	BDD [63]	0.66 nM		Aminothiols, disulfides and thioethers in plasma or tissue

WE, working electrode; LOD, limit of detection; CE-AD, capillary electrophoresis combined with amperometric detection; HPLC-ECD, High Performance Liquid Chromatography with electrochemical detection.

## 5.4 Summary

Many of the electrochemical methods discussed here to detect sulfide, including inorganic sulfide and organic sulfide, with different working electrodes, showed different analytical characteristics (Table 2). It can be seen from the table that cyclic voltammetry was observed with the highest limit of detection (4.2  $\mu\text{M}$ ), yet it also had very broad detection

range. In other words, CV can be used to detect a high concentration of sulfide. On the other hand, the photo-electrochemical method is uniquely capable of detecting sulfide when the concentration is extremely low, as the limit of detection is 0.31 nM and the detection range is from  $1 \times 10^{-8}$  to  $1 \times 10^{-3}$  M. The amperometric method is another sensitive method to detect sulfide in water. The limit of detection was only 12 nM with FeCN-PIL-SPCE working electrode. In addition, electrochemical techniques coupled with other devices such as capillary electrophoresis or HPLC developed into more promising methods to test organic sulfide in real blood and other bodily fluids and tissues.

In conclusion, there is a sufficiently large range of electrochemical techniques developed recently for sulfide detection. Compared with non-electrochemical techniques, the electrochemical techniques reported here are clearly superior with respect to sensitivity, selectivity, portability of the instrumentation and the relative ease of use. In the future, the development of new electrochemical technology, such as using new types of Q-dots or the other nano-particles based electrochemical detection methods, or the application of new modified sensors, will make electrochemical detection of sulphide even more specific and efficient.

## References

- [1] Bineesh, K. V.; Kim, M.-i.; Lee, G.-H.; Selvaraj, M.; Hyun, K.; Park, D.-W. Production of Elemental Sulfur and Ammonium Thiosulfate by the Oxidation of H<sub>2</sub>S Containing Water Vapor and Ammonia Over V/Zr-PILC Catalysts. *J. Ind Eng Chem* **2012**, 18, 1845-1850.
- [2] Gruhlke, M. C. H.; Slusarenko, A. J., The Biology of Reactive Sulfur Species (RSS). *Plant Physiol. Bioch.* **2012**, 59, 98-107.
- [3]. Sheng, Y.; Chen, F.; Yu, Y.; Wang, X.; Sheng, G.; Fu, J.; Zeng, E. Y., Emission of Volatile Organic Sulfur Compounds from a Heavily Polluted River in Guangzhou, South China. *Environ. Monit. Assess.* **2008**, 143, 121-130.
- [4] Joseph, A. P.; Keller, J.; Bustamante, H.; Bond, P. L., Surface Neutralization and H<sub>2</sub>S Oxidation at Early Stages of Sewer Corrosion: Influence of Temperature, Relative Humidity and H<sub>2</sub>S Concentration. *Water Res.* **2012**, 46, 4235-4245.
- [5] Hettmann, K.; Wenzel, T.; Marks, M.; Markl, G., The Sulfur Speciation in S-Bearing Minerals: New Constraints by a Combination of Electron Microprobe Analysis and DFT Calculations With Special Reference to Sodalite-Group Minerals. *Am. Mineral.* **2012**, 97, 1653-1661.
- [6] Yin, H.-B.; Fan, C.-X.; Ding, S.-M.; Zhang, L.; Li, B.; Liu, X.-B., Distribution Characteristic and Correlation Relationship of Reactive Sulfur and Heavy Metals in Sediments of Meiliang Bay and Wuli Lake of Taihu Lake. *Huan jing ke xue* **2008**, 29, 1791-1796.
- [7] Ehsan, M. A.; Ming, H. N.; Misran, M.; Arifin, Z.; Tiekink, E. R. T.; Safwan, A. P.; Ebadi, M.; Basirun, W. J.; Mazhar, M., Effect of AACVD Processing Parameters on the

Growth of Greenockite (CdS) Thin Films using a Single-Source Cadmium Precursor. *Chem. Vapor Depos.* **2012**, 18, 191-200.

[8] Muchez, P.; Corbella, M., Factors Controlling the Precipitation of Copper and Cobalt Minerals in Sediment-Hosted Ore Deposits: Advances and Restrictions. *J. Geochem. Explor.* **2012**, 118, 38-46.

[9] Zhao, S.; Peng, Y., The Oxidation of Copper Sulfide Minerals During Grinding and Their Interactions with Clay Particles. *Powder Technology* **2012**, 230, 112-117.

[10] Yuan, W.; Li, J.; Zhang, Q.; Saito, F., Mechanochemical sulfidization of lead oxides by grinding with sulfur. *Powder Technol.* **2012**, 230, 63-66.

[11] Belin, S.; Chevrel, R.; Sergent, M., Structure of Mo<sub>7</sub>S<sub>8</sub>: A new binary sulfide synthesized by self molybdenum intercalation. *Mater. Res. Bull* **1998**, 33, 43-57.

[12] Barnes, S. J.; Fiorentini, M. L.; Fardon, M. C., Platinum Group Element and Nickel Sulphide Ore Tenors of the Mount Keith Nickel Deposit, Yilgarn Craton, Australia. *Mineralium Deposita* **2012**, 47, 129-150.

[13] Yao, J.; Li, Y.; Li, N.; Le, S., Theoretical investigations of the effect of vacancies on the geometric and electronic structures of zinc sulfide. *Physica B.* **2012**, 407, 3888-3892.

[14] Rodriguez, M. M.; Stubbert, B. D.; Scarborough, C. C.; Brennessel, W. W.; Bill, E.; Holland, P. L., Isolation and Characterization of Stable Iron(I) Sulfide Complexes. *Angew. Chem. Int. Edit.* **2012**, 51, 8247-8250.

[15] Krivolutskaya, N. A.; Sobolev, A. V.; Snisar, S. G. e.; Gongalskiy, B. I.; Kuzmin, D. V.; Hauff, F.; Tushentsova, I. N.; Svirskaya, N. M.; Kononkova, N. N.; Schlychkova, T. B. Mineralogy, Geochemistry and Stratigraphy of the Maslovsky Pt-Cu-Ni Sulfide Deposit,

Noril'sk Region, Russia Implications for Relationship of Ore-Bearing Intrusions and Lavas. *Miner. Deposita* **2012**, 47, 69-88.

[16] Tang, K.; Baskaran, V.; Nemati, M., Bacteria of The Sulphur Cycle: An Overview of Microbiology, Biokinetics and their Role in Petroleum and Mining Industries. *Biochem. Eng. J.* **2009**, 44, 73-94.

[17] Lawrence, N. S.; Davis, J.; Compton, R. G., Analytical Strategies for the Detection of Sulfide: a Review. *Talanta* **2000**, 52, 771-784.

[18] Reiffenstein, R. J.; Hulbert, W. C.; Roth, S. H., Toxicology of Hydrogen-Sulfide. *Annu. Rev. Pharmacol.* **1992**, 32, 109-134.

[19] Evans, C. L., Toxicity of Hydrogen Sulfide and Other Sulphides. *Q. J. Exp. Physiol. CMS.* **1967**, 52, 231-248.

[20] Gunn, B.; Wong, R., Noxious Gas Exposure in the Outback: Two Cases of Hydrogen Sulfide Toxicity. *Emergen. Med.* **2001**, 13, 240-246.

[21] Kimura, H., Hydrogen Sulfide As a Neuromodulator. *Mol. Neurobiol.* **2002**, 26, 13-19.

[22] Benavides, G. A.; Squadrito, G. L.; Mills, R. W.; Patel, H. D.; Isbell, T. S.; Patel, R. P.; Darley-USmar, V. M.; Doeller, J. E.; Kraus, D. W. Hydrogen Sulfide Mediates the Vasoactivity of Garlic. *P. Natl. Acad. Sci. USA* **2007**, 104, 17977-17982.

[23] Wang, R. Physiological Implications of Hydrogen Sulfide: A Whiff Exploration That Blossomed. *Physiol. Rev.* **2012**, 92, 791-896.

[24] Martelli, A.; Testai, L.; Breschi, M. C.; Blandizzi, C.; Viridis, A.; Taddei, S.; Calderone, V. Hydrogen Sulphide: Novel Opportunity for Drug Discovery. *Med. Res. Rev.* **2012**, 32, 1093-1130.

- [25] Olson, K. R.; Healy, M. J.; Qin, Z.; Skovgaard, N.; Vulesevic, B.; Duff, D. W.; Whitfield, N. L.; Yang, G.; Wang, R.; Perry, S. F. Hydrogen Sulfide As an Oxygen Sensor in Trout Gill Chemoreceptors. *Am. J. Physiol-Reg I.* **2008**, 295, R669-R680.
- [26] Yuan, L.; Lin, W.; Xie, Y.; Zhu, S.; Zhao, S., A Native-Chemical-Ligation-Mechanism-Based Ratiometric Fluorescent Probe for Amino Thiols. *Chemistry (Weinheim an der Bergstrasse, Germany)* **2012**, 18, 14520-6.
- [27] Seshadri, S.; Beiser, A.; Selhub, J.; Jacques, P. F.; Rosenberg, I. H.; D'Agostino, R. B.; Wilson, P. W. F.; Wolf, P. A. Plasma Homocysteine as a Risk Factor for Dementia and Alzheimer's Disease. *New Engl. J. Med.* **2002**, 346, 476-483.
- [28] Ueland, P. M.; Vollset, S. E., Homocysteine and Folate in Pregnancy. *Clin. Chem.* **2004**, 50, 1293-1295.
- [29] Faccenda, A.; Bonham, C. A.; Vacratsis, P. O.; Zhang, X.; Mutus, B. Gold Nanoparticle Enrichment Method for Identifying S-Nitrosylation and S-Glutathionylation Sites in Proteins. *J. Am. Chem. Soc.* **2010**, 132, 11392-11394.
- [30] Khalifa, H.; Abdelghani, N. T.; Rizk, M. S. Use of Iodate and Periodate With Iodide in the Potentiometric Titration of Arsenite, Sulfide, and Sulfite With Mercury (II). *Microchem. J.* **1979**, 24, 310-315.
- [31] Leggett, D. J.; Chen, N. H.; Mahadevappa, D. S. Flow-Injection Method For Sulfide Determination By the Methylene-Blue Method. *Anal. Chim. Acta* **1981**, 128, 163-168.
- [32] Rauh, W.; Hammje, K., Hydrogen Sulfide Determination in Atmospheric Air--Improvement of the Methylene Blue Procedure. *Zeitschrift fur die gesamte Hygiene und ihre Grenzgebiete* **1983**, 29, 159-63.



- [33] Kleemann, D. Experimental Investigations of Photodynamic Treatment of Malignant-Tumors of Oral Cavity, Pharynx, and Larynx With Photosensitizer Methylene-Blue. *Laryngo-Rhino-Otol.* **1990**, 69, 437-439.
- [34] Lai, W. C.; Dixit, N. S.; Mackay, R. A. Formation of H Aggregates of Thionine Dye In Water. *J. Phys. Chem-Us* **1984**, 88, 5364-5368.
- [35] Brown, K. A.; McGreer, E. R.; Taekema, B.; Cullen, J. T. Determination of Total Free Sulphides in Sediment Porewater and Artefacts Related to the Mobility of Mineral Sulphides. *Aquat. Geochem.* **2011**, 17, 821-839.
- [36] Sidi, A.; Paulus, D. A.; Rush, W.; Gravenstein, N.; Davis, R. F. Methylene-Blue and Indocyanine Green Artif Actually Lower Pulse Oximetry Readings of Oxygen-Saturation - Studies in Dogs. *J. Clin. Monitor.* **1987**, 3, 249-256.
- [37] Kuban, V.; Dasgupta, P. K.; Marx, J. N. Nitroprusside and Methylene-Blue Methods for Silicone Membrane Differentiated Flow-Injection Determination of Sulfide in Water and Waste-Water. *Anal. chem.* **1992**, 64, 36-43.
- [38] Eroglu, A. E.; Volkan, M.; Ataman, O. Y. Fiber Optic Sensors Using Novel Substrates for Hydrogen Sulfide Determination by Solid Surface Fluorescence. *Talanta* **2000**, 53, 89-101.
- [39] Spaziani, M. A.; Davis, J. L.; Tinani, M.; Carroll, M. K. On-line determination of sulfide by the 'methylene blue method' with diode-laser-based fluorescence detection. *The Analyst* **1997**, 122, 1555-1557.
- [40] Tang, D. G.; Santschi, P. H. Sensitive Determination of Dissolved Sulfide in Estuarine Water by Solid-Phase Extraction and High-Performance Liquid Chromatography of Methylene Blue. *J. Chromatogr. A.* **2000**, 883, 305-309.

- [41] Isoniemi, E.; Pettersson, M.; Khriachtchev, L.; Lundell, J.; Rasanen, M. Infrared Spectroscopy of H<sub>2</sub>S and SH in Rare-Gas Matrixes. *J. Phys. Chem. A*. **1999**, 103, 679-685.
- [42] Shan, D.; Li, Q.-B.; Ding, S.-N.; Xu, J.-Q.; Cosnier, S.; Xue, H.-G. Reagentless Biosensor for Hydrogen Peroxide Based on Self-Assembled Films of Horseradish Peroxidase/Laponite/Chitosan and the Primary Investigation on the Inhibitory Effect by Sulfide. *Biosens. Bioelectron.* **2010**, 26, 536-541.
- [43]. Hoppstock, K.; Lippert, H., An Improved Gas-Liquid Separator for the Selective Determination of Sulfide by ICP-OES Using the Evolution of Hydrogen Sulfide. *Atom. Spectrosc.* **1997**, 18, 35-40.
- [44]. Safavi, A.; Karimi, M. A. Flow Injection Chemiluminescence Determination of Sulfide by Oxidation with N-Bromosuccinimide and N-Chlorosuccinimide. *Talanta* **2002**, 57, 491-500.
- [45] Kosyakov, A. V.; Zavrazhnov, A. Y.; Naumov, A. V. Refinement of the In-S Phase Diagram Using Spectrophotometric Characterization of Equilibria Between Hydrogen and Indium Sulfides. *Inorg. Mater.* **2010**, 46, 343-345.
- [46] Kumeria, T.; Parkinson, L.; Losic, D. A Nanoporous Interferometric Micro-Sensor for Biomedical Detection of Volatile Sulphur Compounds. *Nanoscale Res. Lett.* **2011**, 6.
- [47] Kolotilina, N. K.; Dolgonosov, A. M. Ion-Chromatographic Determination of Borates and Sulfides With the Use of a Developing Column. *J. Anal. Chem.* **2005**, 60, 738-742.
- [48] Wu, X. C.; Zhang, W. J.; Sammynaiken, R.; Meng, Q. H.; Yang, Q. Q.; Zhan, E.; Liu, Q.; Yang, W.; Wang, R. Non-Functionalized Carbon Nanotube Binding with Hemoglobin. *Colloid. Surface. B.* **2008**, 65, 146-149.

- [49] Wu, X. C.; Zhang, W. J.; Sammynaiken, R.; Meng, Q. H.; Wu, D. Q.; Yang, Q.; Yang, W.; Zhang, E. M.; Wang, R., Measurement of Low Concentration and Nano-Quantity Hydrogen Sulfide in Sera Using Unfunctionalized Carbon Nanotubes. *Meas. Sci. Technol.* **2009**, 20.
- [50] Faccenda, A.; Wang, J.; Mutus, B. Polydimethylsiloxane Permeability-Based Method for the Continuous and Specific Detection of Hydrogen Sulfide. *Anal. Chem.* **2012**, 84, 5243-5249.
- [51] Huang, D.-Q.; Xu, B.-L.; Tang, J.; Yang, L.-L.; Yang, Z.-B.; Bi, S.-P. Bismuth Film Electrodes for Indirect Determination of Sulfide Ion in Water Samples at Trace Level by Anodic Stripping Voltammetry. *Int. J. Electrochem. Sc.* **2012**, 7, 2860-2873.
- [52] Savizi, I. S. P.; Kariminia, H.-R.; Ghadiri, M.; Roosta-Azad, R., Amperometric sulfide detection using *Coprinus cinereus* peroxidase immobilized on screen printed electrode in an enzyme inhibition based biosensor. *Biosens. Bioelectron.* **2012**, 35, 297-301.
- [53] Chang, J.-L.; Wei, G.-T.; Chen, T.-Y.; Zen, J.-M. Highly Stable Polymeric Ionic Liquid Modified Electrode to Immobilize Ferricyanide for Electroanalysis of Sulfide. *Electroanal.* **2013**, 25, 845-849.
- [54] Giovanelli, D.; Lawrence, N. S.; Jiang, L.; Jones, T. G. J.; Compton, R. G., Electrochemical determination of sulphide at nickel electrodes in alkaline media: a new electrochemical sensor. *Sensor. Actuat. B-Chem.* **2003**, 88, 320-328.
- [55] Qi, P.; Wan, Y.; Zhang, D.; Wu, J. Reduced Graphene Sheets Modified Electrodes for Electrochemical Detection of Sulfide. *Electroanal.* **2011**, 23, 2796-2801.

[56] Wang, Y.; Wan, Y.; Zhang, D., Reduced graphene sheets modified glassy carbon electrode for electrocatalytic oxidation of hydrazine in alkaline media. *Electrochem. Commun.* **2010**, 12, 187-190.

[57] Paredes, J. I.; Villar-Rodil, S.; Solis-Fernandez, P.; Martinez-Alonso, A.; Tascon, J. M. D. Atomic Force and Scanning Tunneling Microscopy Imaging of Graphene Nanosheets Derived from Graphite Oxide. *Langmuir : the ACS journal of surfaces and colloids* **2009**, 25, 5957-5968.

[58] Paim, L. L.; Stradiotto, N. R., Electrooxidation of sulfide by cobalt pentacyanonitrosylferrate film on glassy carbon electrode by cyclic voltammetry. *Electrochim. Acta* **2010**, 55, 4144-4147.

[59] Hu, X.; Wang, J. A Simple Route of Modifying Copper Electrodes for the Determination of Methanol and Ethylene Glycol. *Electroanal.* **2012**, 24, 1639-1645.

[60] Gooding, J. J.; Wibowo, R.; Liu, J. Q.; Yang, W. R.; Losic, D.; Orbons, S.; Mearns, F. J.; Shapter, J. G.; Hibbert, D. B., Protein electrochemistry using aligned carbon nanotube arrays. *J. Am. Chem. Soc.* **2003**, 125, 9006-9007.

[61] Li, H.; Tian, Y.; Deng, Z.; Liang, Y., An in Situ Photoelectrochemical Determination of Hydrogen Sulfide Through Generation of CdS Nanoclusters onto TiO<sub>2</sub> Nanotubes. *The Analyst* **2012**, 137, 4605-4609.

[62] Chand, R.; Kumar Jha, S.; Islam, K.; Han, D.; Shin, I.-S.; Kim, Y.-S., Analytical Detection of Biological Thiols in a Microchip Capillary Channel. *Biosen. Bioelectron.* **2013**, 40, 362-367.

[63] Bailey, B.; Waraska, J.; Acworth, I., Direct Determination of Tissue Aminothiols, Disulfide, and Thioether Levels Using HPLC-ECD With a Novel Stable Boron-Doped

Diamond Working Electrode. *Methods in molecular biology (Clifton, N.J.)* **2010**, 594, 327-39.

[64] Cataldi, T. R. I.; Nardiello, D., A Pulsed Potential Waveform Displaying Enhanced Detection Capabilities Towards Sulfur-Containing Compounds At a Gold Working Electrode. *J. Chromatogr. A.* **2005**, 1066, 133-142.

[65] Hiraku, Y.; Murata, M.; Kawanishi, S. Determination of Intracellular Glutathione and Thiols by High Performance Liquid Chromatography with a Gold Electrode at the Femtomole Level: Comparison with a Spectroscopic Assay. *BBA-GAN Subjects* **2002**, 1570, 47-52.

[66] Jang, Y. C.; Jha, S. K.; Chand, R.; Islam, K.; Kim, Y. S. Capillary Electrophoresis Microchip for Direct Amperometric Detection of DNA Fragments. *Electrophoresis* **2011**, 32, 913-919.

[67] Aousgi, F.; Kanzari, M. Structural and Optical Properties of Amorphous Sb<sub>2</sub>S<sub>3</sub> Thin Films Deposited by Vacuum Thermal Evaporation Method. *Curr. Appl. Phys.* **2013**, 13, 262-266.

[68] Pasas, S. A.; Lacher, N. A.; Davies, M. I.; Lunte, S. M. Detection of Homocysteine by Conventional and Microchip Capillary Electrophoresis/Electrochemistry. *Electrophoresis* **2002**, 23, 759-766.

[69] Wang, J.; Mannino, S.; Camera, C.; Chatrathi, M. P.; Scampicchio, M.; Zima, J., Microchip capillary electrophoresis with amperometric detection for rapid separation and detection of seleno amino acids. *J. Chromatogr. A.* **2005**, 1091, 177-182.

[70] Chen, G.; Zhang, L. Y.; Wang, J. Miniaturized Capillary Electrophoresis System with a Carbon Nanotube Microelectrode for Rapid Separation and Detection of Thiols. *Talanta* **2004**, 64, 1018-1023.

## Chapter 6 Conclusions and Future Works

### 6.1 Summary

Polyaniline and its derivatives are the most extensively used among conducting polymers in the construction of different types of electrochemical sensors and biosensors. In the first part of this thesis, PBA film was electrochemically synthesized on gold electrodes for the recognition of amino acid enantiomers. SEM measurements illustrate that the as-prepared PBA film has porous structure and was made up of numerous nano-ribbons. DPVs of L- and D-glutamic acids at the PBA modified Au electrode do not only have very different current densities, but also produce different waveforms, providing an intuitive way to differentiate the two chiral molecules. Similar results are obtained in the analysis of L- and D-aspartic acids. Control experiments suggests that while the observed electro reactivity arises from Au substrate, the coating of the PBA film provides a steric structure needed for differentiating chiral molecules. The approach of utilizing the secondary branches of a polymer chain to build the steric structure needed for chiral sensing may be extended to other monomers which contain various functional groups such as 2-aminophenol.

Halogen ions were subsequently employed in this research as an additive to manifest the properties of the synthesized polymers. In chapter 3 it has been shown that bromide ions could significantly affect the oxidation state of the prepared PANI film, where the results indicated that the bromide ions inhibited the formation of ES and forced the PANI polymer to be dominated by PE and SE forms. When the above synthesized PANI films

were applied for pH sensing, the film obtained under the influence of bromide ions exhibits distinct advantages with regard to larger linear potential response range to pH, a shorter response time, higher accuracy and stability. Such an improvement is attributed to the amine groups in PANI that are more favored in protonation, making the potential response more sensitive in strongly acidic solution.

In addition, motivated by the tremendous research interest in making metal nanoparticle and polymer hybrids, controlled electrodeposition of copper nanoparticles inside or on conductive PDMA matrix was explored. In chapter 4, PDMA film was in-situ synthesized on a glassy carbon electrode with CV technique. The presence of chloride ions in the electrolyte solution was found to have crucial influences on the locations where the copper deposition took place. SEM images illustrate that chloride ions also have significant influence on the size and morphology of the Cu deposit. A transition from octahedral to cubic crystals was seen. Experiments demonstrate that different facets of the Cu nanoparticles give rise to distinctive peak potential for the electrochemical oxidation of glucose, in which glucose oxidation is greatly favored at the (100) cubic facet than at the (111) octahedral facet. The cubic facet exhibits a lower oxidation potential in the electro-oxidation of glucose in alkaline solution with a detection limit of 0.1  $\mu\text{M}$ . The as-prepared PDMA/Cu hybrid electrode also shows great stability for repeated usages.

Finally, a review on electrochemical detection of sulfide was introduced in chapter 5. This review provided an up-to-date overview of the electrochemical detection of sulfide, including hydrogen sulfide, metal sulfide and organic sulfide. Comparing with other detection methods, electrochemical detection represents a highly sensitive, rapid,



affordable and simple technique. This review also detailed different electrochemical approaches and the development of various electrodes, which could be helpful for designing new polymer modified electrodes in our future work.

## 6.2 Future works

Research conducted in this thesis has demonstrated that conductive polymers may have a very promising role in the construction of low cost, highly sensitive sensors by either providing the necessary steric frames or providing more active sites due to its large specific surface area. So far, only monomers of aniline and bromo aniline were explored in this thesis. In the future work, DL-  $\beta$  phenyl-alanine and aniline-2-sulfonic acid can be copolymerized and the properties of copolymer film can be compared with the homopolymers. Most water-soluble ANI monomers, such as aniline-2(or -3)-sulfonic acid, could hardly be homopolymerized because of the withdrawing effect of the sulfonic acid moiety of the phenyl ring. However, the dopant incorporated into inherently conducting polymers could solve this problem and have a profound effect on the physical and chemical properties of the resultant material. Due to the presence of negatively charged sulfonate group, these materials are capable of electrostatic interaction with positively charged groups such as anilinium ions [1].

Our work has demonstrated that the polymer which containing  $-\text{COOH}$  group has capability to distinguish between HQ and CC [2-6]. Benzene derivatives with  $-\text{COOH}$  group can be tried in the future work to be electropolymerized and then explored as the electrochemical sensor to determine HQ and CC. As to the approach employed in the preparation of the metal-polymer hybrid sensors, several directions can be tested. For

example, Xia and his co-workers reported that they could control the ratio of the etching and regrowth rates simply by varying the amount of HCl added to their reaction solution, which resulted in the formation of Pd octahedra or Pd cubes [7]. Inspired by his work, based on our work in chapter 4, the shape of copper nanoparticles may also be controlled to form in the conductive polymer matrix by using different pH values. Then, catalytic performance of nanoparticles with different shapes in the electrochemical oxidation of glucose and other chemicals will be compared.

## References

- [1] Masdarolomoor, F., Innis, P. C., Wallace, G. G. Electrochemical synthesis and Characterisation of Polyaniline/Poly(2-Methoxyaniline-5-Sulfonic Acid) Composites. *Electrochim. Acta* **2008**, 53, 4146-4155.
- [2] Wang, L., Huang, P., Bai, J., Wang, H., Zhang, L., Zhao, Y. Direct simultaneous Electrochemical Determination of Hydroquinone and Catechol at a Poly(glutamic acid) Modified Glassy Carbon Electrode. *Int. J. Electrochem. Sci.* **2007**, 2, 123-132.
- [3] Yang, P., Zhu, Q., Chen, Y., Wang, F. Simultaneous Determination of Hydroquinone and Catechol using Poly(p-Aminobenzoic Acid) Modified Glassy Carbon Electrode. *J. Appl. Polym. Sci.* **2009**, 113, 2881-2886.
- [4] Wang, L., Huang, P. F., Wang, H. J., Bai, J. Y., Zhang, L. Y., Zhao, Y. Q., Covalent Modification of Glassy Carbon Electrode with Aspartic Acid for Simultaneous Determination of Hydroquinone and Catechol. *Ann. Chim.* **2007**, 97, 395-404.

[5] Alemu, Y., Amare, M., Admassie, S., Tessema, M. Simultaneous Determination of Hydroquinone and Catechol at Poly(P-ASA)/MWNTs Composite Film Modified Glassy Carbon Electrode. *Ethiop. J. Sci.* **2012**, 35, 29-40.

[6] Yang, Q. X., Sui, W. P., Fan, D. W., Li, G. B. Simultaneous Determination of Hydroquinone and Catechol at Poly-Histidine Film Modified Glassy Carbon Electrode. *Adv. Mat. Res.* **2013**, 89, 781-784.

[7] Liu, M., Zheng, Y., Zhang, L., Guo, L., Xia, Y. Transformation of Pd Nanocubes into Octahedra with Controlled Sizes by Maneuvering the Rates of Etching and Regrowth, *J. Am. Chem. Soc.* **2013**, 135, 11752-11755.

## APPENDICES

## Appendix A Copyright Releases Electroanalysis

JOHN WILEY AND SONS LICENSE  
TERMS AND CONDITIONS

May 20, 2014

---



---

This is a License Agreement between xuefeng hu ("You") and John Wiley and Sons ("John Wiley and Sons") provided by Copyright Clearance Center ("CCC"). The license consists of your order details, the terms and conditions provided by John Wiley and Sons, and the payment terms and conditions.

**All payments must be made in full to CCC. For payment instructions, please see information listed at the bottom of this form.**



License Number	3393130878004
License date	May 20, 2014
Licensed content publisher	John Wiley and Sons
Licensed content publication	Electroanalysis
Licensed content title	Electrochemical Recognition of Chiral Molecules with Poly(4-bromoaniline) Modified Gold Electrode
Licensed copyright line	Copyright © 2013 WILEY-VCH Verlag GmbH & Co. KGaA, Weinheim
Licensed content author	Jun Li, Xuefeng Hu, Jichang Wang
Licensed content date	Jul 16, 2013
Start page	1975
End page	1980
Type of use	Dissertation/Thesis
Requestor type	Author of this Wiley article
Format	Electronic
Portion	Full article
Will you be translating?	No
Title of your thesis / dissertation	The Development of Polymer-coated Electrodes for Chemical Detection

## APPENDICES

Expected completion date	May 2014
Expected size (number of pages)	125
Total	0.00 USD

## Terms and Conditions

**TERMS AND CONDITIONS**

This copyrighted material is owned by or exclusively licensed to John Wiley & Sons, Inc. or one of its group companies (each a "Wiley Company") or handled on behalf of a society with which a Wiley Company has exclusive publishing rights in relation to a particular work (collectively "WILEY"). By clicking  accept  in connection with completing this licensing transaction, you agree that the following terms and conditions apply to this transaction (along with the billing and payment terms and conditions established by the Copyright Clearance Center Inc., ("CCC's Billing and Payment terms and conditions"), at the time that you opened your Rightslink account (these are available at any time at <http://myaccount.copyright.com/>).

**Terms and Conditions**

- The materials you have requested permission to reproduce or reuse (the "Wiley Materials") are protected by copyright.
- You are hereby granted a personal, non-exclusive, non-sub licensable (on a stand-alone basis), non-transferable, worldwide, limited license to reproduce the Wiley Materials for the purpose specified in the licensing process. This license is for a one-time use only and limited to any maximum distribution number specified in the license. The first instance of republication or reuse granted by this licence must be completed within two years of the date of the grant of this licence (although copies prepared before the end date may be distributed thereafter). The Wiley Materials shall not be used in any other manner or for any other purpose, beyond what is granted in the license. Permission is granted subject to an appropriate acknowledgement given to the author, title of the material/book/journal and the publisher. You shall also duplicate the copyright notice that appears in the Wiley publication in your use of the Wiley Material. Permission is also granted on the understanding that nowhere in the text is a previously published source acknowledged for all or part of this Wiley Material. Any third party content is expressly excluded from this permission.
- With respect to the Wiley Materials, all rights are reserved. Except as expressly granted by the terms of the license, no part of the Wiley Materials may be copied, modified, adapted (except for minor reformatting required by the new Publication), translated, reproduced, transferred or distributed, in any form or by any means, and no derivative works may be made based on the Wiley Materials without the prior permission of the respective copyright owner. You may not alter, remove or

suppress in any manner any copyright, trademark or other notices displayed by the Wiley Materials. You may not license, rent, sell, loan, lease, pledge, offer as security, transfer or assign the Wiley Materials on a stand-alone basis, or any of the rights granted to you hereunder to any other person.

- The Wiley Materials and all of the intellectual property rights therein shall at all times remain the exclusive property of John Wiley & Sons Inc, the Wiley Companies, or their respective licensors, and your interest therein is only that of having possession of and the right to reproduce the Wiley Materials pursuant to Section 2 herein during the continuance of this Agreement. You agree that you own no right, title or interest in or to the Wiley Materials or any of the intellectual property rights therein. You shall have no rights hereunder other than the license as provided for above in Section 2. No right, license or interest to any trademark, trade name, service mark or other branding ("Marks") of WILEY or its licensors is granted hereunder, and you agree that you shall not assert any such right, license or interest with respect thereto.
- NEITHER WILEY NOR ITS LICENSORS MAKES ANY WARRANTY OR REPRESENTATION OF ANY KIND TO YOU OR ANY THIRD PARTY, EXPRESS, IMPLIED OR STATUTORY, WITH RESPECT TO THE MATERIALS OR THE ACCURACY OF ANY INFORMATION CONTAINED IN THE MATERIALS, INCLUDING, WITHOUT LIMITATION, ANY IMPLIED WARRANTY OF MERCHANTABILITY, ACCURACY, SATISFACTORY QUALITY, FITNESS FOR A PARTICULAR PURPOSE, USABILITY, INTEGRATION OR NON-INFRINGEMENT AND ALL SUCH WARRANTIES ARE HEREBY EXCLUDED BY WILEY AND ITS LICENSORS AND WAIVED BY YOU
- WILEY shall have the right to terminate this Agreement immediately upon breach of this Agreement by you.
- You shall indemnify, defend and hold harmless WILEY, its Licensors and their respective directors, officers, agents and employees, from and against any actual or threatened claims, demands, causes of action or proceedings arising from any breach of this Agreement by you.
- IN NO EVENT SHALL WILEY OR ITS LICENSORS BE LIABLE TO YOU OR ANY OTHER PARTY OR ANY OTHER PERSON OR ENTITY FOR ANY SPECIAL, CONSEQUENTIAL, INCIDENTAL, INDIRECT, EXEMPLARY OR PUNITIVE DAMAGES, HOWEVER CAUSED, ARISING OUT OF OR IN CONNECTION WITH THE DOWNLOADING, PROVISIONING, VIEWING OR USE OF THE MATERIALS REGARDLESS OF THE FORM OF ACTION, WHETHER FOR BREACH OF CONTRACT, BREACH OF WARRANTY, TORT, NEGLIGENCE, INFRINGEMENT OR OTHERWISE (INCLUDING, WITHOUT LIMITATION, DAMAGES BASED ON LOSS OF PROFITS, DATA, FILES, USE, BUSINESS OPPORTUNITY OR CLAIMS OF THIRD PARTIES), AND WHETHER OR NOT THE PARTY HAS BEEN ADVISED OF THE POSSIBILITY OF SUCH DAMAGES. THIS LIMITATION SHALL APPLY

NOTWITHSTANDING ANY FAILURE OF ESSENTIAL PURPOSE OF ANY LIMITED REMEDY PROVIDED HEREIN.

- Should any provision of this Agreement be held by a court of competent jurisdiction to be illegal, invalid, or unenforceable, that provision shall be deemed amended to achieve as nearly as possible the same economic effect as the original provision, and the legality, validity and enforceability of the remaining provisions of this Agreement shall not be affected or impaired thereby.
- The failure of either party to enforce any term or condition of this Agreement shall not constitute a waiver of either party's right to enforce each and every term and condition of this Agreement. No breach under this agreement shall be deemed waived or excused by either party unless such waiver or consent is in writing signed by the party granting such waiver or consent. The waiver by or consent of a party to a breach of any provision of this Agreement shall not operate or be construed as a waiver of or consent to any other or subsequent breach by such other party.
- This Agreement may not be assigned (including by operation of law or otherwise) by you without WILEY's prior written consent.
- Any fee required for this permission shall be non-refundable after thirty (30) days from receipt by the CCC.
- These terms and conditions together with CCC's Billing and Payment terms and conditions (which are incorporated herein) form the entire agreement between you and WILEY concerning this licensing transaction and (in the absence of fraud) supersedes all prior agreements and representations of the parties, oral or written. This Agreement may not be amended except in writing signed by both parties. This Agreement shall be binding upon and inure to the benefit of the parties' successors, legal representatives, and authorized assigns.
- In the event of any conflict between your obligations established by these terms and conditions and those established by CCC's Billing and Payment terms and conditions, these terms and conditions shall prevail.
- WILEY expressly reserves all rights not specifically granted in the combination of (i) the license details provided by you and accepted in the course of this licensing transaction, (ii) these terms and conditions and (iii) CCC's Billing and Payment terms and conditions.
- This Agreement will be void if the Type of Use, Format, Circulation, or Requestor Type was misrepresented during the licensing process.
- This Agreement shall be governed by and construed in accordance with the laws of the State of New York, USA, without regards to such state's conflict of law rules. Any legal action, suit or proceeding arising out of or relating to these Terms and Conditions or the breach thereof shall be instituted in a court of competent

jurisdiction in New York County in the State of New York in the United States of America and each party hereby consents and submits to the personal jurisdiction of such court, waives any objection to venue in such court and consents to service of process by registered or certified mail, return receipt requested, at the last known address of such party.

## **WILEY OPEN ACCESS TERMS AND CONDITIONS**

Wiley Publishes Open Access Articles in fully Open Access Journals and in Subscription journals offering Online Open. Although most of the fully Open Access journals publish open access articles under the terms of the Creative Commons Attribution (CC BY) License only, the subscription journals and a few of the Open Access Journals offer a choice of Creative Commons Licenses:: Creative Commons Attribution (CC-BY) license [Creative Commons Attribution Non-Commercial \(CC-BY-NC\) license](#) and [Creative Commons Attribution Non-Commercial-NoDerivs \(CC-BY-NC-ND\) License](#). The license type is clearly identified on the article.

Copyright in any research article in a journal published as Open Access under a Creative Commons License is retained by the author(s). Authors grant Wiley a license to publish the article and identify itself as the original publisher. Authors also grant any third party the right to use the article freely as long as its integrity is maintained and its original authors, citation details and publisher are identified as follows: [Title of Article/Author/Journal Title and Volume/Issue. Copyright (c) [year] [copyright owner as specified in the Journal]. Links to the final article on Wiley's website are encouraged where applicable.

### **The Creative Commons Attribution License**

The [Creative Commons Attribution License \(CC-BY\)](#) allows users to copy, distribute and transmit an article, adapt the article and make commercial use of the article. The CC-BY license permits commercial and non-commercial re-use of an open access article, as long as the author is properly attributed.

The Creative Commons Attribution License does not affect the moral rights of authors, including without limitation the right not to have their work subjected to derogatory treatment. It also does not affect any other rights held by authors or third parties in the article, including without limitation the rights of privacy and publicity. Use of the article must not assert or imply, whether implicitly or explicitly, any connection with, endorsement or sponsorship of such use by the author, publisher or any other party associated with the article.

For any reuse or distribution, users must include the copyright notice and make clear to others that the article is made available under a Creative Commons Attribution license, linking to the relevant Creative Commons web page.

To the fullest extent permitted by applicable law, the article is made available as is and without representation or warranties of any kind whether express, implied, statutory or



otherwise and including, without limitation, warranties of title, merchantability, fitness for a particular purpose, non-infringement, absence of defects, accuracy, or the presence or absence of errors.

### **Creative Commons Attribution Non-Commercial License**

The [Creative Commons Attribution Non-Commercial \(CC-BY-NC\) License](#) permits use, distribution and reproduction in any medium, provided the original work is properly cited and is not used for commercial purposes.(see below)

### **Creative Commons Attribution-Non-Commercial-NoDerivs License**

The [Creative Commons Attribution Non-Commercial-NoDerivs License](#) (CC-BY-NC-ND) permits use, distribution and reproduction in any medium, provided the original work is properly cited, is not used for commercial purposes and no modifications or adaptations are made. (see below)

### **Use by non-commercial users**

For non-commercial and non-promotional purposes, individual users may access, download, copy, display and redistribute to colleagues Wiley Open Access articles, as well as adapt, translate, text- and data-mine the content subject to the following conditions:

- The authors' moral rights are not compromised. These rights include the right of "paternity" (also known as "attribution" - the right for the author to be identified as such) and "integrity" (the right for the author not to have the work altered in such a way that the author's reputation or integrity may be impugned).
- Where content in the article is identified as belonging to a third party, it is the obligation of the user to ensure that any reuse complies with the copyright policies of the owner of that content.
- If article content is copied, downloaded or otherwise reused for non-commercial research and education purposes, a link to the appropriate bibliographic citation (authors, journal, article title, volume, issue, page numbers, DOI and the link to the definitive published version on **Wiley Online Library**) should be maintained. Copyright notices and disclaimers must not be deleted.
- Any translations, for which a prior translation agreement with Wiley has not been agreed, must prominently display the statement: "This is an unofficial translation of an article that appeared in a Wiley publication. The publisher has not endorsed this translation."

### **Use by commercial "for-profit" organisations**

Use of Wiley Open Access articles for commercial, promotional, or marketing purposes requires further explicit permission from Wiley and will be subject to a fee. Commercial

purposes include:

- Copying or downloading of articles, or linking to such articles for further redistribution, sale or licensing;
- Copying, downloading or posting by a site or service that incorporates advertising with such content;
- The inclusion or incorporation of article content in other works or services (other than normal quotations with an appropriate citation) that is then available for sale or licensing, for a fee (for example, a compilation produced for marketing purposes, inclusion in a sales pack)
- Use of article content (other than normal quotations with appropriate citation) by for-profit organisations for promotional purposes
- Linking to article content in e-mails redistributed for promotional, marketing or educational purposes;
- Use for the purposes of monetary reward by means of sale, resale, licence, loan, transfer or other form of commercial exploitation such as marketing products
- Print reprints of Wiley Open Access articles can be purchased from: [corporatesales@wiley.com](mailto:corporatesales@wiley.com)

Further details can be found on Wiley Online Library  
<http://olabout.wiley.com/WileyCDA/Section/id-410895.html>

Other Terms and Conditions:

**v1.9**

**If you would like to pay for this license now, please remit this license along with your payment made payable to "COPYRIGHT CLEARANCE CENTER" otherwise you will be invoiced within 48 hours of the license date. Payment should be in the form of a check or money order referencing your account number and this invoice number 501307666.**

**Once you receive your invoice for this order, you may pay your invoice by credit card. Please follow instructions provided at that time.**

**Make Payment To:  
Copyright Clearance Center  
Dept 001**

## APPENDICES

**P.O. Box 843006  
Boston, MA 02284-3006**

**For suggestions or comments regarding this order, contact RightsLink Customer Support: [customercare@copyright.com](mailto:customercare@copyright.com) or +1-877-622-5543 (toll free in the US) or +1-978-646-2777.**

**Gratis licenses (referencing \$0 in the Total field) are free. Please retain this printable license for your reference. No payment is required.**

---

---

## Appendix B Copyright Releases ECS Electrochemistry Letter

### Request for Permission to Reproduce or Re-Publish ECS Material

Please fax (or email) to: The Electrochemical Society (ECS), Attn: Permissions Requests, 1.606.730.0629  
 You may also e-mail your request to: [copyright@electrochem.org](mailto:copyright@electrochem.org). Include all the information as required on this form. Please allow 3-7 days for your request to be processed.

I am preparing a (choose one):  paper  chapter  book  thesis

entitled The Development of Polymer-coated Electrodes for Chemical Detection  
 to be published by will be listed in University of Windsor Library

in an upcoming publication entitled: The Development of Polymer-coated Electrodes for Chemical Detection

I request permission to use the following material in the publication noted above, and request nonexclusive rights for all subsequent editions and in all foreign language translations for distribution throughout the world.

Description of material to be used—Indicate what material you wish to use (figures, notes, text, etc.) and give the full bibliographic reference for the source publication. You may attach a separate list, reproducible by ECS title.

I wish to use a full article in my thesis, and I will make 2 copies.  
 The article is: "Designed Deposition of Copper Nanoparticles on/in a  
 Conductive Polymer Matrix" Xuefeng Hu, Jun Li, Licheng Wang  
 ECS Electrochemistry Letters, 3 (6) D15 - D16 (2014)  
 The deadline is May 23<sup>rd</sup>, 2014.

Signature: Xuefeng Hu Date: May-20-2014

Name: Xuefeng Hu

Address: 125 1980 Wyandotte Street West, Windsor, ON, Canada

Telephone: 519-253-3600 - 2618 Fax: \_\_\_\_\_

E-mail: hu.x.f.l@uwindsor.ca

Permission is granted to include the above-referenced paper in your thesis, provided that you obtain permission of the other individual authors. In the thesis, please acknowledge the authors and the citation given above, and include the words: "Reproduced by permission of ECS - The Electrochemical Society."

5/20/14  
Date

  
John Lewis, Associate Director of Publications

## Appendix C Copyright Releases Reviews in Analytical Chemistry



DE GRUYTER

**PERMISSION REQUEST****1. Contact Details**

Company / Institution: University of Windsor  
Address: 401 Sunset Avenue  
Contact Person: Xuefeng Hu  
Telephone / Fax: 5192533000-2648  
E-Mail: hu11b@uwindsor.ca

**2. De Gruyter Title:**

Book  Journal  Online/Website  Other: Reviews in Analytical Chemistry

Author(s)/Editor(s): Xuefeng Hu, Bulent Mutus

Title: Electrochemical Detection of Sulfide

Year of Publication: 2013

Volume / Issue Number: 32

ISBN / ISSN: 0793-0135

Are you the author of the requested material?  Yes  No

If not, is the author employed at your company/institute?  Yes  No

**Please specify the requested material:**

Whole Book

Chapter / Article, Author:

Title:

Page(s):

Illustration(s) / Figure(s), Title:

Credit Line:

Page number/Number of illustration(s) or figure:

**3. Please specify how the requested material will be used:**

Reprint  Translation, language:

Book  Journal  Online/Website  Dissertation

Other: Thesis

Author(s)/Editor(s): Xuefeng Hu

Title: The Development of Polymer-coated Electrodes for Chemical Detection

Publisher: Will not publish (will be list in U Windsor's library)

ISBN / ISSN:

Total Number of Pages: 133

Language(s): English

**VITA AUCTORIS**

**NAME:** Xuefeng Hu

**PLACE OF BIRTH:** China

**YEAR OF BIRTH:** 1982

**EDUCATION:** University of Anqing, B.Sc., China, 2005  
China University of Mining and Technology, M.Sc., China, 2009  
University of Windsor, M. Sc., Canada, 2014